

HSV-1 INDUCES FILOPODIA FORMATION IN ACTIVATED T LYMPHOCYTES



A Thesis Submitted in Partial Fulfillment of the Requirements
for the Degree of Master of Science in Medical Microbiology

Medical Microbiology, Interdisciplinary Program

GRADUATE SCHOOL

Chulalongkorn University

Academic Year 2018

Copyright of Chulalongkorn University

ไวรัสเฮอริสซิมเพล็กซ์ไทป์ 1 เหนี่ยวนาให้ทีลิมโพซัยต์ที่ถูกกระตุ้น สร้างไฟโลโปเดีย



วิทยานิพนธ์นี้เป็นส่วนหนึ่งของการศึกษาตามหลักสูตรปริญญาวิทยาศาสตรมหาบัณฑิต

สาขาวิชาจุลชีววิทยาทางการแพทย์ สหสาขาวิชาจุลชีววิทยาทางการแพทย์

บัณฑิตวิทยาลัย จุฬาลงกรณ์มหาวิทยาลัย

ปีการศึกษา 2561

ลิขสิทธิ์ของจุฬาลงกรณ์มหาวิทยาลัย

Thesis Title HSV-
1 INDUCES FILOPODIA FORMATION IN ACTIVATED T LYMPHOCYTES

By Mr. Thanayod Sasivimolrattana

Field of Study Medical Microbiology

Thesis Advisor Associate Professor Parvapan Bhattarakosol, Ph.D.

Accepted by the GRADUATE SCHOOL, Chulalongkorn University in Partial Fulfillment of the Requirement for the Master of Science

..... Dean of the GRADUATE SCHOOL
(Associate Professor Thumnoon Nhujak, Ph.D.)

THESIS COMMITTEE

..... Chairman
(Associate Professor Kanitha Patarakul, M.D., Ph.D.)

..... Advisor
(Associate Professor Parvapan Bhattarakosol, Ph.D.)

..... Examiner
(Rangsima Reantragoon, M.D., Ph.D.)

..... External Examiner
(Professor Wasun Chantratita, Ph.D.)

ธนยศ ศศิวิมลรัตนานา : ไวรัสเฮอร์ปีสซิมเพล็กซ์ไทป์ 1 เหนี่ยวานำให้ทีลิมโฟซัยต์ที่ถูกกระตุ้น สร้างไฟโลโปเดีย.
(HSV-1 INDUCES FILOPODIA FORMATION IN ACTIVATED T LYMPHOCYTES) อ.ที่ปรีกษา
วิทยานิพนธ์หลัก : รศ. ดร.ภาวพันธ์ ภัทรโกศล

Herpes simplex virus type 1(HSV-1) เป็นไวรัสที่พบว่ามีการแพร่ระบาดอย่างกว้างขวาง ซึ่งสามารถก่อโรคได้ทั้งแบบติดเชื้อเฉพาะตำแหน่ง อาการไม่รุนแรง ไปจนถึงอาการโรครุนแรง มีการแพร่กระจายไปทั่วร่างกายทำให้เกิดอันตรายถึงชีวิตได้ โดยปกติแล้วเซลล์เป้าหมายของ HSV-1 คือ เซลล์เยื่อบุผิว และเซลล์เยื่อเมือก อย่างไรก็ตาม ไวรัสชนิดนี้สามารถเพิ่มจำนวนได้ในเซลล์เม็ดเลือดขาวชนิด T lymphocytes ซึ่งเป็นสาเหตุของการติดเชื้อ HSV-1 ในกระแสโลหิต ในงานวิจัยนี้ใช้ CD3⁺CD4⁻CD8⁻ Jurkat T lymphocytes โดยเมื่อเซลล์ถูกกระตุ้นจะมีการแสดงออกของโมเลกุล CD69 เพิ่มขึ้นบริเวณผิวของเซลล์ จากการทดลองพบว่า HSV-1 มีปริมาณเพิ่มขึ้นใน T lymphocytes ที่ถูกกระตุ้น นอกจากนี้ภายหลังการเพิ่มจำนวนใน T lymphocytes อนุภาคไวรัสจะถูกปล่อยออกมาภายนอกเซลล์ ซึ่งน่าจะเป็นสาเหตุของการแพร่กระจายของไวรัสในกระแสเลือด ปัจจุบันกลไกที่สนับสนุนการติดเชื้อ HSV-1 ใน T lymphocytes ที่ถูกกระตุ้นยังไม่เป็นที่ทราบแน่ชัด แต่ในเซลล์เยื่อบุผิว HSV-1 สามารถที่จะเหนี่ยวนำให้เซลล์เกิดการสร้าง filopodia ซึ่งเกิดจากการจัดเรียงตัว และการต่อสายยาวของ actin ซึ่งโครงสร้างดังกล่าวจะทำให้เซลล์ติดเชื้อ HSV ได้มากยิ่งขึ้น นอกจากนั้นการเกิด filopodia ยังถูกควบคุมโดย Cdc42 ซึ่งเป็นโปรตีนที่จัดอยู่ในกลุ่ม Rho GTPase จากการทดลองพบว่า การแสดงออกของ β -actin mRNA เพิ่มขึ้นเล็กน้อยอย่างไม่เป็นนัยสำคัญ ในเซลล์ติดเชื้อ HSV-1 T lymphocytes ที่ถูกและไม่ถูกกระตุ้น แต่พบความแตกต่างอย่างมีนัยสำคัญของการแสดงออกในระดับโปรตีน โดยพบว่า การแสดงออกของโปรตีน β -actin เพิ่มขึ้นในเซลล์ที่ถูกกระตุ้นและติดเชื้อ HSV และลดลงในเซลล์ที่ถูก treat ด้วย cytochalasin D (cyto D) ซึ่งจะไปยับยั้งการต่อสายยาวของ actin และยังทำให้ actin filament เกิดการ depolymerization จากผลการทดลองดังกล่าว ชี้ให้เห็นว่า actin มีบทบาทในการเข้าสู่เซลล์ของ HSV-1 ใน T lymphocytes ที่ถูกกระตุ้น และยังพบว่า การแสดงออกของโปรตีน Cdc42 ถูกเหนี่ยวนำโดย HSV-1 ในขณะที่การแสดงออกของโปรตีนอื่นๆในกลุ่ม Rho GTPase ไม่เปลี่ยนแปลง ขณะ HSV-1 กำลังจะเข้าสู่เซลล์พบมีการสร้าง filopodia ในเซลล์ T lymphocytes ที่ถูกกระตุ้น เช่นเดียวกับที่พบในเซลล์เยื่อบุผิว ชี้ให้เห็นว่า filopodia formation มีบทบาทต่อการเข้าสู่เซลล์ของไวรัสชนิดนี้ จากการสังเกตภายใต้กล้องจุลทรรศน์อิเล็กตรอนพบว่า HSV-1 สามารถเข้าสู่เซลล์ T lymphocytes ที่ถูกกระตุ้นได้ทั้งวิธี fusion และ endocytosis นอกจากนั้นเมื่อทำการ treat เซลล์ด้วย cyto D พบว่าปริมาณของไวรัสที่ลดลง แสดงให้เห็นว่า actin polymerization มีบทบาทสำคัญต่อการติดเชื้อ HSV-1 ใน T lymphocytes จากผลการทดลองทั้งหมดจึงสรุปได้ว่า ใน T lymphocytes ที่ถูกกระตุ้น filopodia ถูกสร้างขึ้นโดยอาศัยการต่อสายยาวของแอกติน และเพื่อเพิ่มประสิทธิภาพในการติดเชื้อ HSV-1 สามารถเหนี่ยวนำให้ T lymphocytes ที่ถูกกระตุ้น เกิดการสร้าง filopodia อีกด้วย

| | | |
|------------|----------------------------------|---|
| ภาควิชา | สหสาขาวิชาจุลชีววิทยาทางการแพทย์ | ลายมือชื่อนิสิต |
| สาขาวิชา | จุลชีววิทยาทางการแพทย์ | ลายมือชื่อ อ.ที่ปรีกษาวิทยานิพนธ์หลัก |
| ปีการศึกษา | 2561 | |

5987144320 : MASTER OF SCIENCE

Herpes simplex virus type 1, Filopodia formation, T lymphocytes, Actin

Thanayod Sasivimolrattana : HSV-1 INDUCES FILOPODIA FORMATION IN ACTIVATED T LYMPHOCYTES. ADVISOR: Assoc. Prof. Parvapan Bhattarakosol, Ph.D.

Herpes simplex virus type 1 (HSV-1) is a widespread pathogen, which has diverse clinical manifestations from mild localized infection to severe systemic infection. The tissue tropism of HSV-1 is mainly epithelial and mucosal cells. However, it can also multiply in T lymphocytes suggesting a cause of viremia. In this study, CD3⁺CD4⁻CD8⁻ Jurkat T lymphocytes were used. Under activation, up-regulation of CD69 molecules on cell surface was observed. Increase yield of HSV-1 production in activated T lymphocytes was demonstrated. In addition, most of HSV-1 virion progenies from infected T lymphocytes were released extracellularly, suggesting the cause of dissemination. The mechanism which supports HSV-1 infection in activated T lymphocytes is unclear. In epithelial cells, HSV-1 induce filopodia formation which constructed by actin polymerization to support their infectivity. Moreover, in those type of cell, filopodia formation are regulated by Cdc42, a member of Rho GTPase protein. In this study, the trend of β -actin mRNA expression was increased after HSV-1 infection in both activated and non-activated cell while the statistically different was found at protein level. β -actin expression was overexpressed after HSV-1 infection in activated T lymphocytes and decreased in cytochalasin D (cyto D), an inhibitor of actin polymerization and depolymerization of actin filaments formed, treated cells. This result indicated that actin plays role during HSV-1 entry in activated T cells. Moreover, Cdc42 was induced by HSV-1 whereas the expression of other Rho GTPase proteins was not changed. During viral entry, filopodia formation was observed in HSV-1-infected activated T lymphocytes suggesting filopodia formation might play role in HSV-1 entry in T-lymphocytes similar to epithelial cells. Observation under electron microscope suggested that HSV-1 entered into activated T lymphocytes via fusion and endocytosis pathway. In addition, HSV-1 titer in cyto D treated activated T lymphocytes was decreased indicating that actin polymerization plays role in HSV-1 infection of activated T lymphocytes. In conclusion, in activated T lymphocytes, filopodia formation, induced by HSV-1 infection was constructed by actin polymerization through Cdc42 which then resulted in increased yield of HSV-1 production.

| | | |
|-----------------|---|---------------------------|
| Department: | Medical Microbiology, Interdisciplinary Program | Student's Signature |
| Field of Study: | Medical Microbiology | Advisor's Signature |
| Academic Year: | 2018 | |

ACKNOWLEDGEMENTS

I would like to express my sincere gratitude to my advisor Associate Professor Parvapan Bhattarakosol, Ph.D., Department of Microbiology, Faculty of Medicine, Chulalongkorn University for the invaluable advice, helpful guidance, encouragement and continuous support of my M.Sc. study and related research. All of this has enabled me to carry out my study successfully.

I gratefully acknowledge Assistant Professor Pokrath Hansasuta, MD, DPhil (Oxon), Department of Microbiology, Faculty of Medicine, Chulalongkorn University for his kindly advises, supports and suggestions even though I am not his advisee.

I am also very grateful to Assistant Professor Supang Maneesri Le Grand, Ph.D. and Ms. Wilawan Ji-Au, Department of Pathology, Faculty of Medicine, Chulalongkorn University for transmission electron microscope processing and performing.

I am also greatly appreciated Professor Tanapat Palaga, Ph.D., Department of Microbiology, Faculty of Science, Chulalongkorn University for providing Jurkat cells and Assistant Professor Monthon Lertworapreecha, Ph.D., Faculty of Science, Thaksin University for giving Vero cell.

I am very grateful to the members of the thesis committee, Associate Professor Kanitha Patarakul, M.D., Ph.D. and Rangsimaa Reantragoon, M.D., Ph.D. Department of Microbiology, Faculty of Medicine, Chulalongkorn University, Professor Wasun Chantratitra, Ph.D., Director of Center for Medical Genomics, Faculty of Medicine, Ramathibodi Hospital, Mahidol University for their kindness, constructive criticisms and helpful suggestion for completeness and correction of the thesis.

I also wish to express special thanks to Arkhom Chaiwongkot, Ph.D., Supranee Buranapraditkun, Ph.D., Yada Tansiri, Ph.D., Mrs. Vanida Mungmee, Ms. Prathanporn Kaewpreedee, Ph.D. student, Ms. Fern Baedyananda, Ph.D. student, Ms. Sasiprapa Anoma, Ph.D. student, Ms. Parichat Kanyaboon, Ms. Aphinya Suroengrit, Mr. Chaichontat Sriworarat, Ms. Sasiprapa Liewchalermwong, Ms. Sonsavan Ruechukorndamrong and every one, whose names cannot be fully listed for their experimental assistance, kind support and cheerfulness throughout the study.

Lastly, I would like to thank my family for supporting me spiritually throughout writing this thesis and my life in general.

Thanayod Sasivimolrattana

TABLE OF CONTENTS

| | Page |
|---------------------------------------|------|
| ABSTRACT (THAI)..... | iii |
| ABSTRACT (ENGLISH)..... | iv |
| ACKNOWLEDGEMENTS | v |
| TABLE OF CONTENTS | vi |
| LIST OF TABLES..... | x |
| LIST OF FIGURES | xi |
| CHAPTER I INTRODUCTION..... | 1 |
| CHAPTER II OBJECTIVE..... | 3 |
| CHAPTER III REVIEW OF LITERATURE..... | 4 |
| Herpes simplex virus | 4 |
| HSV entry..... | 7 |
| HSV replication cycle | 11 |
| HSV latency and reactivation | 14 |
| Filopodia formation..... | 15 |
| HSV infection..... | 22 |
| Transmission | 22 |
| Epidemiology | 23 |
| Pathology..... | 23 |
| Immunity to HSV infection..... | 23 |
| Diseases | 25 |
| Laboratory diagnosis | 25 |

| | |
|--|----|
| Activation of T lymphocytes | 26 |
| HSV replication in T lymphocyte..... | 28 |
| CHAPTER IV MATERIALS AND METHODS..... | 30 |
| Part I: Cell cultures and viral stock preparation..... | 30 |
| 1. Cell cultures..... | 30 |
| 1.1 Jurkat cell..... | 30 |
| 1.2 Vero cell | 30 |
| 1.3 Peripheral Blood Mononuclear Cells (PBMC)..... | 30 |
| 2. Virus stock preparation | 31 |
| 3. Viral plaque assay | 31 |
| PART II: T cell activation..... | 32 |
| 1. T cell activation..... | 32 |
| 1.1 Dynabeads preparation | 32 |
| 1.2 Activation process..... | 32 |
| 1.3 Study of activated Jurkat cell growth..... | 32 |
| 2. Flow cytometry | 32 |
| 2.1 Characterization of Jurkat cell phenotype | 32 |
| 2.2 Detection of activation markers on activated T lymphocytes | 33 |
| PART III: β -actin expression | 34 |
| 1. Real-time polymerase chain reaction | 34 |
| 1.1 RNA extraction..... | 34 |
| 1.2 First-stranded cDNA synthesis..... | 35 |
| 1.3 RT-qPCR | 35 |
| 1.4 Double delta Ct analysis..... | 36 |

| | |
|---|----|
| 2. Cytochalasin D treatment | 36 |
| 2.1 Viable cell count..... | 36 |
| 2.2 Cytotoxicity assay (Tetra Z assay)..... | 37 |
| 3. Actin polymerization | 38 |
| 3.1 SDS-PAGE | 38 |
| 3.2 Western blot..... | 38 |
| 3.3 Re-probing | 39 |
| 3.4 Protein band intensity analysis | 39 |
| PART IV: Filopodia formation..... | 40 |
| 1. Detection of GTPase of the Rho family (Cdc42, RhoA, Rac1) by Western blot | 40 |
| 2. Immunofluorescence | 40 |
| 2.1 Optimization of antibody and fluorescence dye | 40 |
| 2.2 Sample preparation..... | 41 |
| 2.3 Immunostaining..... | 42 |
| 3. Transmission electron microscope (TEM)..... | 42 |
| 3.1 Sample preparation..... | 42 |
| 3.2 Dehydration and Embedding..... | 42 |
| 3.3 Sectioning and Imaging | 43 |
| PART V: Role of actin on HSV-1 production in activated T lymphocytes..... | 44 |
| CHAPTURE V RESULTS | 45 |
| Part I: Cell cultures and viral stock preparation..... | 45 |
| 1. Jurkat cell growth curve | 45 |
| 2. HSV-1 stock titers | 47 |

| | |
|--|-----|
| PART II: T cell activation | 48 |
| 1. Growth of activated and non-activated T lymphocytes..... | 48 |
| 2. Characterization of Jurkat cell phenotype..... | 50 |
| 3. Detection of activation markers on activated T lymphocytes | 51 |
| 4. HSV-1 growth in activated and non-activated T lymphocytes | 54 |
| PART III: β -actin expression..... | 56 |
| 1. Detection of β -actin mRNA..... | 56 |
| 2. Cytochalasin D treatment..... | 58 |
| 3. Detection of β -actin expression at translational level | 61 |
| PART IV: Filopodia formation during HSV-1 entry..... | 63 |
| 1. Rho GTPase family expression..... | 63 |
| 2. Detection of HSV-1 and actin on filopodia..... | 67 |
| 3. Detection of HSV-1 entry and filopodia by electron microscopy..... | 74 |
| PART V: Effect of actin on the yield production of HSV-1 in activated T lymphocytes | 76 |
| CHAPTURE VI DISCUSSION..... | 80 |
| REFERENCES | 89 |
| APPENDIX A REGENTS, MATERIALS AND INSTRUMENTS | 106 |
| APPENDIX B REAGENTS PREPARATION | 112 |
| VITA..... | 121 |

LIST OF TABLES

| | Page |
|--|------|
| Table 1. Properties of human Herpesviruses..... | 6 |
| Table 2. The specific primers for RT-qPCR..... | 36 |
| Table 3. The specific antibodies for Western blot | 40 |
| Table 4. The expression of CD38, CD69 and HLA-DR on activated T lymphocytes after 72 hours activation..... | 53 |



LIST OF FIGURES

| | Page |
|---|------|
| Figure 1. Structure of the herpesvirus virion..... | 5 |
| Figure 2. Herpes simplex virus (HSV) attachment and entry mechanism..... | 10 |
| Figure 3. Herpes simplex virus replication cycle..... | 12 |
| Figure 4. Envelopment and egression theories of herpes simplex virus..... | 13 |
| Figure 5. Three steps of the polymerization of actin..... | 16 |
| Figure 6. Filopodium, lamellipodium and stress fiber structure..... | 18 |
| Figure 7. A model of filopodia formation..... | 19 |
| Figure 8. HSV-1 induces filopodia formation support viral entry and cell-to-cell spread. | 20 |
| Figure 9. The actin polymerizing and depolymerizing molecules..... | 22 |
| Figure 10. Mean growth curve of Jurkat cell..... | 46 |
| Figure 11. The plaque titration assay | 47 |
| Figure 12. Growth rate of activated and non-activated T lymphocytes. | 49 |
| Figure 13. The phenotypic markers on surface of Jurkat cells. | 50 |
| Figure 14. The expression of activation markers on activated T lymphocytes and PBMCs..... | 52 |
| Figure 15. Mean HSV-1 titers from 72 hours activated and non-activated T lymphocytes at 24, 48 and 72 hpi..... | 55 |
| Figure 16. β -actin mRNA expression in activated and non-activated T lymphocytes without HSV-1 and with HSV-1 inoculation (30 mpi)..... | 57 |
| Figure 17. The cell survival after cyto D treatment at various concentrations. | 59 |
| Figure 18. The cell survival rate (%) after cyto D treatment..... | 60 |

| | |
|--|----|
| Figure 19. The expression of β -actin during HSV-1 entry..... | 62 |
| Figure 20. The Cdc42 expression during HSV-1 entry. | 64 |
| Figure 21. The RhoA expression during HSV-1 entry. | 65 |
| Figure 22. The Rac1 expression during HSV-1 entry. | 66 |
| Figure 23. Optimization of goat polyclonal anti-HSV-1 conjugated with FITC..... | 69 |
| Figure 24. Optimization of rhodamine phalloidin..... | 70 |
| Figure 25. Detection of filopodia formation in HSV-1-infected Vero cell. | 71 |
| Figure 26. HSV-1 attaches to filopodia on activated T lymphocytes. | 72 |
| Figure 27. HSV-1 attaches to cyto D treated activated and non-activated T lymphocytes..... | 73 |
| Figure 28. Cell morphology during HSV-1 entry..... | 75 |
| Figure 29. The role of actin in HSV-1-infected, activated T lymphocytes after cyto D treatment. | 78 |
| Figure 30. Percentage of plaque reduction after cyto D treatment. | 79 |

CHAPTER I

INTRODUCTION

Herpes simplex virus (HSV) is a widespread pathogen which has diverse clinical manifestations ranging from mild to severe diseases leading to death, for example, cold sores, herpetic whitlow, gingivostomatitis and neonatal herpes (1-4). HSV belongs to family *Herpesviridae*, subfamily *Alphaherpesvirinae*. There are 2 types, i.e., HSV-1 and HSV-2 (5). HSV-1 causes oropharyngeal lesions and transmits by contact while HSV-2 is a sexually transmitted disease and generally infects the genital mucosa (6). HSV is a double-stranded DNA virus containing in an icosahedral capsid. The viral envelope comes from the host nuclear membrane which contains various types of viral glycoproteins, for instance, glycoprotein (g) B, D, H and L. These glycoproteins are very essential for herpesvirus attachment and entry (7). The tissue tropism of HSV is epithelial and mucosal cells. After HSV-infection, the virus can cause latent infection by persisting in the neuronal ganglion (6). The recurrent infection can occur time to time when reactivation is induced by stimuli such as burn, cold, stress and immunosuppressive drug. During latency the virus stays in nerve cell without replication.

Cytoskeleton is an essential structure in all domains, including archaea, bacteria and eukaryotes. The cytoskeleton is divided into 3 types, including microtubules, 10-nm (intermediate) filaments, and microfilaments (8, 9). Microfilaments are filamentous structure that comes from the polymerization of actin. Actin is the main component of the actin cytoskeleton (10) and plays an important role in various cell functions including intracellular transport, uptake of extracellular substance, migration, adherence and cell division (11). There are 6 isoforms of actin that present in mammals, including 4 muscle isoforms (α_{skeletal} -actin, α_{cardiac} -actin, α_{smooth} -actin and γ_{smooth} -actin) which are expressed in cardiac, skeletal and smooth muscle (12). The other groups of actin isoforms are 2

cytoplasmic (non-muscle) isoforms (β_{cyto} -actin and γ_{cyto} -actin) which differ only at 4 amino acids at N-terminus end of the structure (10, 12, 13). These 2 types of cytoplasmic isoforms are encoded by *ACTB* and *ACTG1* gene respectively (10). Muscle actins are specific to the type of tissue but non-muscle actins are conserved in various cell types and are important for living cells (13). There are 2 basic types of actin which present in cell including globular or monomeric actin (G-actin) and linear polymer or filamentous actin (F-actin) (11). Both of them are essential for cell functions such as contraction of cells during cell division (10). The polymerization of actin plays an important role in cell morphogenesis, i.e., filopodia and lamellipodium (14). HSV and some viruses can use this structure, especially filopodia for viral entry (7).

Although HSV-1 normally infects epithelial cells, previous studies showed the possibility of HSV replication in a human T lymphocyte (15, 16). HSV-1 and HSV-2 production in Jurkat cells, an immortalized cell line of human T lymphocyte, were lower than those in epithelial cells (Vero and HEp-2 cells) (16). However, after PHA-activation, viral production and percentage of viral infected T-cells were increased. HVEA, a HSV gD receptor normally expressed on T lymphocytes but its expression were also increased in HSV-1-infected, activated T lymphocytes (17). Not only the increased of HVEA, but also filopodia formation was also observed in the HSV-1 infected, activated T lymphocytes (18). Thus, this study aims to investigate the role of filopodia formation in association with the viral entry in HSV-1-infected, activated T lymphocytes.

CHAPTER II

OBJECTIVE

The objective of this study is to investigate filopodia formation in HSV-1-infected activated T lymphocytes.



CHAPTER III

REVIEW OF LITERATURE

Herpes simplex virus

Herpes simplex virus (HSV) is a member of *Herpesviridae* family (19). This family is divided into 3 subfamilies, i.e., *Alphaherpesvirinae*, *Betaherpesvirinae* and *Gammapherpesvirinae* (6). Herpesviruses can infect human or animal depending on their types. However, there are only 8 human herpesviruses (HHVs) present nowadays (Table 1). Among each group of these viruses, some viral properties are different for example base composition and sequence arrangements of their genome but some of their properties are shared, such as ability to latency (20). Many herpesviruses infect animals, for example, B viruses (herpesvirus simian or cercopithecine herpesvirus 1) of monkeys, marmoset herpesvirus and pseudorabies virus of pigs (6).

Since ancient Greek times, herpes infection had been discovered. The word “herpes” means creeping and crawling indicating the behavior of skin lesions (19). At present, HSV is known to be the causative pathogen. There are 2 types of HSV. HSV-1 usually involves in nongenital infection and spreads by contact, usually associated with infected saliva. HSV-2 causes genital diseases and transmits sexually or from HSV-infected mothers to their child (6, 19, 21). HSV-1 not only causes nongenital infection, but also genital infection. In some country, HSV-1 infection is a main cause of genital herpes and probably neonatal herpes (22). Moreover, HSV-1 infection also plays a critical role in immunocompromised host (23).

HSV contains 125-240 kilobase pairs (kbp) double-stranded linear DNA genome (5). The viral genome consists of long and short components. These components consist of UL and US sequences. The UL sequence contains 65 protein coding sequences, whereas US sequence contains 14 protein coding sequences. The HSV genome contains in viral nucleocapsid. There are many types of protein (about 14 virus-coded proteins) which contain between nucleocapsid and envelope, called

the tegument proteins (5). HSV envelope is acquired by budding of nucleocapsid through the host nuclear membrane. The glycoproteins (gB, gC, gD, gE, gG, gH, gI, gK, gL, gM, gJ and gN) are on envelope surface (24) (Figure 1). The diameter of HSV virion is about 150-200 nanometers (25), depends on the amount of the tegument proteins (26). The diameter of naked HSV is 125 nanometers. The HSV genome encodes about 100 different proteins. Over 35 polypeptides are viral structure; at least 10 are viral envelope glycoproteins (6).

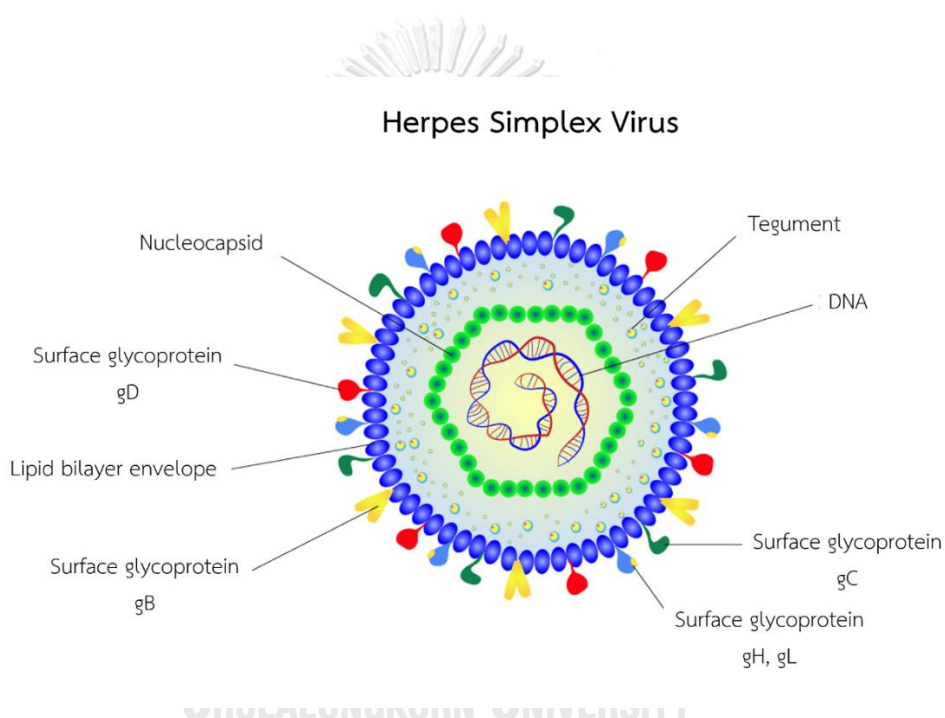


Figure 1. Structure of the herpesvirus virion
(24)

Table 1. Properties of human Herpesviruses

| Subfamily/genus | Official name (Human herpes virus; HHV) | Common name | Biological properties |
|----------------------------|---|--|---|
| <i>Alphaherpesvirinae</i> | | | |
| <i>Simplexvirus</i> | HHV-1 | Herpes simplex virus 1 (HSV-1) | Fast-growing, Cytolytic, Latent in dorsal root ganglion |
| | HHV-2 | Herpes simplex virus 2 (HSV-2) | |
| <i>Varicellovirus</i> | HHV-3 | Varicella-zoster virus (VZV) | |
| <i>Betaherpesvirinae</i> | | | |
| <i>Cytomegalovirus</i> | HHV-5 | Cytomegalovirus (CMV) | Slow-growing, Cytomegalic, Latent in myeloid progenitor cell and leukocytes |
| <i>Roseolovirus</i> | HHV-6 HHV-7 | | Latent in monocyte and CD4 ⁺ T lymphocytes |
| <i>Gammapherpesvirinae</i> | | | |
| <i>Lymphocryptovirus</i> | HHV-4 | Epstein-Barr virus (EBV) | Lymphoproliferative, Latent in B lymphocytes |
| <i>Rhadinovirus</i> | HHV-8 | Kaposi's sarcoma-associated herpesvirus (KSHV) | |

HSV entry

HSV requires various molecules for entry into host cells. They interact with their specific molecules (receptors) successively. Firstly, HSV uses glycoprotein (g) B and/or gC, located on the envelope, to attach to the heparan sulfate proteoglycans (HSPG) which express on the membrane of target cell, called the attachment step. Although gC is the first glycoprotein that HSV uses to contact HSPG on the cell surface, gC-deficient HSV can use only gB for attachment (7). Alternatively, filopodia formation, actin-rich plasma-membrane protrusions, can increase the opportunity of HSV attachment (27). HSV surfing along surface of these filopodia by using their gB attach to HSPG cause actin remodeling (28). Oh *et al.* demonstrated that HSPG expression is increased on the filopodia while the expression gD receptor is located only at the cell surface (27). Moreover, filopodia formation is induced by the interaction of HSV and the cell. The chances of others HSV binding is increased after the first HSV particle binds (28). After HSV arrives at cell surface, it uses the gD to bind to the gD receptors on host cell surface (7). There are 3 kinds of gD receptors expressing in different cell types including Nectin-1 and 2, HVEM and 3-OS-HS.

Nectin-1 and Nectin-2

Nectin-1 and -2, members of the immunoglobulin superfamily, play role in cell adhesion. Nectin-1 plays a major role in gD receptor for HSV-1 attachment at epithelial cells, endothelial cells, neuronal cells and keratinocytes (29-31). Cell expressing Nectin-2 needs more HSV particles than Nectin-1 for infection (32). Nectin-2 is expressed in epithelial, endothelial and neuronal cells (31). The amino acid sequence of Nectin-1 is 30% different from Nectin-2. Nectin-1 or -2 can mediate HSV-2 entry but wide-type HSV-1 can interact with nectin-1 only (33).

Herpes virus entry mediator (HVEM)

HVEM or herpes virus entry protein A (HveA) is a tumor necrosis factor receptor superfamily (34, 35). This receptor is necessary for HSV entry in T

lymphocytes and many kinds of ocular epithelial cells. HVEM is expressed in many immune cells, e.g., natural killer (NK) cells, B and T lymphocytes, dendritic cells (DC) and myeloid cells (36). Moreover, HVEM is also found on fibroblasts, epithelial cells and endothelial cells (37). Natural ligands of HVEM is BTLA (B- and T-cell attenuator) (38). Another HVEM ligand is LIGHT, stands for "homologous to lymphotoxin, exhibits inducible expression and competes with HSV glycoprotein D for binding to herpesvirus entry mediator, a receptor expressed on T lymphocytes, which has an effect to regulate lymphocyte activation (39, 40). The efficiency of gD binding to Nectin-1 and HVEM is really different. Previous study found that the HSV entry in HVEM-transfected Chinese hamster ovary (CHO) cells is blocked by soluble Nectin-1 (41). HVEM also plays role in HSV latency and reactivation. Latency-associated transcript (LAT), HSV-1 gene transcript abundantly expressed throughout latency, enhances HVEM expression (but not other gD receptors) in HSV infected mouse ocular (42). Moreover, the amount of HSV-1 DNA in trigeminal ganglion (TG) from wide type (WT) mice which infected with LAT (+) HSV-1 is higher than those infected with LAT (-) HSV-1. Additionally, the number of HSV-1 latent genomes from HVEM knockout mice which infected with LAT (+) HSV-1 is lower than those infected with LAT (+) HSV-1. This indicates that LAT induces the over expression of HVEM leading to increase the amount of HSV-1 latency. This suggests that HSV-1 reactivation is also increased (43).

3-O-sulfated heparan sulfate (3-OS HS)

3-OS HS is polysaccharide which contains various modification of heparan sulfate (44). This gD receptor is an important receptor for human herpesviruses attachment except EBV (45). HS is modified by the 3-OST (3-O-Sulfotransferase) family to turn to 3-OS HS, modified at C3 position of glucosamine precursor, as a gD receptor (46-50). HSV-1 binds to 3-OS HS on primary culture of corneal fibroblast cell, lack of Nectin-1 expression and very low expression of HVEM, for entry (51). Multiple 3-OST isoform expressing zebrafish model can generate HSV-1 entry

receptor (52). Moreover, soluble 3-OS HS supports HSV-1 entry in CHO cells which lack of gD receptors (53). 3-OS HS not only induces HSV-1 entry but also cell-cell fusion (48, 53). 3-OS HS is expressed on some kinds of human tissue and cell line, less than other gD receptors. This gD receptor is found in liver, placenta, heart, kidney, pancreas and human epithelial cell (54).

After gD binds to one of its receptors, a conformational change of this glycoprotein's structure drives the recruitment of a fusion complex including gB, gH and gL. gB, a member of class III fusogen (55), binds to one of its receptors to initiate membrane fusion. There are 3 types of gB receptors including paired immunoglobulin-like receptor (PILR α), an inhibitory receptor found on macrophages, dendritic cells and monocytes (56), myelin-associated glycoprotein (MAG) which expresses on glial cells (57), and non-muscle myosin heavy chain-IIA (NMHC-IIA) on human tissue (7). Recent study investigated that $\alpha_v\beta_6$ - and $\alpha_v\beta_8$ -integrins are gH/gL receptors (58). HSV envelope fusions with the plasma membrane via pH-independent process requires gB, gD, gH and gL. This fusion complex leads HSV to merge their envelope with the lipid bilayer of host membrane and releases viral nucleocapsid and tegument proteins into the host cytoplasm (7) (Figure 2). In conclusion, cell to cell fusion after HSV-1 and HSV-2 entry is induced by gD, gB and gH/gL (59-61).

Alternatively, HSV can enter into the cell by endocytosis and phagocytosis-like uptake (28, 62). HSV binds to gD receptor which localizes in endosome for fusion with endosomal membrane (28). HSV-1 and HSV-2 can enter into HeLa cells and CHO cells expressing gD receptors by endocytosis with low pH-dependent (63). The phagocytosis-like uptake is induced by Rho GTPase activation and cytoskeleton rearrangement. The pathway that HSV uses for entry depends on cell types (64). HSV prefers fusion with plasma membrane to enter into Vero cells, human neurons, human foreskin fibroblasts and Hep-2 cells (65-67). On the other hand, HSV enters into retinal pigment epithelial cells, human conjunctival epithelial cells, human

epidermal keratinocytes and HeLa cells by endocytosis (62, 68) (Figure 2). In conclusion, gB, gD and gH/gL are essential for both HSV entry pathway (67, 69).

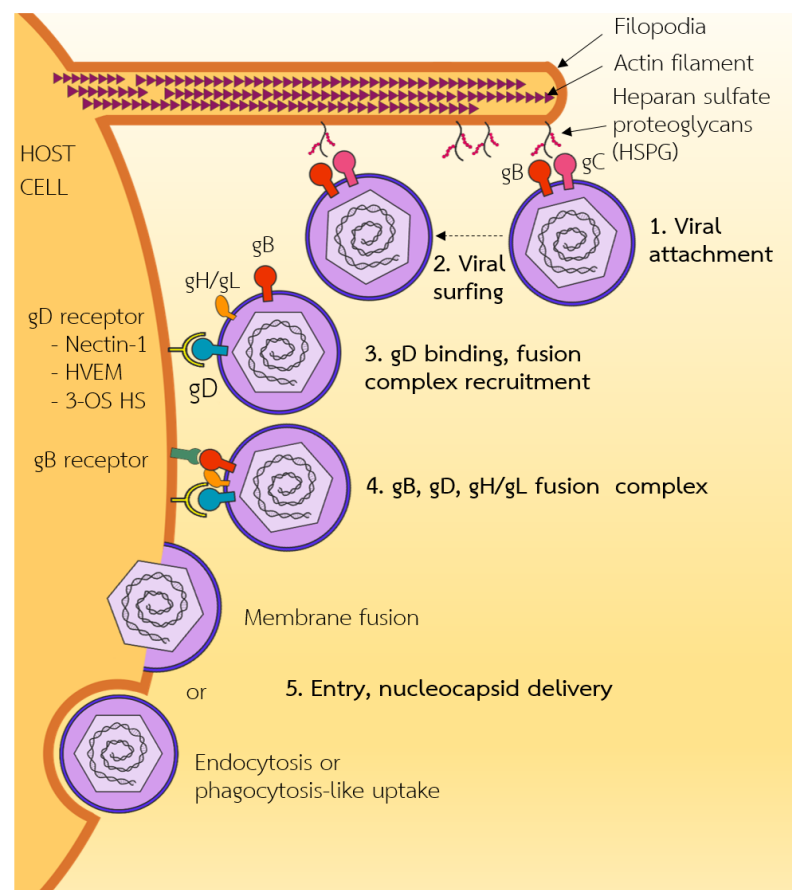


Figure 2. Herpes simplex virus (HSV) attachment and entry mechanism.

[1] HSV glycoprotein B and/or glycoprotein C bind to HSPG. [2] HSV surfs along filopodia to the cell surface. [3] The interaction of HSV glycoprotein D with one of their receptors (Nectin-1, HVEM and 3-OS HS) induces a conformational change. [4] The recruitment of a fusion complex including gB, gD and gH/gL is induced. [5] HSV enters into cells by fusion, endocytosis or phagocytosis-like uptake. (24)

HSV replication cycle

After HSV enters into the cell, HSV icosahedral capsid goes through cytoplasm to nuclear pore (6). Some tegument proteins, e.g., US11 and virion host shut-off protein (vhs), is digested while HSV transports through cytoplasm. Virion-specific protein (VP) 16, a tegument protein, and HSV capsid protein go to the nucleus (70). After uncoating step occurs, HSV DNA is released into the nucleus. After that, HSV transcription is started to produce various types of proteins, such as infected cell proteins (ICP) and VP (24). The HSV genes transcription requires host RNA polymerase II. Three groups of HSV genes expression are initiated like a cascade (6) (Figure 3).

First, immediate early (IE) genes are expressed, producing immediate early proteins (α -proteins), e.g. ICP4, ICP0, ICP27/UL54, ICP22/US1, and ICP47/US12 (24). These genes are expressed after 2-4 hours post-infection (hpi) by the activation of VP16 and several cellular proteins (6, 19). ICP4 is a regulatory protein for early and late protein productions (71). ICP0, usually working with ICP4, is an important protein to regulate virion production and latent infection (72). ICP27 is a phosphoprotein which is important for HSV transcriptional and post-transcriptional processes (73). Moreover, ICP27 plays role in proteins production switching from early to late proteins (74). ICP22 plays role in gene regulation as other proteins but is not essential for HSV growth (75). ICP47 is a protein that can inhibit antigen presentation process. Therefore, HSV infected cells are not destroyed by cytotoxic T cells (76).

Second, early (E) genes are expressed by the activation of ICP4, a α -protein. Early proteins (β -proteins), mostly related with HSV DNA replication, are produced, e.g. viral DNA-dependent-DNA polymerase (UL30), DNA binding protein (UL42, UL29 or ICP8), Origin-binding protein (OBP or UL9) and viral helicase/primase complex (UL5, UL8 and UL52). These genes are expressed at 4-8 hpi. If the E (β) proteins production are increased, IE (α) proteins are decreased. However, the expression of late (L) genes are initiated by E genes expression (6, 24). β -proteins are divided into 2

groups, $\beta 1$ and $\beta 2$ which produced by α -proteins activation (24). ICP8 is a single-stranded DNA binding protein (5, 77). To initiate HSV replication, OBP (UL19) binds to the origin of replication. Helicase activity of OBP is activated by ICP8 binding (78). ICP8 and OBP interaction induces a DNA destabilization at the origin of replication. Next, HSV double-stranded (ds) DNA are unwired by helicase-primase complex. After that, short RNA primers are synthesized. Lastly, leading and lagging strands are synthesized by DNA polymerase holoenzyme (79).

Third, late (L) genes are expressed by the activation of the viral DNA synthesis while E gene expression is decreasing (79). Most of L (γ) proteins are virus structural components (6). These group of proteins are transported to nucleus where capsid assembly occurs. HSV dsDNA are packed in the icosahedral capsid. The component of HSV capsid includes VP5 (UL19; Major capsid protein), VP23 (UL18), VP19c (UL38), VP26 (UL35), UL6 and UL25/UL17 (24).

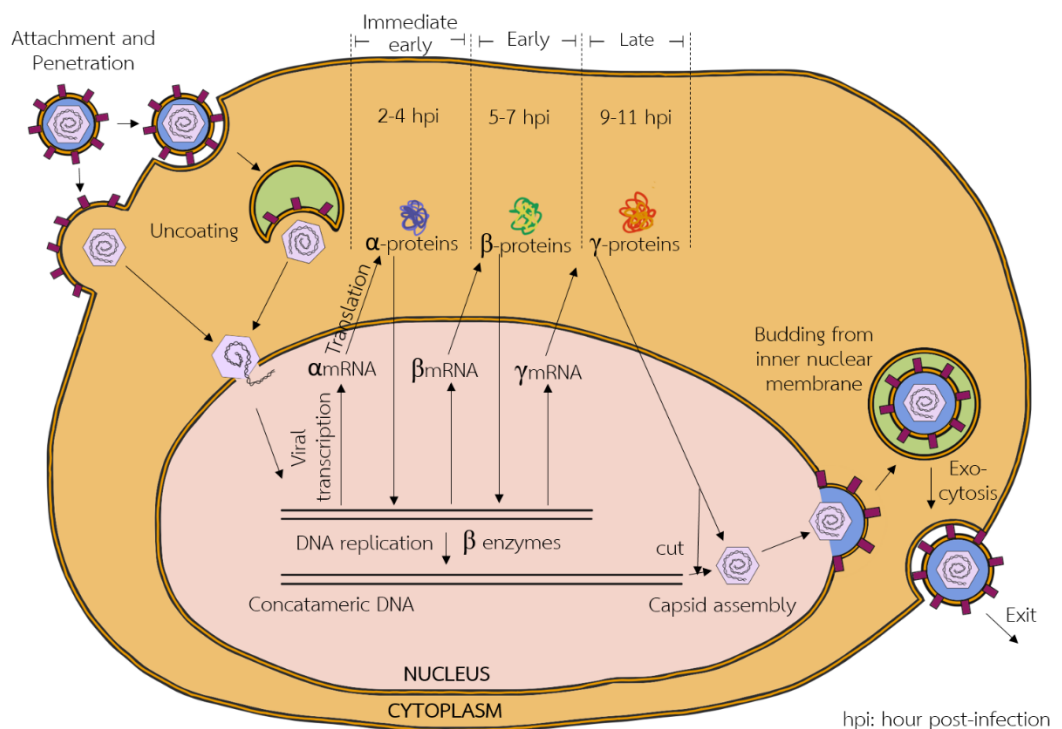


Figure 3. Herpes simplex virus replication cycle

(24)

Once the genome is packed into the capsid, the nucleocapsid goes through nuclear membrane to acquire the envelope. There are 2 main theories of HSV envelopment which are envelopment-deenvelopment-reenvelopment pathway and luminal pathway. First, envelopment-deenvelopment-reenvelopment pathway, HSV acquires primary envelope by budding through inner nuclear membrane, called envelopment. After that, the envelope of the virus fuses with outer nuclear membrane to exit into cytosol, called deenvelopment. Next, HSV nucleocapsid buds through trans-golgi network to acquire the envelope again, called reenvelopment. Another pathway is luminal pathway, HSV acquires envelope by budding through nuclear membrane and transports along the luminal pathway from inside out to the surface membrane. Finally, both pathways, HSV virion egresses the cell by directed exocytosis (5, 24) (Figure 4).

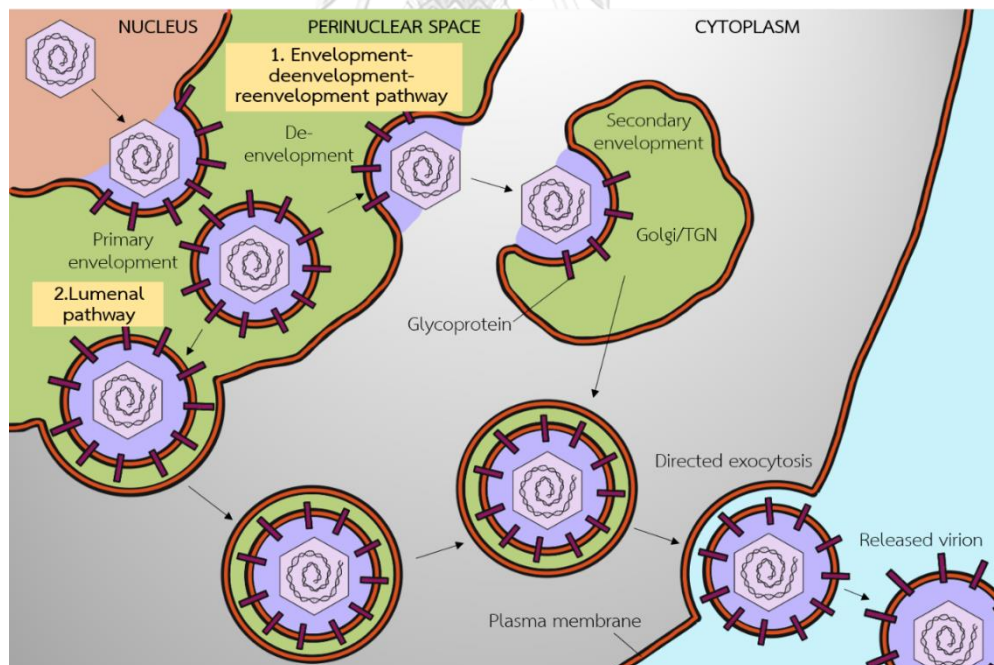


Figure 4. Envelopment and egression theories of herpes simplex virus (24)

HSV latency and reactivation

The first place where HSV-1 starts replication is the site of infection. After that, HSV-1 travels along an axon to establish latency stage at dorsal root ganglia, called the latent infection (80, 81). During this period, HSV-1 turns to non-infectious state and waits for reactivation (82). The fusion with neuronal membrane lets HSV enter into sensory neurons. HSV capsid transports through cell body to the nucleus, called retrograde movement (83). HSV DNA which is contained in capsid is released into the nucleus, latent infection is established. HSV IE genes are downregulated by the interaction of histone and heterochromatin with circular episomal form of HSV DNA while HSV reproductive genes are not expressed. Thus, HSV replication cycle is stopped (84-89). LAT (latency-associated transcripts) RNA coded from non-coding protein region, are overexpressed at latency stage (90, 91). LAT RNA downregulate the lytic gene expression, especially IE gene (89, 92), and inhibit apoptotic activity during HSV infection (93, 94). At this stage, no virus can be isolated at the site of lesions (6).

HSV is reactivated from latency by the activation of ICP0 (72, 95). HSV components assembly in the axon and release at the site of recurrent infection (96). Axonal injury, fever, physical or emotional stress and exposure to ultraviolet light can reactivate HSV from the latent stage. Many recurrences are asymptomatic, investigated only by viral shedding in secretions (6). In neonates or immunocompromised individuals, HSV can cause more severe and persistent lesions than immunocompetent hosts.

Filopodia formation

Filopodia are actin-rich structure that contain strongly bound horizontal actin bundles which are polymerized in this structure, called filamentous actin (F-actin) polymerization. In mammals, there are 6 actin genes (*Acta1*, *Acta2*, *Actc1*, *Actb*, *Actg1* and *Actg2*), each gene encodes one protein isoform including α_{skeletal} -actin, α_{smooth} -actin, α_{cardiac} -actin, β_{cyto} -actin, γ_{cyto} -actin and γ_{smooth} -actin, respectively. The amino acid sequences of these isoforms are more than 93% similarity (12). There are 2 basic types of actin which localize in various cells including globular or monomeric actin (G-actin) and linear polymer or filamentous actin (F-actin) (11). Both of them are essential for cell functions such as contraction of cells during cell division and filopodia formation (10, 14). The dimension of actin monomer are about 5.5 x 5.5 x 3 nm (97). F-actin, physiologically active form of actin, is obtained by the polymerization of G-actin monomers (12, 98). The F-actin polymerization process is divided into 3 steps including nucleation, elongation and steady state (98) (Figure 5). G-actin is bound by one molecule of ATP to maintain their native configuration. After G-actin interaction in a growing filament, the bound ATP is hydrolyzed rapidly and turned to ADP and inorganic phosphate (Pi). Because of the structural polarity of F-actin, the polymerization rates at both ends of filament are different. The fast-growing end is called barbed end (+) whereas the slow-growing end is called pointed end (-). The F-actin has a diameter about 8 to 10 nm and contains about 1,000 G-actin monomers along 1 μm length (97). The property of F-actin depends on the isoforms which mix in the filament (12). The polymerization and depolymerization rates of β_{cyto} -actin is faster than γ_{cyto} -actin. However, both isoforms can copolymerize together and the polymerization rates depend on β_{cyto} -actin and γ_{cyto} -actin ratio (99).

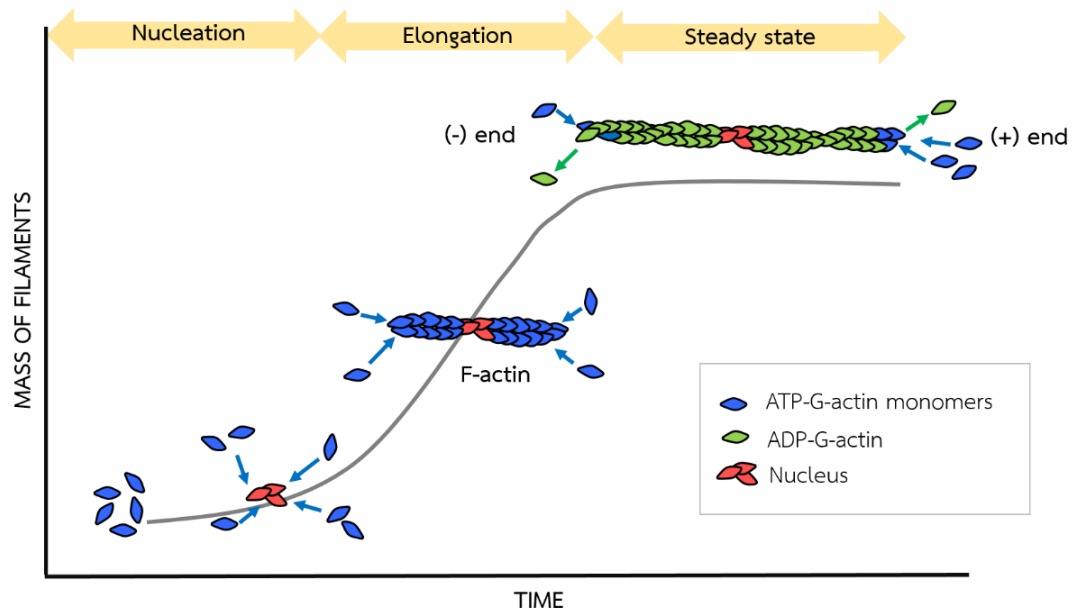


Figure 5. Three steps of the polymerization of actin.

First, nucleation phase, a stable complex of actin is obtained by gathering 3 molecules of ATP-G-actin monomers. Second, elongation phase, ATP-G-actin monomers are added at both end of filament, the pointed (-) end is rather stable than the barbed (+) end, quickly elongate. Third, steady state, after the polymerization process of G-actin to F-actin, the ATP-G-actin turns to be a stable ADP-F-actin by ATP hydrolyzing. This step G-actin molecules exchange with the filament ends without increasing the total F-actin amount. (Adapted and redrawn from <https://www.mechanobio.info/cytoskeleton-dynamics/what-is-the-cytoskeleton/what-are-actin-filaments/how-do-actin-filaments-grow/>)

There are 3 basic types of actin networks which are caused by actin polymerization including stress fibers, filopodia and lamellipodia (Figure 6). Stress fibers are networks which constructed by the arrangement of F-actin bundles with alternating polarity. These filaments are combined together via interactions between dimeric bundling protein α -actinin and the motor protein myosin II. Stress fibers play role in maintaining cell attachment to the platform and changing the cell

morphology. Filopodia formation consists of compact and strongly bound parallel F-actin bundles which polymerize along the cell membrane forming a spike-like structure (11). This spike plays an important role in the process of wound healing and extracellular matrix adhesion (100). Moreover, the function of this formation is a sensors of extracellular environment which contains various receptors for signaling, for example, cell adhesion molecules including integrins and cadherins. Lamellipodia consist of the actin networks which extremely branch near cell membrane. Emanation of these formation initiated by the activation of Rho GTPase (11). These proteins are regulated by GTP/GDP binding, GTP-bound is an active form whereas GDP-bound is an inactive form (101, 102). There are 3 extensive Rho family members involve in actin rearrangement including RhoA, Rac1 and Cdc42. Ras homolog gene family, member A (RhoA) plays role in gathering of F-actin to produce stress fibers. Ras-related C3 botulinum toxin substrate 1 (Rac1) is associated with lamellipodia and ruffling. Cell division control protein 42 (Cdc42) is essential for filopodia formation (11). Moreover, Rho GTPase is involved in phagocytosis uptake (102). Phagocytosis uptake requires receptors, e.g. Fc receptor (FcR), to mediate actin rearrangement and to transport actin to the site of stimulating particle (103).

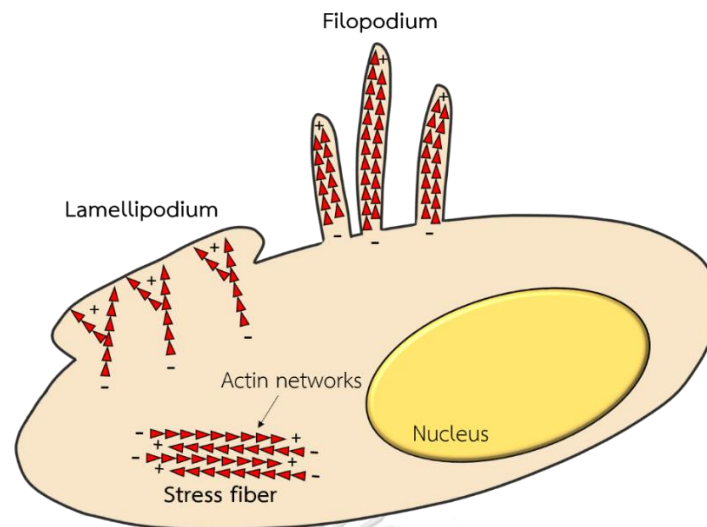


Figure 6. Filopodium, lamellipodium and stress fiber structure

(Adapted and redrawn from Roberts and Baines, 2011) (11)

To initiate filopodia formation, the cell requires Cdc42 to induce the complex of actin-related proteins-2/3 (ARP2/3), a seven-subunit protein complex which plays role in the regulation of the actin cytoskeleton, and actin filament. The components of filopodium are prepared by the interaction of myosin-X, diaphanous-related formin-2 (Dia2), enabled/vasodilator-stimulated phosphoprotein (ENA/VASP) with barbed ends of uncapped or formin-nucleated actin filament nearly the plasma membrane (Figure 7A). F-actin is gathering towards the cell membrane via the activity of myosin-X. The uncapped actin filament is a target of formin Dia2 and/or ENA/VASP which is essential for the actin elongation step. Next, plasma membrane is deformed by the interaction of IRSp53, scaffolding protein which involves in the plasma membrane deforming, with plasma membrane and actin filament (Figure 7B). Then, each actin bundle cross-links together by fascin and ENA/VASP protein to build filopodial actin filament bundle (Figure 7C) (14). The length of this formation is about 1 to 100 μm (104). Filopodia can also build on the lamellipodia as a thin fingers-like structure. However, the activities and interactions of key proteins in pathway depend on different organisms and type of cells.

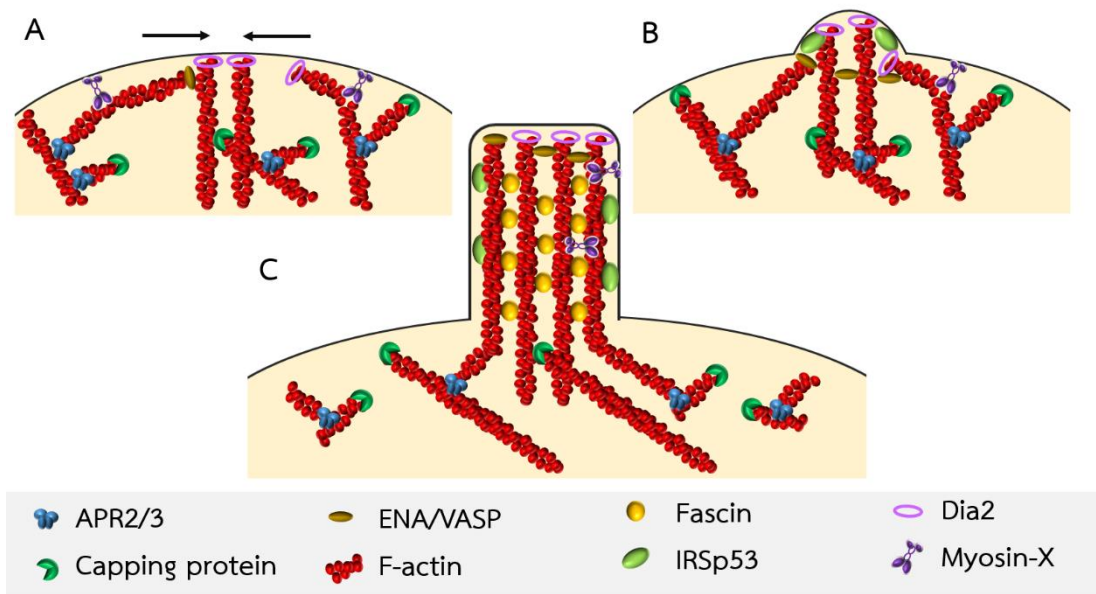


Figure 7. A model of filopodia formation
(Adapted and redrawn from Mattila et al., 2008) (14)

Another role of filopodia formation is supporting pathogens, especially virus, entry and spread. F-actin is remodeled along viral life cycle (entry, assembly and egress) by the activation of RhoA, Cdc42 and Rac1 (105). Filopodia formation is regulated by Cdc42 to induce ARP2/3 complex actin filaments (14, 104). Cdc42 is also activated by the interaction of HSV-1 and epithelial cells, lead to filopodia formation (Figure 8A-1). Oh *et al.* investigated that filopodia are induced in Vero cell after exposure with HSV-1 for 15 minutes. Filopodia formation and HSV-1 entry are decreased by Cdc42 down-regulation (27). Another Rho GTPase protein, Rac-1, is activated together with Cdc42 during HSV-1 infection in fibroblasts and epithelial cells (106). After filopodia induced via HSV-1 attachment, other HSV-1 particles bind to their receptor, HS, which express on filopodia and surf along these structures to go to cell surface (Figure 8A-2, 8B). At the early stage during HSV-1 infection, F-actin assembly rates is increased (104). Actin cytoskeleton rearrangements are not only promoted HSV-1 infection by filopodia formation, but also HSV-1 transport to the cell body and nucleus (107). Human immunodeficiency virus (HIV) and human

papillomavirus (HPV) can also surf along filopodia formation too (104). Sometimes filopodia is retracted after viral, such as HPV, binds on this structure to promote viral entry (108). Filopodia can be used as a marker for viral infection. The amount of this actin rich structures increase during HSV-1, CMV or HHV-8 infection (104). Moreover, virus can travel along filopodia to transport to another cell (Figure 8C). HSV gE, gI and/or gK are essential for cell-to-cell spread (109, 110). There are several advantages of viral spreading by cell-to-cell contact. The duration of viral spread by cell-to-cell spreading is faster than cell-free spreading. Another benefit is immune evasion due to the absence of viral antigens which present to the environment. This suggests that neutralizing antibodies cannot work because there are no free viruses outside the cell (111).

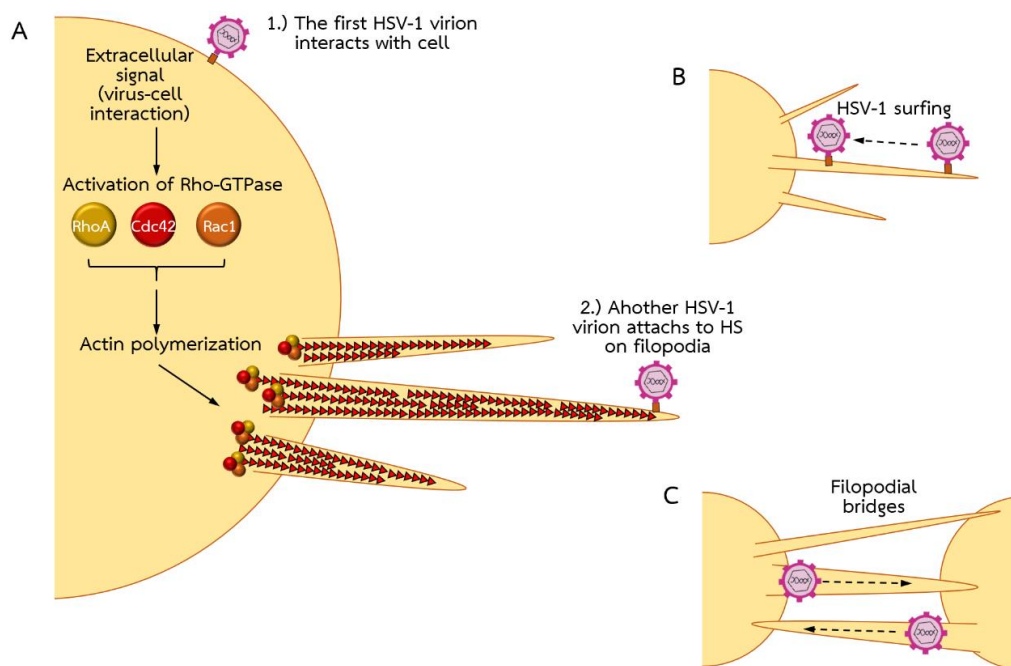


Figure 8. HSV-1 induces filopodia formation support viral entry and cell-to-cell spread.

(A) HSV-1 induces filopodia formation by the activation of Rho-GTPases, especially Cdc42, support other HSV-1 particles attachment. (B) HSV-1 surfs along the filopodia. (C) HSV-1 cell-to-cell spread through filopodial bridges. (Adapted and redrawn from Chang *et al.*, 2016) (104)

There are many types of small molecules which can interact with actin molecule to promote actin polymerization and depolymerization which may affect to the formation of filopodia. Phalloidins, a toxin of death cap mushroom (*Amanita phalloides*), can support F-actin polymerization by inhibition of actin filament disassembly. Jasplakinolides, a cytotoxin which is isolated from marine sponge *Jaspis splendens*, enhances actin filament assembly by stabilization of G-actin monomers (112). On the other hand, Latrunculin A and cytochalasin D are actin depolymerizing agents. Latrunculin A, toxin which produced by sponges (genus *Latrunculia* and *Negombata*), binds to G-actin monomers leading to inhibit their polymerization activity and promote F-actin disassembly (113, 114). Cytochalasin (cyto) D, a mycotoxin produced by *Helminthosporium* and other molds, binds to the barbed (+) end of F-actin to prevent G-actin assembly and promote F-actin disassembly at that site (Figure 9). Many previous studies use cyto D to block filopodia formation and reduce the infectivity of some viruses. Filopodia induction and viral surfing are completely inhibited via cyto D treated neurons (115). The amount of HSV-1 entry in Chinese hamster ovary (CHO) cells are decreased when the cells are treated with cyto D (116).

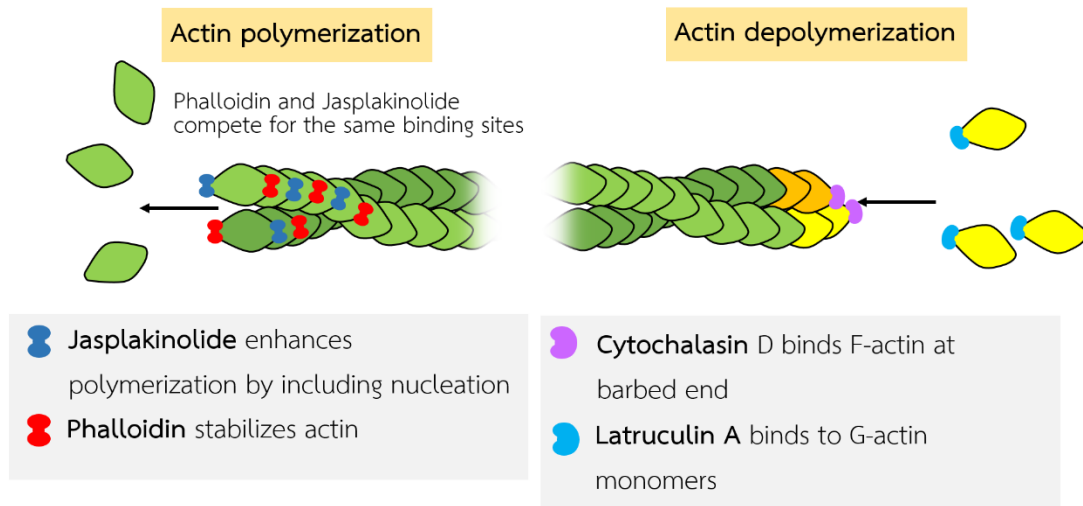


Figure 9. The actin polymerizing and depolymerizing molecules

(Adapted and redrawn from <https://www.mechanobio.info/cytoskeleton-dynamics/what-is-the-cytoskeleton/what-are-actin-filaments/what-factors-influence-actin-filament-length-and-treadmilling/>)

HSV infection

Transmission

HSV infects human only. This virus spreads by aerosol droplets or direct contact and must interact a broken skin or mucosal surface for infection. There is no carrier of this virus. HSV is transmitted via contact of a HSV infected patient and susceptible person (6). There are 2 main ways of HSV transmission including vertical and horizontal transmission. Vertical transmission is an infection of HSV from mother to the baby. This transmission is divided into 3 groups including postpartum, *In utero* and intrapartum. Postpartum transmission begins immediately after the birth of a child whereas intrapartum is a transmission that the viruses from mothers transmit to their babies while laboring. *In utero* transmission is an infection that acquires before

laboring. Horizontal transmission is delivered from person to another person by directly or sexually contact (24).

Epidemiology

HSV widely spreads around the world. There are no animal reservoirs for HSV. More than 70% of adults in many countries have anti-HSV-1 positive (6). HSV-1 infection is a main cause of HSV primary infection in new born babies which are transmitted by contact with their mothers or babysitters who are previously infected with HSV-1 (117, 118). The HSV-2 antibodies are hardly found before adolescence since this type of virus is transmitted mainly by sexual contact. The average age of HSV-1 infected individuals in under-developed countries is lower than developed countries (6). In 2004, there are 64.44% of HSV infected individuals in Thailand (24).

Pathology

The tissue tropism of HSV is skin, mucous membrane and epithelial cells. During HSV infection, the properties of the infected cells are changed, called cytopathic effect (CPE). The CPE of HSV infected cell is multinucleated giant cell (polykaryocyte), caused by changing of plasma membrane property to induce cell fusion (24). Because of cytolytic infection, HSV can induce infected cell to necrosis with the inflammatory response. There are several characteristic histopathologic changes in HSV infected cell including Cowdry type A intranuclear inclusion bodies production, ballooning of infected cell, margination of chromatin and induction of multinucleated giant cell (6).

Immunity to HSV infection

In newborns, anti-HSV antibodies which are transferred from mothers, maternal antibodies, are lost after 6 months of their life. The 6 months to 2 years old children are really susceptible to primary HSV infection. Anti-HSV-1 antibodies are usually found in early childhood but anti-HSV-2 antibodies are usually found in the period of adolescence (6).

During HSV infection, the viral proteins are detected by immune responses. To start with innate immune responses, the viral pathogen-associated molecular patterns (PAMPs) are detected by pattern recognition receptors (PRRs), e.g., Toll-like receptors (TLRs) and retinoic acid inducible gene-I (RIG-I)-like receptors (RLRs) to induce viral infected cells produce cytokine and interferon (IFN) type I, IFN- α and IFN- β , to inhibit viral replication by breaking down the viral mRNA and inhibition of IE proteins (24, 119). Moreover, IFN can also enhance the efficacy of macrophage and natural killer (NK) cell to destroy virus and infected cell (24). Neutrophils, macrophages, NK cells, monocytes and dendritic cells (DCs) play important role in innate immune response to HSV infection (119). After that, acquired (adaptive) immunity is initiated. Cytotoxic T cells (CD8⁺ T cells) and helper T cells (CD4⁺ T cells) play important roles in inhibition of HSV-1 infection and reactivation and force HSV-1 into latency (119). IFN- γ is secreted by CD8⁺ T cells while responding to viral infection. This IFN inhibits viral infection and promotes immune response via support antigen presentation on MHC class I (120, 121). During HSV-1 infection, CD8⁺ T cells interact with many antigen presenting cells, e.g., DCs and ganglionic cells. Another type of T cell which responds to HSV-1 infection is CD4⁺ T cell. CD4⁺ T cell is divided into 4 subpopulations including Th1, Th2, Th17 and induced regulatory T (iTreg) (119). Th2 can induce B cell to differentiate and produce HSV-1 specific antibody to neutralize HSV-1 infectivity, called neutralizing antibody, and collaborative with macrophage to destroy infected cell specifically, called antibody-dependent cell-mediated cytotoxicity (ADCC) (24). HSV antigens are not only induced cell mediated immune response (CMIR), but also humoral immune response (HIR). IgM is the first immunoglobulin that presents in a short period during HSV infection and followed by IgG and IgA which present continuously for a long time (122). However, HSV can evade immune responses by inhibition of apoptosis, inhibition of antibody-mediated complement activation, downregulation of MHC class I, and initiation of latency stage, etc. (123-125)

Diseases

HSV-1 and HSV-2 cause various clinical findings ranging from primary to recurrent infection. HSV that infects in a person without anti-HSV antibodies is called primary infection and HSV that is reactivated in a person who already had anti-HSV antibodies is called recurrent infection (6). During the first year of infection, HSV from 90% of infected individuals are reactivated once (122). HSV is ubiquitous pathogen which has various clinical manifestations for example oropharyngeal disease, primary herpetic gingivostomatitis, recurrent herpes labialis, genital herpes, herpetic whitlow, eczema herpeticum, herpes gladiatorum, herpes keratitis, herpes neonatorum and neurological disease (6, 24). Moreover, HSV can cause severe infection in immunocompromised hosts. HIV infected individuals and some kind of transplant recipients have more risk and severe HSV infections (6). New born babies also have a risk for severe HSV infection since they are not fully immune response (24).

Laboratory diagnosis

There are many methods which can detect HSV infection including HSV isolation, identification, antigen detection, antibodies detection and genome detection. HSV identification is divided into 2 kinds, i.e., specific and non-specific methods. Non-specific identification can rapidly detect by staining the scraping which acquires from the base of vesicle with Giemsa or Wright stain, called Tzanck test. The present of multinucleated giant cells refers to either HSV-1, HSV-2 or VZV infections. Specific identification can detect by staining samples with HSV-1 or -2 specific antibodies conjugated with fluorescence or enzyme, called immunofluorescence (IF) or immunoperoxidase (IP) assay, respectively. Enzyme-linked immunosorbent (ELISA) assay can also be used to detect HSV specific antigens. Another method is HSV specific antibodies detection, also known as serological test. HSV specific IgM, IgG and IgA can be detected by ELISA. Polymerase chain reaction (PCR) can be used to detect HSV DNA in many types of specimens. Because of high specificity and

sensitivity, this assay is a standard assay for specific diagnosis of HSV infection in nervous system (6, 24, 122).

HSV isolation by cell culture is usually used as routine diagnostic method (122). Due to the fast replication period (about 13-18 hours per 1 replication cycle), HSV is easy to isolate in many types of cell culture, e.g. MRC-5, WI-38, HeLa, Hep-2 and Vero cell (24). Moreover, another viral culture based method which can determine viral concentration is plaque titration assay (126). This method performs by growing the cells, e.g. Vero cells, to be a monolayer following by viral inoculation of various concentrations. Because of semi-solid medium condition, the virus from viral-infected monolayer cells cannot move far from each infected cell. The new progeny virions infect other cells around the infected cell by cell-to-cell spread. The infected cells are then float out of the surface. Finally, the cells are stained with dye which can stain only living cells and the death infected cell are removed out. The clear area is observed as a plaque. This method measures the production of virus from samples as plaque forming unit per milliliters (PFU/mL).

Activation of T lymphocytes

T lymphocytes are involved in regulation of immune response and in cell-mediated immunity (127). T lymphocytes recognize antigens and are activated to perform effective functions which response to antigen, e.g. microorganisms. Naïve T lymphocytes arrive to secondary lymphoid organs, where they interact with antigen presenting cells (APC) and thus become activated. This activation process requires 3 signals. First, interaction of MHC molecules, in the form of peptide-MHC complexes, on APC, e.g. dendritic cells, and T cell receptor (TCR). Second, APCs are induced to express costimulatory molecules, e.g. B7 proteins. These molecules interact with costimulatory receptors, CD28 molecules, which express on the T cell to provide second signals to naïve T cells. Third, the cytokine, interleukin-2 (IL-2), drives

autocrine signals to activate T lymphocytes by interacting with its receptors on T cell. Activated T cells are differentiated to effector or memory cells (128). T lymphocytes activation can be occurred in vitro via interaction with nonspecific manner by lectins, for instance, phytohemagglutinin (PHA), pokeweed mitogen (PWM) and concanavalin A (Con A), and can also be mimicked via the interaction of TCR and co-stimulatory receptors with specific antibodies, e.g. anti-CD3 and anti-CD28 antibodies (129, 130).

There are several molecules that express on the surface of activated T lymphocytes, which discriminates from naïve T lymphocytes such as adhesion molecules, receptors, co-stimulatory molecules, chemokine receptors and MHC class II molecules. Examples of receptor which upregulated on activated T lymphocytes is CD25 (interleukin-2 receptor) and CD69 (type II C-lectin receptor) (130). CD69 is an early molecules which initiates to express in a few hours after TCR ligation then expression is lost after 48-72 hours but CD25 is up regulated a bit later than CD69. CD69 is detected within 1 hour of activation with anti-CD3/CD28 antibodies (129). Examples of co-stimulatory molecules which observed to be an activation marker is members of the IgG superfamily, including CD28 (T cell-specific surface glycoprotein) and CD279 (programmed cell death 1; PD-1), members of the TNF-TNF-receptor super family, including CD134 (Tumor necrosis factor receptor superfamily member 4; OX40), CD137 (Tumor necrosis factor receptor superfamily member 94-1BB; ILA) and CD154 (CD40 ligand) (130). MHC molecules which also observed to be an activation makers include HLA-DP, HLA-DQ and HLA-DR. These molecules are upregulated only after 3-5 days after activation (130, 131). Moreover, some activation marker is selected to use for observation of disease progression. For example, in HIV patients, the expression of CD38, cyclic ADP ribose hydrolase, is utilized as a predictor of HIV-1 induced disease progression (132).

HSV replication in T lymphocyte

Although the common tissue tropism of HSV is fibroblast, epithelial and mucosal cells, HSV can also infect in T lymphocytes (15, 16, 133, 134). Previous study shows that HSV can replicate in Jurkat cell, an immortalized line of human T lymphocyte cells, but its production from T lymphocytes is lower than from epithelial cells, Vero and HEp-2 cells (16). HSV-1 and HSV-2 can evade immune responses by the induction of apoptosis in HSV-infected T lymphocytes via caspase-dependent pathway (135). The number of HSV-1 infected T lymphocytes increase when the cells are activated by phytohemagglutinin (PHA), a mitogen inducing activation and proliferation of lymphocytes. HSV replication in non-activated T lymphocytes are delayed at least 2 hours and the production of HSV-1 from T lymphocytes is higher than HSV-2 (16). HVEA, a HSV gD receptor which presents on T lymphocytes, mRNA is over expressed after PHA activation but HVEA mRNA expression cannot detect in non-activated T lymphocytes (17). Another study investigates that HSV-1 production from anti-CD3-activated T lymphocytes are higher than non-activated cells (18). These results suggest that HSV-1 can be spread in blood through T lymphocytes to be a viremia. Activating T lymphocytes with PHA or anti-CD3 antibody may mimic *in vivo* situation, such as HSV coinfection in a patient who already has a latent stage by other organisms. In HIV infection, T cell activation is induced (136, 137). Since their T cells are already activated, HSV-1 production in T cells obtained from HIV-infected individuals is significantly higher than those from healthy donors (138). Moreover, both CD4⁺ and CD8⁺ T lymphocytes are shown to be susceptible for HSV-1 replication (138). In addition, one of the mechanisms that might support HSV-1 infection in activated T lymphocytes is filopodia formation (18). There are many previous studies investigate that the formation of filopodia plays an important role in HSV-1 infection in various cell types, e.g., Vero (monkey kidney epithelial cells), HeLa (human cervical cancer cells), RPE (human Retinal pigment epithelium), ZF-3-OST-3 (zebrafish cells), Differentiated P19 (neural cells from mice),

HCjE (human conjunctival epithelial cells) and CHO-K1 cells (Chinese hamster ovary cells) (27, 115, 116, 139-142). Actin cytoskeleton rearrangement plays a role in formation of filopodia for HSV surfing, HSV entry and HSV production (115, 116, 139, 141). However, the role of actin in filopodia formation of activated T lymphocytes for HSV-1 entry is under investigated. Therefore, aim of this study is to investigate whether HSV-1 can induce filopodia formation in activated T lymphocytes to support HSV-1 entry.



CHAPTER IV

MATERIALS AND METHODS

Part I: Cell cultures and viral stock preparation

1. Cell cultures

1.1 Jurkat cell

Jurkat cells, an immortalized human T lymphocyte cell line isolated from the peripheral blood of a boy suffering from leukemia since 1976, (kindly provided by Professor Tanapat Palaga, Ph.D., Department of Microbiology, Faculty of Sciences, Chulalongkorn University) were cultured in growth medium, RPMI 1640 (Gibco, USA) (see Appendix B). The cells were sub-cultured every 3-4 days at a split-ratio of 1:5 and grown under 5% CO₂ at 37°C.

1.2 Vero cell

Vero cells, a continuous epithelial cell line isolated from African green monkey kidney cells (*Cercopithecus aethiops*) since 1967, were cultured in growth medium (Medium 199; Gibco, USA) (see Appendix B). The cells were sub-cultured every 2-3 days. When the cell monolayer was observed, the medium was discarded. Then, the cell monolayer was washed with 1x phosphate buffer saline (PBS; see Appendix B) twice. Next, pre-warmed 1x trypsin (see Appendix B) was added and incubated at 37°C for 2-3 minutes or until the round shape cell was observed. After that, trypsin was discarded and the cell culture flask was gently knocked to detach the cells. Then, the cells were resuspended with M199 growth medium (see Appendix B) and sub-cultured at a split-ratio of 1:3 and grown at 37°C.

1.3 Peripheral Blood Mononuclear Cells (PBMC)

PBMCs from single donor were separated by density-gradient centrifugation method. Briefly, the whole blood was mixed with the equal volume of RPMI 1640 growth medium. Then, the mixture was overlaid on ficoll-hypaque and spun at 1,500 rpm 25°C for 30 minutes. After that, PBMCs were collected and washed twice with

the equal volume of RPMI 1640 growth medium. The PBMCs were harvested by suspending in RPMI 1640 growth medium.

2. Virus stock preparation

Vero cell monolayer was infected with HSV-1 (KOS) at multiplicity of infection (MOI) of 0.01. After viral inoculation, the cells were incubated for 1 hour at 37°C (Rocking every 15 minutes) and washed once with 1xPBS. Next, maintenance medium (Medium 199 supplemented with 2% FBS; see Appendix B) was added and incubated at 37°C until the CPE was observed more than 75%. The cells were frozen at -80°C and thawed at 37°C for 3 times and centrifuged at 1,500 rpm, 4°C for 5 minutes. The virus in supernatant was aliquot and kept at -70°C until used. The titer of HSV-1 (KOS) stock was determined by viral plaque assay.

3. Viral plaque assay

The stock seed HSV-1 was diluted (10-fold serial dilutions) and 50 µl of the diluted HSV-1 were added to 96-well plate (Thermo Scientific, China) in quadruplicate. Next, 50 µL of Vero cells (3×10^4 cells/well) were added to each well. The plate was incubated at 37°C for 3 hours. After that, 100 µL of overlay medium with 0.8% gum tragacanth in M199 growth medium (see Appendix B) were added and incubated at 37°C for 3-4 days, the plaque can be observed under inverted light microscopy. Then, the cultured supernatant was removed and replaced by 100 µL 1% crystal violet solution (see Appendix B). After 45 minutes later, the plate was washed with running tap-water and air-dried at room temperature. The number of plaques was counted. Finally, the viral titers were calculated (Plaque forming units per milliliter; PFU/mL).

$$\text{PFU/mL} = \frac{\text{Number of plaques}}{\text{Dilution} \times \text{Volume of HSV inoculation per well (mL)}}$$

PART II: T cell activation

1. T cell activation

1.1 Dynabeads preparation

Dynabeads® Human T-Activator CD3/CD28 (Invitrogen, USA) were mixed in the vial by vortex up to 30 seconds and transferred the expected volume to a new tube. The equal volume (at least 1 mL) of washing buffer (0.1% bovine serum albumin (BSA; Sigma, USA), 2 mM EDTA in 1x PBS, pH 7.4; see Appendix B) was added and mixed by vortex for 5 seconds. Then, the tube was placed on a DynaMag™-2 magnetic particle concentrator (Invitrogen, Norway) for 1 minute and supernatant was discarded. Finally, the tube was removed from magnetic particle concentrator and the residue was resuspended with the same volume of 10% RPMI equal to the initial volume of Dynabeads® at the beginning.

1.2 Activation process

Activated Jurkat cells were achieved by using 10^6 of 24 hours pre-grown Jurkat cells co-incubated with 25 μ L of pre-washed Dynabeads® Human T-Activator CD3/CD28 (bead-to-cell ratio of 1:1) for 72 hours (or indicated time points) in RPMI 1640 medium supplemented with 10% FBS, 100 units/mL penicillin, 100 μ g/mL of streptomycin and 0.01 M HEPES. The cells were growth in 5% CO₂ at 37°C (18).

1.3 Study of activated Jurkat cell growth

Jurkat cells (5×10^5 cells/mL) were activated by Dynabeads and the number of viable cells were counted on hemocytometer (Spencer, USA) under microscopy at 24, 48, 72 and 96 hours by staining with trypan blue (Invitrogen, USA). The non-activated Jurkat cells (negative control) were performed similarly to the activated Jurkat cells.

2. Flow cytometry

2.1 Characterization of Jurkat cell phenotype

The property of Jurkat cell was characterized. The cells were centrifuged at 500 x g for 2 minutes and the medium was discarded. Next, the cell pellet was

washed with 500 μ L 1x PBS (centrifugation at 500 x g for 2 minutes) and resuspended with 100 μ L 1x PBS. Then, the cells were stained with PE/Cy7 conjugated anti-human CD3 antibody, brilliant violet 421 conjugated anti-human CD8 antibody and FITC conjugated anti-human CD4 antibody (Biolegend, USA) for 30 minutes at 4°C. After that, the cells were washed with 500 μ L 1x PBS (centrifugation at 500 x g for 2 minutes) and resuspended with 300 μ L 1x PBS. Next, the cell properties were analyzed by flow cytometer (BD FACSAriaII, BD Biosciences) and FlowJo® v10.3 software. The Jurkat cell phenotyping analysis was kindly performed by Ms. Fern Baedyananda, Ph.D. student, Biomedical Sciences and Biotechnology, Faculty of Medicine, Chulalongkorn University, and Mr. Chaichontat Sriworarat, research scientist at Faculty of Medicine, Chulalongkorn University.

2.2 Detection of activation markers on activated T lymphocytes

After 72 hours activation (or indicated time points), the activated Jurkat cells were determined for the activation phenotype. The magnetic beads (Dynabeads® Human T-Activator CD3/CD28) were separated from the solution by DynaMag™-2 magnetic particle concentrator. The cells were washed with 1x PBS following the methods which were described above and were stained with Pacific blue™ mouse anti-Human CD3 Clone: UCHT1 following by one of several anti-activation marker antibodies including PE/Cy5 conjugated anti-human CD38, PE conjugated anti-human CD69 or PE conjugated anti-human CD137 for 30 minutes at 4°C. After that, the cells were washed with 500 μ L 1x PBS (centrifugation at 500 x g for 2 minutes) and resuspended with 300 μ L 1x PBS. The cell properties were analyzed by flow cytometer (BD FACSAriaII, BD Biosciences) and FlowJo® v10.3 software. The non-activated Jurkat cells were used as negative control. PBMC (unstimulated and post-stimulated) from a single donor were used as control for activation process. The activation marker analysis was kindly performed by Ms. Prathanporn Kaewpreedee, Ph.D. student, Medical Microbiology, Graduate school, Chulalongkorn University, and Mr. Chaichontat Sriworarat, research scientist at Faculty of Medicine, Chulalongkorn

University. The mean fluorescence intensity (MFI) were measured and the percentage of increased fluorescence intensity was calculated.

$$\text{Increased fluorescence intensity (\%)} = \left[\frac{\text{Intensity from experiment}}{\text{Intensity from control}} \times 100 \right] - 100$$

PART III: β -actin expression

1. Real-time polymerase chain reaction

To investigate the expression of β -actin mRNA in HSV-1 infected activated T lymphocytes, one day pre-cultured Jurkat cells were activated by co-cultured with Dynabeads[®] Human T-Activator CD3/CD28 for 72 hours. Activated Jurkat cells were washed with 1x PBS (centrifugation at 1,500 rpm, 4 °C for 5 minutes). The 1.5×10^6 activated Jurkat cells suspended in 1 mL of 2% RPMI 1640 medium (maintenance medium) were plated in 24 well-plate (Nunc, China) following by HSV-1 inoculation at MOI of 10 and incubated at 37°C for 30 minutes. Next, the samples were collected for RNA extraction. Activated Jurkat cells without HSV-1 inoculation, non-activated Jurkat cells without HSV-1 inoculation and non-activated with HSV-1 inoculation (30 minutes) were used as control.

1.1 RNA extraction

RNA extraction was performed by using NucleoSpin RNA plus (MACHEREY-NAGEL, Germany). Cells of each sample were centrifuged at 1,500 rpm, 4°C for 5 minutes. Cell pellet was resuspended with 350 μ L Buffer LBP by pipetting up and down. The sample was transferred to NucleoSpin[®] gDNA Removal Column and centrifuged at 11,000 x g for 30 seconds. Next, 100 μ L Binding Solution (BS) was added to the flow-through and mixed by pipetting up and down for several times. The whole lysate was transferred to the Nucleospin[®] RNA Plus Column and centrifuged at 11,000 x g for 15 seconds. Then, 200 μ L Buffer WB1 was added and centrifuged at 11,000 x g for 15 seconds. The flow-through was discarded. Next, 600

μL Buffer WB2 was added to the column and centrifuged at $11,000 \times g$ for 15 seconds. The flow-through was again discarded. $250 \mu\text{L}$ Buffer WB2 was added to the column and centrifuged at $11,000 \times g$ for 2 minutes to dry the membrane completely. The column was placed into a new 1.5 mL nuclease-free Collection Tube. Finally, $15 \mu\text{L}$ RNase-free H_2O was added to the column and centrifuged at $11,000 \times g$ for 1 minute (twice). The RNA sample was stored at -80°C until used.

1.2 First-stranded cDNA synthesis

RNA sample was synthesized first-stranded by using SuperScript™ III Reverse Transcriptase (Invitrogen, USA). To prepare a cDNA synthesis master mix for 1x reaction, $1 \mu\text{L}$ of $100 \mu\text{M}$ oligo (dt)₁₈ primer, $1 \mu\text{L}$ of 10mM dNTP Mix and $10 \mu\text{L}$ distilled water were added into 0.2 mL tube. After that, $1 \mu\text{L}$ of RNA sample was added and mixed gently. The mixture was heated at 65°C for 5 minutes and incubated on ice for 1 minute. The mixture of $4 \mu\text{L}$ 5X First-Strand Buffer, $1 \mu\text{L}$ RNaseOUT™ Recombinant RNase Inhibitor and $1 \mu\text{L}$ of 200 units/ μL Superscript™ III RT were added and mixed by pipetting gently. The mixture was heated at 50°C for 60 minutes followed by 70°C for 15 minutes. The cDNA sample was then stored at -20°C until used.

1.3 RT-qPCR

To detect β -actin mRNA expression, the cDNA was amplified by real-time polymerase chain reaction (PCR) using Luna® Universal qPCR Master Mix (New England Biolabs, UK). To prepare a master mix for 1x reaction, $10 \mu\text{L}$ of 1x Luna® Universal qPCR Master Mix, $0.5 \mu\text{L}$ of $10 \mu\text{M}$ forward primer, $0.5 \mu\text{L}$ of $10 \mu\text{M}$ reverse primer (see Table 2) and $6.5 \mu\text{L}$ nuclease-free water were mixed in a Vari-Strip (4titude, UK). Next, $2.5 \mu\text{L}$ template (cDNA) was added to the mixture. The strip was spun briefly to collect liquid and remove bubbles. The real-time PCR was started by heating the reaction mixture at 95°C for 60 seconds (initial denaturation). After that, the sample was denatured at 95°C for 15 seconds, and extended at 60°C for 30 seconds, 45 cycles. These reactions were performed by Step One Plus Real-Time PCR

System (Applied Biosystems, USA) and Step One Plus software. Glyceraldehyde-3-phosphate dehydrogenase (GAPDH) gene was used as a housekeeping gene.

Table 2. The specific primers for RT-qPCR

| Target gene | Primer | Sequence | Product length (bp) | Reference |
|-------------|---------|----------------------------|---------------------|-----------|
| β-actin | Forward | 5'-AGAGCTACGAGCTGCCTGAC-3' | 579 | (143) |
| | Reverse | 5'-CACCTTCACCGTTCCAGTTT-3' | | |
| GAPDH | Forward | 5'-GAGTCAACGGATTTGGTCGT-3' | 238 | (143) |
| | Reverse | 5'-TTGATTTTGGAGGGATCTCG-3' | | |

1.4 Double delta Ct analysis

To calculate the level of β-actin mRNA expression, Ct values from RT-qPCR experiment were calculated by following formula. Non-activated Jurkat cell without HSV-1 was used as control compared with activated Jurkat cell without HSV-1, activated Jurkat cell with HSV-1 (30 minutes) and non-activated Jurkat cell with HSV-1 (30 minutes).

$$\text{Gene expression} = 2^{-(\Delta\Delta\text{CT})} = 2^{-(\Delta\text{CTE}-\Delta\text{CTC})}$$

ΔCTE = ΔCT value from experiments

ΔCTC = ΔCT value from control (non-activated Jurkat cell without HSV-1)

2. Cytochalasin D treatment

2.1 Viable cell count

Cytochalasin (cyto) D, an actin depolymerizing agent (Cyto D; Sigma, USA) was used. To determine the suitable cyto D concentration to be used in this study, viable cell count and the cell cytotoxicity assay were performed. One mL of Jurkat cells (2×10^6 cells/well) were plated in 24 well-plate. Various cyto D (dissolved in DMSO)

concentrations (0, 0.5, 1, 2.5, 5 and 10 $\mu\text{g/mL}$) were added into each well. The cell culture plate was incubated at 37°C for 1 hour. The number of living cells after cyto D treatment was counted. Ten μL from each well was stained with 10 μL trypan blue (Invitrogen, USA) and the cells were counted on hemocytometer (Spencer, USA) under microscopy for 4 areas (16 corner squares = 1 area). The living cells (unstained) were counted and calculated by following formula (the dead cell is stained blue).

$$\text{Live cell count (cells/mL)} = \frac{\text{Area}_1 + \text{Area}_2 + \text{Area}_3 + \text{Area}_4}{4} \times 10^4 \times \text{dilution factor}$$

2.2 Cytotoxicity assay (Tetra Z assay)

Besides cell viability count, a cell metabolic assay (Tetra Z assay) was used. The principle is based on if the cells were not damaged by cyto D, electrons were produced by cellular mechanism and transformed the tetrazolium salt (Tetra Z reagent) into a colored product, formazan. The Jurkat cells were treated with cyto D for 1 hour similar to previous experiment. Ten μL of cyto D treated Jurkat cells were then transferred into 96 well-plate (2×10^4 cells/well) and mixed with 90 μL of growth medium RPMI 1640. To perform cytotoxicity assay, Tetra ZTM (Biolegend, USA) was added to each well (10 μL /well) and incubated at 37°C for 2 hours. The mixture was measured at the absorbance 450 nm using a microplate reader (PerkinElmer, USA). Survival rate (%) was calculated by following formula. This experiment was done in triplication.

$$\text{Survival rate (\%)} = \frac{\text{OD}_{\text{Sample}} - \text{OD}_{\text{Background}}}{\text{OD}_{\text{Control}} - \text{OD}_{\text{Background}}} \times 100\%$$

$\text{OD}_{\text{Sample}}$ = OD_{450} from each sample

$\text{OD}_{\text{Background}}$ = OD_{450} from 10% RPMI 1640 medium + Tetra Z (Blank)

$\text{OD}_{\text{Control}}$ = OD_{450} from 100% viability (untreated cells)

3. Actin polymerization

To determine whether cyto D affect actin polymerization, 1.5×10^6 cells/mL activated Jurkat cells suspended in 1 mL of maintenance RPMI 1640 medium (RPMI 1640 supplemented with 2% FBS) were plated in 24 well-plate. Next, the cells were pre-incubated with cyto D at concentrations of 0, 2.5 and 5 $\mu\text{g}/\text{mL}$ at 37°C for 1 hour before HSV-1 at MOI of 10 was added to 1.5×10^6 of cyto D treated activated and non-activated Jurkat cell. The cells were incubated at 37°C for 30 minutes, then collected by centrifugation at 1,500 rpm, 4°C for 5 minutes. The supernatant was discarded. Seventy-five μL of Lysis M (See appendix B; Roche, Germany) was added to each sample and resuspended for several times. After that, the cells were incubated for 5 minutes at room temperature. Finally, the cells were centrifuged at $14,000 \times g$ for 5 minutes and protein samples were collected by transfer the supernatant to a new tube. Both activated and non-activated Jurkat cells with and without cyto D treatment were also performed and used as controls. The protein samples were stored at -20°C until used.

3.1 SDS-PAGE

5 μL of protein sample (equal to 1×10^5 cells) was mixed with 5 μL SDS loading buffer (see Appendix B) and heated at 95°C for 5 minutes. After that, 10 μL of the mixture was loaded onto polyacrylamide gel (4% stacking gel and 10% resolving gel; see Appendix B) and separated by using Mini-PROTEAN[®] Tetra system (BIO-RAD, USA) in 1x Tris/Glycine/SDS Buffer (BIO-RAD; see Appendix B) at 70 V for stacking gel and 135 V for resolving gel.

3.2 Western blot

After SDS-PAGE process, all separated proteins in gel were transferred to Nitrocellulose membrane (BioRad, USA) which was pre-soaked in blotting buffer for 5 minutes (see Appendix B) by TRANS-BLOT[®] SD SEMI-DRY TRANSFER CELL (BioRad, USA) at 16 V for 45 minutes. After that, the membrane was blocked by 3% Bovine serum albumin (BSA; Sigma, USA) in 0.05% Tween-Tris-buffered saline (TTBS) (Life

science, US) (see Appendix B) for 1 hour. The blocked membrane was washed by TTBS for 3 times. Then, the membrane was incubated with 1:1,000 primary antibody, mouse anti-beta-actin antibodies (Santa cruz biotechnology, USA) diluted in 1% BSA in TTBS at 4°C overnight. Next, the membrane was washed by TTBS for 3 times and incubated with 1:15,000 secondary antibody, goat polyclonal antibody to mouse IgG conjugated with horseradish peroxidase (HRP) (Abcam, USA) diluted in 1% BSA in TTBS for 1 hour. The membrane was washed again with TTBS for 3 times. The target band was developed by SuperSignal[®] West Femto Maximum Sensitivity Substrate (Thermo Scientific, USA) and detected by C-DiGit Blot Scanner (LI-COR, USA).

3.3 Re-probing

To quantify the amount of β -actin protein, GAPDH was used as comparative control. After detecting β -actin protein, the membrane was re-probed. The membrane was washed twice with removal buffer (see Appendix B) for 5 minutes at room temperature. The membrane was washed with 1x PBS for 10 minutes and washed again with 1x PBS for 5 minutes at room temperature. Next, the membrane was washed twice by TTBS for 5 minutes each. The re-probed membrane was started from blocking step followed by mouse anti-GAPDH antibodies (Santa cruz biotechnology, USA) as primary antibody). The rest was performed the same as detecting β -actin protein.

3.4 Protein band intensity analysis

The protein band intensities were quantified by Image J software. The band intensities represented the amount of protein expression. The β -actin expression was calculated by using the relative ratio of β -actin and GAPDH intensities.

PART IV: Filopodia formation

1. Detection of GTPase of the Rho family (Cdc42, RhoA, Rac1) by Western blot

To investigate the role of Rho GTPase family in filopodia formation during HSV-1 infection, HSV-1 at MOI of 10 were incubated with 1×10^6 activated or non-activated Jurkat cells for 10 minutes at 37°C. Each sample was centrifuged at 1,500 rpm, 4°C for 5 minutes and the supernatant was discarded. Twenty μL SDS loading buffer and 20 μL lysis M were added to the pellet and extremely mixed by vortex. Whole cell lysate was achieved by heating the mixture at 95°C for 5 minutes. Then, all amount of mixture was spun briefly and loaded onto 12.5% polyacrylamide gel and performed the SDS-PAGE and Western blot as already described above. The transferred nitrocellulose membrane was immunoblotted with primary antibodies either mouse anti-Cdc 42 or RhoA or Rac1 antibodies (Santa cruz biotechnology, USA) (Table 3). GAPDH was used as comparative control. Activated and non-activated Jurkat cells without HSV-1 were also used as controls.

Table 3. The specific antibodies for Western blot

| Target | Dilution | Expected protein size (kDa) |
|--------------|----------|-----------------------------|
| Rho A (26C4) | 1:200 | 24 |
| Cdc42 (B-8) | 1:200 | 25 |
| Rac1 (G-2) | 1:200 | 22 |

2. Immunofluorescence

2.1 Optimization of antibody and fluorescence dye

To determine the suitable dilutions of antibody specific to HSV-1 and fluorescence dye, rhodamine phalloidin specific to actin to be used in this study, the titrations were performed. Vero cells were infected with HSV-1 (KOS) at MOI of 10 for

24 hours. Then, the cells were centrifuged at 1,500 rpm, 4°C for 5 minutes. The pellet was resuspended with 1x PBS and smeared on glass slide (Thermo Scientific, USA). After that, the slides were air-dried at room temperature. Next, the slides were fixed by cold acetone (Emsure, Germany) at -20°C for 10 minutes and air-dried at room temperature. The slides were stored at -20°C until used.

2.1.1 Optimization of goat polyclonal anti-HSV-1 conjugated with FITC

The infected cells were stained with various concentrations of goat polyclonal anti-HSV-1 conjugated with FITC (Abcam, USA) (1:5, 1:10, 1:20 and 1:40) which were diluted in 1x PBS and incubated at 37°C for 1 hour in a moisture chamber. Next, the slide was washed twice with 1x PBS and mounted with mounting fluid (glycerol and 0.1% sodium azide) (Diagnostic Hybrids, USA). Fluorescence microscope (OLYMPUS BX50) and DP controller software were used to observe fluorescence imaging.

2.1.2 Optimization of rhodamine phalloidin

The infected cells were stained with various concentration of rhodamine phalloidin (Invitrogen, USA) (1:10, 1:20, 1:40 and 1:80) which were diluted in 1x PBS and incubated at 37°C for 1 hour in a moisture chamber. Next, the slide was washed twice with 1x PBS and mounted with mounting fluid. Fluorescence microscope (OLYMPUS BX50) and DP controller software were used to observe fluorescence imaging.

2.2 Sample preparation

Activated and non-activated T lymphocytes were treated with Cyto D (0 and 5 µg/mL) for 1 hour and incubated with HSV-1 at MOI of 10 at 37°C for 30 minutes. The cells were collected by centrifugation at 1,500 rpm, 4°C for 5 minutes. The pellet was resuspended with 1x PBS and transferred to the glass slide (Thermo Scientific, USA). After that, the slides were air-dried at room temperature. Next, the

slides were fixed by cold acetone at -20°C for 10 minutes and air-dried at room temperature. The samples were blocked with 1% BSA in 1x PBS at room temperature for 60 minutes and completely air-dried. The slides were stored at -20°C until used. Activated and non-activated Jurkat cells without HSV-1 were also prepared as control.

2.3 Immunostaining

The slide was stained with 15 μL of the fluorescence dye mixture including 1:10 rhodamine phalloidin and 1:20 goat polyclonal anti-HSV-1 conjugated with FITC diluted with 1% BSA in PBS and incubated at 37°C for 1 hour in a moisture chamber. After that, the slide was washed and incubated with 1x PBS for 15 minutes twice. Then, the slide was rinsed with 1x PBS several times to remove all free fluorescence dye. Finally, fluorescence microscopy (OLYMPUS BX50) and DP controller software were used to observe fluorescence imaging on the slide.

3. Transmission electron microscope (TEM)

3.1 Sample preparation

One million and five hundred thousand of activated Jurkat cells and non-activated Jurkat cells were inoculated with HSV-1 at MOI of 10 and incubated at 37°C for 15 minutes. After that, the cells were fixed with 3% glutaraldehyde in 0.1 M phosphate buffer (PB) at 4°C for 30 minutes. Next, the cells were spun at 1,500 rpm, 4°C for 5 minutes. The supernatant was replaced by PBS and stored at 4°C until used.

3.2 Dehydration and Embedding

The fixed cells were washed 3 times with 0.1 M PB for 2 minutes on rotator. The cells were post-fixed with 2% OsO_4 in 0.1 M PB for 45 minutes on rotator. Then, the cells were washed twice with PB for 2 minutes on rotator and dehydrated (for 3 times each) in 50%, 70%, 85% and 95% ethanol alcohol (EtOH) for 2 minutes on rotator and dehydrate again in absolute EtOH for 3 minutes (3 times). The cells were

further incubated with propylene oxide for 3 minutes (3 times). The cells were incubated once with the mixture of propylene oxide and resin (Epon812) at the ratio of 1:1 and 3:1 at 37°C for 10 and 15 minutes, respectively. Next, the cells were incubated with 100% resin at 37°C for 15 minutes (3 times). The cell pellet was transferred to a new capsule tube and fulfilled with 100% resin. The capsule was incubated overnight at 37°C and removed from the sample after incubation. The samples were ready for sectioning.

3.3 Sectioning and Imaging

Thick sections (survey sections) were obtained by trimming the resin stick with glass knife and ultramicrotome. After that, the thick sections were stained with Toluidine blue for 1 minute and observed under light microscope. Then, the resin sticks were retrimmed to be thin sections by using diamond knife. The thin sections were stained with uranyl acetate and lead citrate for 20 and 30 minutes respectively. The transmission electron microscope (JEM-1400 series, USA) processing was kindly performed by Assistant Professor Supang Maneesri Le Grand, Ph.D. and Ms. Wilawan Ji-Au, Department of Pathology, Faculty of medicine, Chulalongkorn University.

PART V: Role of actin on HSV-1 production in activated T lymphocytes

To investigate the role of actin, 1×10^6 cells/mL of activated and non-activated Jurkat cells were treated with Cyto D (2.5 and 5 $\mu\text{g}/\text{mL}$) at 37°C for 1 hour followed by HSV-1 at MOI of 10 inoculation and incubated at 37°C for 24 hours. After that, the cells were transferred to a new tube and centrifuged at 1,500 rpm, 4°C for 5 minutes. The supernatant (extracellular HSV-1) was collected and stored at -80°C . The pellet was frozen at -80°C and thawed at 37°C for 3 times and centrifuged at 1,500 rpm, 4°C for 5 minutes. The supernatant (intracellular HSV-1) was collected and stored at -80°C . Cyto D untreated activated and non-activated Jurkat cells were used as controls. HSV-1 titers were measured by plaque titration assay. The percentage of plaque reduction was calculated by following formula.

$$\text{Plaque reduction (\%)} = 100 - \left[\frac{\text{Viral titers from experiment}}{\text{Viral titers from control}} \times 100 \right]$$

Viral titers from experiment = HSV-1 titers from Cyto D-treated (2.5 or 5 $\mu\text{g}/\text{mL}$)
activated or non-activated Jurkat cells

Viral titers from control = HSV-1 titers from Cyto D untreated activated or non-
activated Jurkat cells

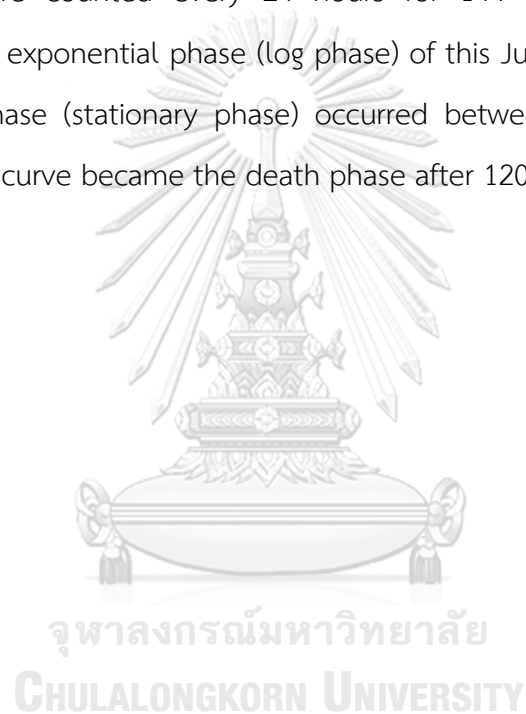
CHAPTURE V

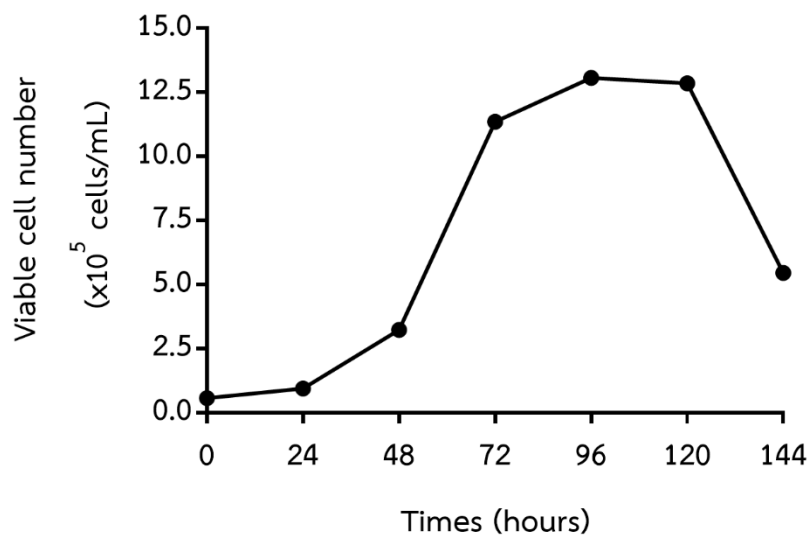
RESULTS

Part I: Cell cultures and viral stock preparation

1. Jurkat cell growth curve

To determine Jurkat cell growth rate, Jurkat cell growth curve was generated. Fifty thousand of Jurkat cells were cultured in growth medium (RPMI 1640). Viable cell numbers were counted every 24 hours for 144 hours. The growth curve indicated that the exponential phase (log phase) of this Jurkat cell line started at 48 hours. Plateau phase (stationary phase) occurred between 72 to 120 hours. The Jurkat cell growth curve became the death phase after 120 hours (Figure 10).





| Time (hours) | Cell number (Mean $\times 10^5$ cells/mL) |
|--------------|--|
| 0 | 0.575 |
| 24 | 0.950 |
| 48 | 3.225 |
| 72 | 11.350 |
| 96 | 13.075 |
| 120 | 12.850 |
| 144 | 5.450 |

Figure 10. Mean growth curve of Jurkat cell

5×10^4 Jurkat cells were continuously counted every 24 hours until 144 hours. This experiment was done in duplicate.

2. HSV-1 stock titers

To determine the titer of HSV-1 stock, plaque assay was performed. Thirty thousand of Vero cells per well in 96-well plate were infected with 10-fold dilution of HSV-1 stock for 3-4 days, the plaque were counted. The titer of this viral stock was 4.8×10^7 PFU/mL (Figure 11).

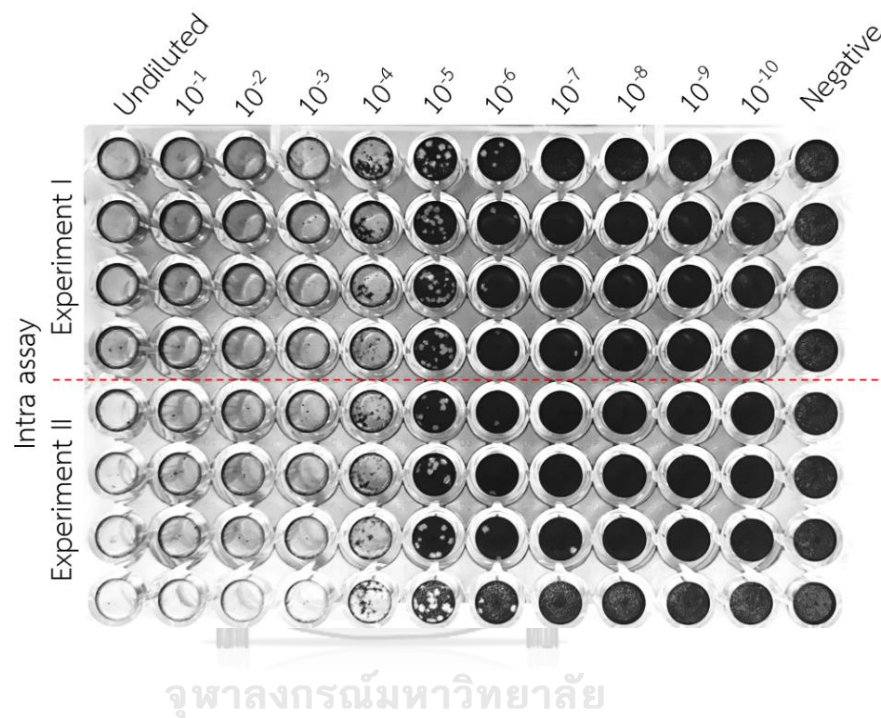


Figure 11. The plaque titration assay

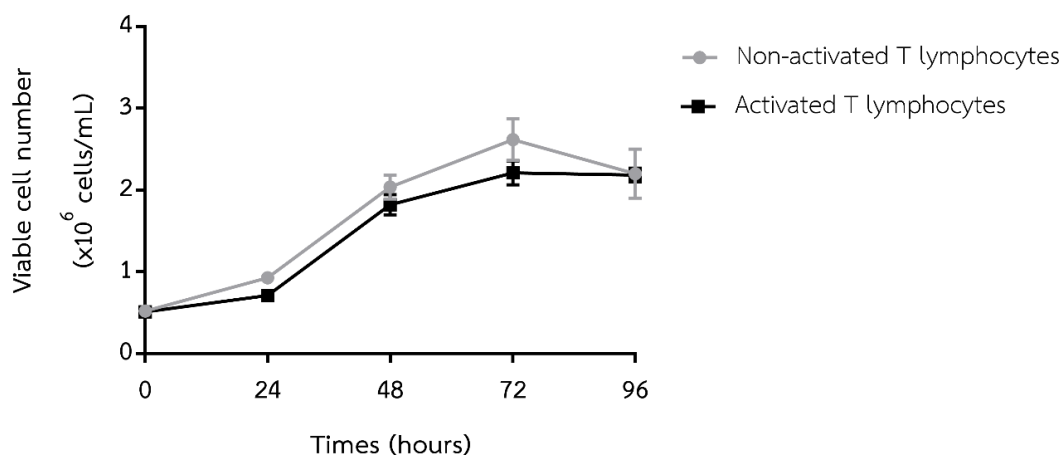
HSV-1 stock titer was determined by plaque assay. Maintenance media without HSV-1 was used as negative control. The data was from three independent experiments and each experiment was done in quadruplicate.

PART II: T cell activation

1. Growth of activated and non-activated T lymphocytes

To measure the growth rate of activated T lymphocytes at various time points during activation process, 5×10^5 of Jurkat cells were activated with Dynabeads Human T-Activator CD3/CD28 in growth medium (RPMI1640). The number of viable activated T lymphocytes were counted every 24 hours after adding beads and compared to non-activated T lymphocytes. The results showed that the growth rate of activated T lymphocytes was slightly lower than non-activated T lymphocytes at every time points (Figure 12). Both cells grew after 24 hours of plating and trended to plateau after 72 hours. Therefore, T cell activation at 72 hours was selected for further study.





| Hours | Cell number (Mean±SEM x10 ⁶ cells/mL) | |
|-------|--|-------------------------|
| | Non-activated T lymphocytes | Activated T lymphocytes |
| 0 | 0.520±0.010 | 0.513±0.011 |
| 24 | 0.927±0.022 | 0.712±0.009 |
| 48 | 2.037±0.148 | 1.822±0.122 |
| 72 | 2.618±0.254 | 2.213±0.150 |
| 96 | 2.200±0.300 | 2.185±0.085 |

Figure 12. Growth rate of activated and non-activated T lymphocytes.

The data was from three independent experiments. Error bars represented SEM.

2. Characterization of Jurkat cell phenotype

To determine the properties of Jurkat cells, the Jurkat cells were stained with PE/Cy7 conjugated anti-human CD3 antibody, brilliant violet 421 conjugated anti-human CD8 antibody and FITC conjugated anti-human CD4 antibody and were analyzed by flow cytometry. The results indicated that the Jurkat cells were mainly CD3⁺ T cell (97.2%) while only 0.37% and 0.17% were CD4⁺ and CD8⁺ T cell, respectively (Figure 13). Thus, 97.2% of this Jurkat cell line was CD3⁺CD4⁻CD8⁻ T cells.

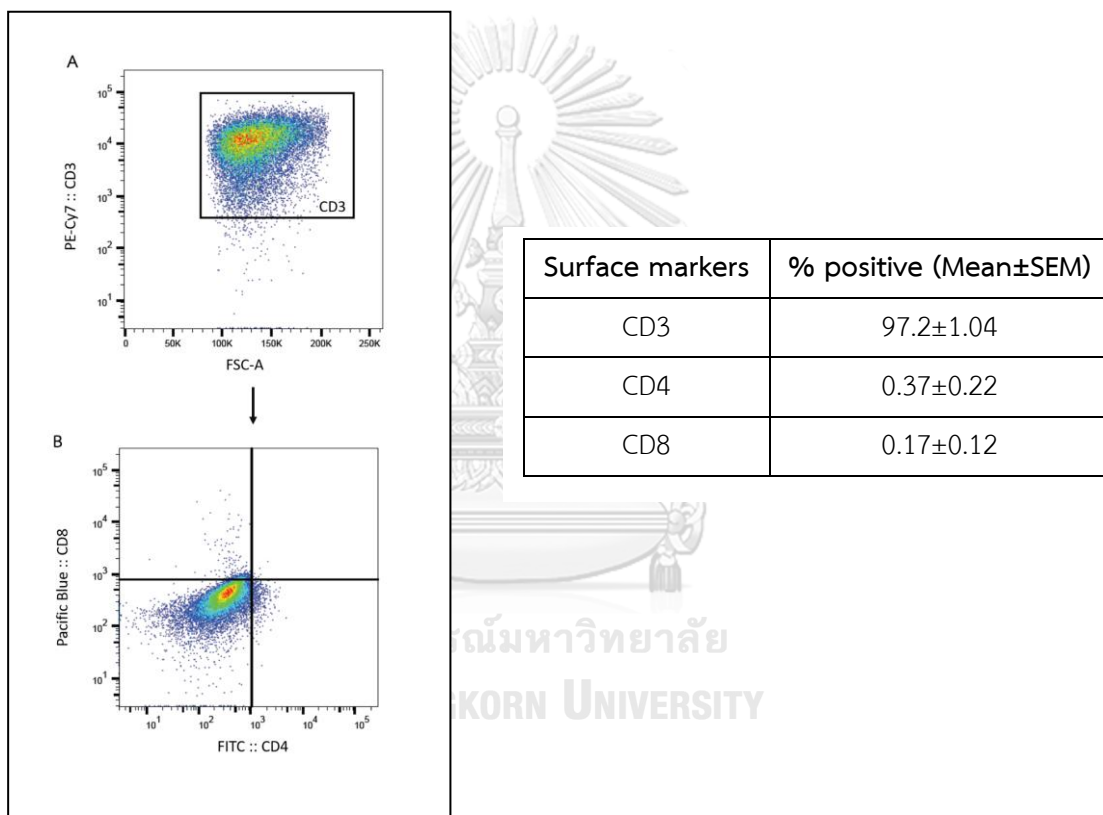


Figure 13. The phenotypic markers on surface of Jurkat cells.

Jurkat cell phenotypes were determined by flow cytometry. Three independent experiments were done. (A) CD3 expression (B) CD4 and CD8 expression from CD3⁺ population.

3. Detection of activation markers on activated T lymphocytes

When T lymphocytes are activated, several activation markers appear on their surface such as CD38, CD69, CD137 and HLA-DR (130). To characterize the phenotypes of Jurkat cells after activation, antibody specific to those markers were used to stain the surface of the cells and analyzed by flow cytometry.

Jurkat cells (1×10^6 cell/mL) were activated with Dynabeads Human T-Activator CD3/CD28 in growth medium (RPMI1640) at 37°C for 24, 48 and 72 hours. After activation, the activation markers were detected by staining with PE conjugated anti-human CD69 and PE conjugated anti-human CD137 antibodies and analyzed by flow cytometry. Increased median fluorescence intensities (MFI) and the number of positive cells (%) were calculated by comparing with non-activated Jurkat cells. Activated PBMCs were used as positive controls. Figure 14 showed that after activation, the percentage number of CD69 expressing Jurkat cells were increased 8.20% and 3.50% at 24 and 72 hours but 9.30% decreased at 48 hours. In contrast, CD69 expressing PBMCs were decreased 0.1% at 24 hours but 14.48% and 1.74% increased at 48 and 72 hours. The number of CD137 expressing Jurkat cells increased 12.77% and 3.09% at 24 and 48 hours but decreased 2.28% after 72 hours of activation whereas CD137 expressing PBMCs were decreased 0.11% at 24 hours but 10.71% and 8.03% increased after 48 and 72 hours of activation. Not only the percentage number of positive cells was measured, but also the MFI was determined. During 24, 48 and 72 hours of activation period, the fluorescence intensities of CD69 positive activated Jurkat cells were increased 43.95%, 7.80% and 31.98%, respectively similar to those of activated PBMCs, i.e., 0.53%, 157.74% and 57.70%, respectively (Figure 14). The fluorescence intensities of CD137 positive activated Jurkat cells were also increased 7.12% and 3.09% at 24 and 48 hours post-activation but decreased 2.44% at 72 hours while those of activated PBMCs were increased 2.81%, 156.48% and 36.09% at 24, 48 and 72 hours, respectively (Figure 14). In conclusion, after 72 hours activation, the number of CD69 positive cells was

slightly increased (3.50%) but the number of CD69 molecules on their surface was highly increased (31.98%). In contrast, the number of CD137 positive cells was 8.03% increased but the number of CD137 molecule was decreased 2.44%.

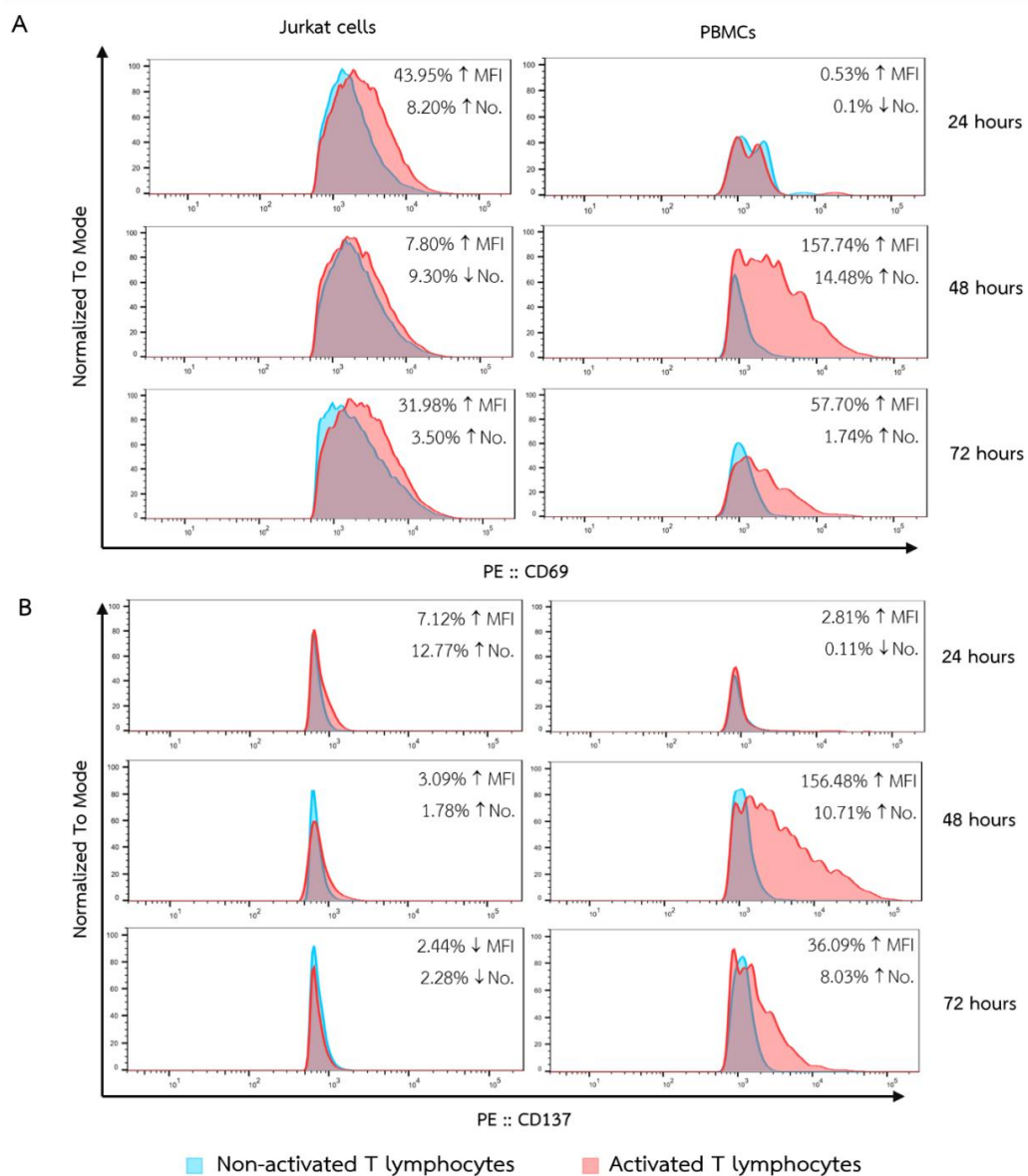


Figure 14. The expression of activation markers on activated T lymphocytes and PBMCs.

The increasing of median fluorescence intensities (%) was calculated. All cells were CD3⁺CD69⁺ or CD3⁺CD137⁺ populations. (A) CD69 expression (B) CD137 expression (↑ = increase, ↓ = decrease, MFI = median fluorescence intensities, No. = Number of positive cells)

In order to confirm the expression of activation phenotypes after 72 hours activation, activated T lymphocytes were stained with PE/Cy5 conjugated anti-human CD38, PE conjugated anti-human CD69 and PE/Cy7 conjugated anti-human HLA-DR. MFI and number of positive cells (%) were calculated. The results showed that the mean fluorescent intensities of CD69 activated T lymphocyte was increased $51.690 \pm 19.710\%$ when compared with non-activated cell. Mean MFI of HLA-DR expression on activated T lymphocyte was barely increased ($5.410 \pm 3.710\%$) whereas the opposite results were found in mean MFI of CD38 expressing cells ($16.390 \pm 1.280\%$ decreased after activation). The percentage number of positive cells ($CD3^+CD38^+$, $CD3^+CD69^+$ and $CD3^+HLA-DR^+$) were shifted 10.200 ± 3.00 , 6.100 ± 2.600 and $4.150 \pm 2.750\%$ after activation, respectively (Table 4). In conclusion, after 72 hours of dynabeads activation, the number of positive cells with all activation markers were increased however, up-regulated activation surface marker was mainly CD69.

Table 4. The expression of CD38, CD69 and HLA-DR on activated T lymphocytes after 72 hours activation.

The data was from two independent experiments.

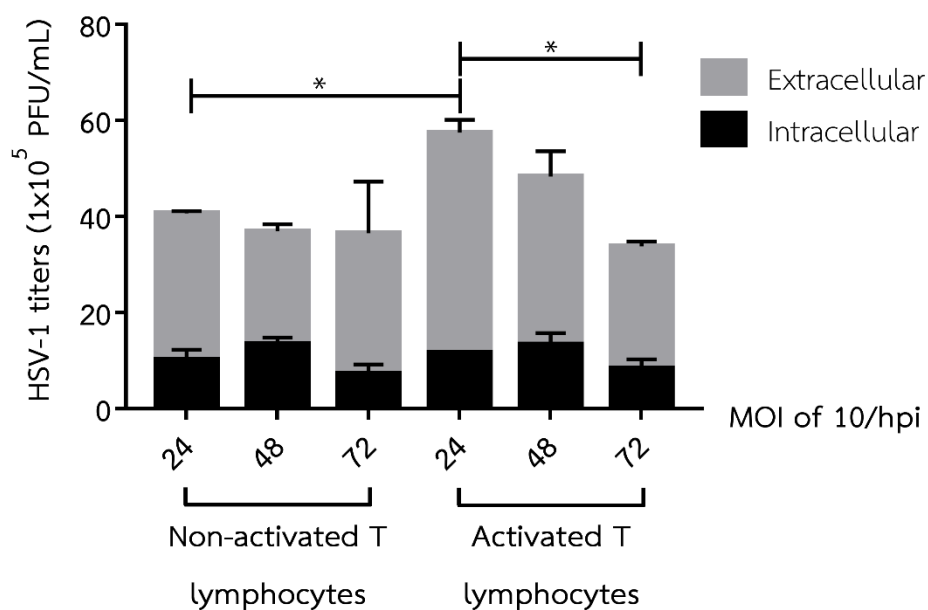
| Markers | %increased (Mean \pm SEM) | |
|-----------------|-----------------------------|--------------------|
| | MFI | Positive cells |
| $CD3^+CD38^+$ | -16.390 ± 1.280 | 10.200 ± 3.000 |
| $CD3^+CD69^+$ | 51.690 ± 19.710 | 6.100 ± 2.600 |
| $CD3^+HLA-DR^+$ | 5.410 ± 3.710 | 4.150 ± 2.750 |

(-) = decreased

4. HSV-1 growth in activated and non-activated T lymphocytes

In order to investigate the yield production of HSV-1 in activated and non-activated T lymphocytes, 72-hour activated and non-activated T lymphocytes were infected with HSV-1 at MOI of 10. The HSV-1 titers were measured at 24, 48 and 72 hours post-infection (hpi). The results indicated that, production of intracellular HSV-1 in both activated and non-activated T lymphocytes were lower than extracellular HSV-1 at every time points. Mean HSV-1 titer from activated T lymphocytes was statistically significant different higher than those from non-activated T lymphocytes at 24 hpi (57.515 ± 2.465 vs. 40.690 ± 2.610 PFU/mL, $p=0.0426$). Increase mean HSV-1 titer at 48 hpi was found in activated cells compared to that of non-activated cells (48.360 ± 2.840 vs. 36.955 ± 2.895 PFU/mL) but lower mean titer was shown at 72 hpi (33.840 ± 2.990 vs. 36.538 ± 8.838 PFU/mL). Mean HSV-1 titer from activated T lymphocytes at 24 hpi was also significantly higher than that at 72 hpi (57.515 ± 2.465 vs. 33.840 ± 2.990 , $p=0.0258$) whereas HSV-1 production from 24, 48 and 72 hours from non-activated T lymphocytes were not different (Figure 15).





| | Mean ± SEM HSV-1 titer (x10 ⁵ PFU/mL) | | | |
|---------------|--|---------------|---------------|--------------|
| | Hours postinfection (hpi) | Intracellular | Extracellular | Total |
| Activated | 24 | 11.640±0.160 | 45.875±2.625 | 57.515±2.465 |
| | 48 | 13.360±2.410 | 35.000±5.250 | 48.360±2.840 |
| | 72 | 8.340±1.990 | 25.000±1.000 | 33.840±2.990 |
| Non-activated | 24 | 10.190±2.110 | 30.500±0.500 | 40.690±2.610 |
| | 48 | 13.455±1.395 | 23.500±1.500 | 36.955±2.895 |
| | 72 | 7.288±1.913 | 29.250±10.750 | 36.538±8.838 |

Figure 15. Mean HSV-1 titers from 72 hours activated and non-activated T lymphocytes at 24, 48 and 72 hpi.

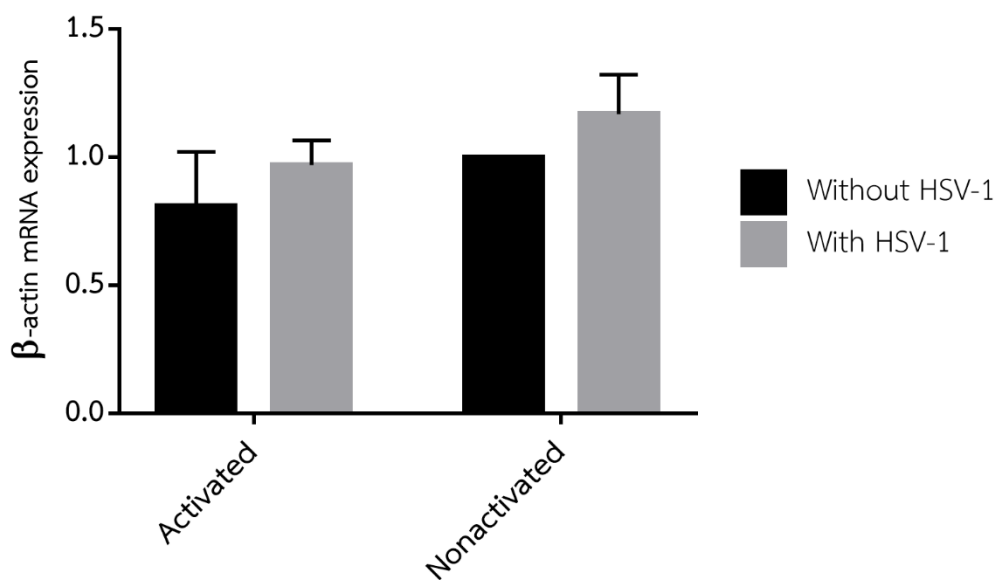
The titers were measured by plaque titration assay. The data was from two independent experiments. Error bars represented SEM.

PART III: β -actin expression

Previous study indicated that HSV-1 entry was enhanced in activated T lymphocytes (18). One of mechanisms supporting HSV-1 uptake in neuronal, fibroblast and epithelial cells was filopodia formation (104, 115, 116, 140). Thus, enhance HSV-1 entry in activated T lymphocyte might cause by the filopodia formation similar to those cells. The essential component for filopodia construction was actin which was polymerized toward along the filopodia to increase the length (14, 104). Therefore, detection of β -actin expression was performed.

1. Detection of β -actin mRNA

To detect the expression of β -actin mRNA, activated and non-activated T lymphocytes were infected with HSV-1 at MOI of 10. RNA from each sample was harvested before adding HSV-1 and at 30 minutes post-infection (mpi). Each RNA samples were converted to be cDNA by SuperScript III Reverse Transcriptase. Real-time polymerase chain reaction and double delta Ct analysis were used to quantitate the amount of β -actin expression. GAPDH was used as housekeeping gene. Activated and non-activated T lymphocytes without HSV-1 inoculation was used as base line of β -actin mRNA expression. The results indicated that the expression of β -actin mRNA in HSV-1 infected non-activated T lymphocytes (1.170 ± 0.153) was higher than HSV-1 infected activated T lymphocytes (0.970 ± 0.097) without significant difference. However, the trend of β -actin mRNA expression was increased after HSV-1 infection in both activated and non-activated cell (Figure 16).



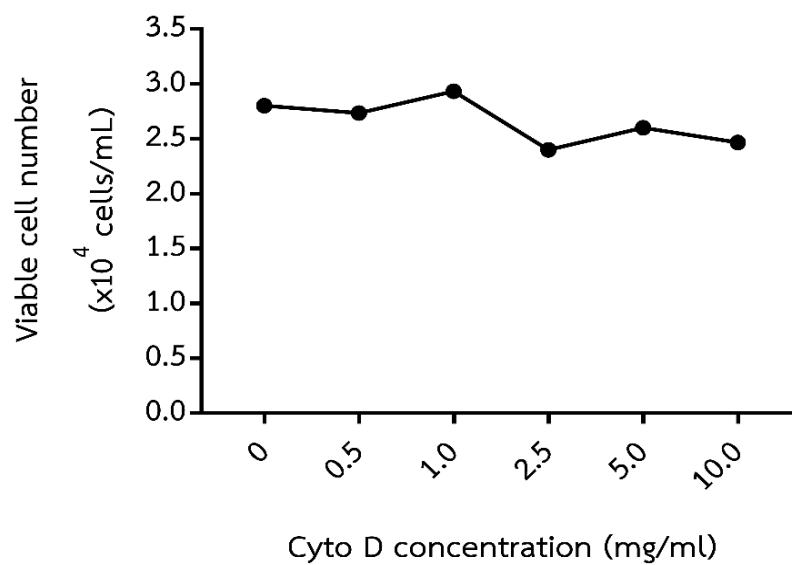
| Cell types | β -actin mRNA expression (Mean \pm SEM) | |
|---------------|---|---------------------|
| | Without HSV-1 | With HSV-1 (30 mpi) |
| Activated | 0.810 \pm 0.212 | 0.970 \pm 0.097 |
| Non-activated | 1.000 \pm 0.000 | 1.170 \pm 0.153 |

Figure 16. β -actin mRNA expression in activated and non-activated T lymphocytes without HSV-1 and with HSV-1 inoculation (30 mpi).

β -actin mRNA expression was detected by real-time PCR. The data was from three independent experiments. Error bars represented SEM.

2. Cytochalasin D treatment

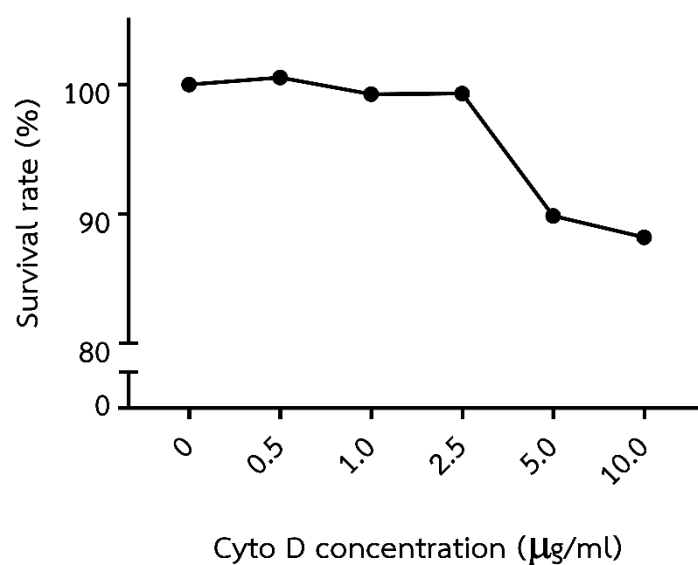
In order to confirm whether actin played role in filopodia formation, inhibition of actin polymerization by cytochalasin D (Cyto D) was studied. To optimize the suitable cyto D concentration, viable cell count and cell cytotoxicity assay were performed. Two million of Jurkat cells were treated with 0, 0.5, 1, 2.5, 5 and 10 $\mu\text{g}/\text{mL}$ of cyto D for 1 hour. The number of living cells after treatment was counted by trypan blue staining. The results showed that the declining trend of living cells was observed since cytoD concentration of 2.5 $\mu\text{g}/\text{mL}$ without significant difference (Figure 17). The cytotoxicity assay was also performed to quantify the toxicity of cyto D to the Jurkat cells. The cells were treated with indicated concentration of cyto D for 1 hour. Then, tetra Z assay was performed and the survival rate (%) was calculated. The Jurkat cells without cyto D treatment was used as control (100% viability). Growth medium alone was used as background control. The results indicated that the cell survival rate approximately 10% decreased after cyto D treatment at concentration of 5.0 and 10.0 $\mu\text{g}/\text{mL}$ (Figure 18). Thus, 2.5 and 5.0 $\mu\text{g}/\text{mL}$ of cyto D treatment were selected for future experiments.



| Cyto D concentration ($\mu\text{g}/\text{mL}$) | Viable cell number (Mean $\times 10^4$ cells/mL) |
|---|---|
| 0 | 2.800 |
| 0.5 | 2.733 |
| 1.0 | 2.933 |
| 2.5 | 2.400 |
| 5.0 | 2.600 |
| 10.0 | 2.476 |

Figure 17. The cell survival after cyto D treatment at various concentrations.

After 1 hour of cyto D treatment (0, 0.5, 1, 2.5, 5 and 10 $\mu\text{g}/\text{mL}$), living cells were counted by trypan blue staining. An experiment was done in triplicate.



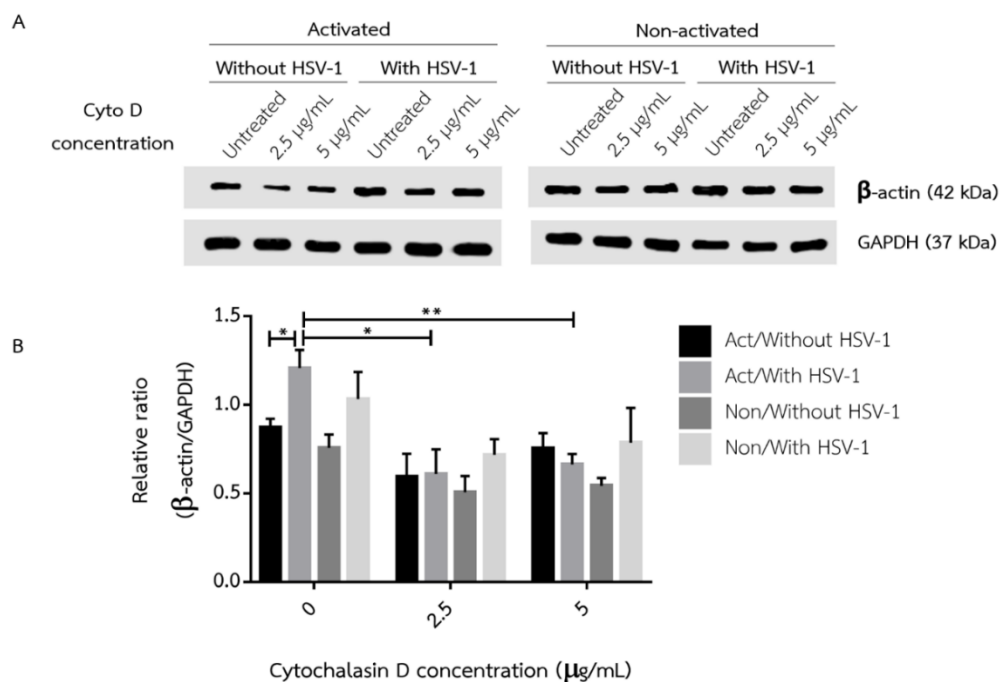
| Cyto D concentration (µg/mL) | Survival rate (%) (Mean) |
|------------------------------|--------------------------|
| 0 | 100.00 |
| 0.5 | 100.55 |
| 1.0 | 99.27 |
| 2.5 | 99.32 |
| 5.0 | 89.87 |
| 10.0 | 88.21 |

Figure 18. The cell survival rate (%) after cyto D treatment.

Jurkat cell survival rate after 1 hour of cyto D treatment (0, 0.5, 1.0, 2.5, 5.0 and 10.0 µg/mL) were measured by cytotoxicity (tetra Z) assay. An experiment was done in triplicate.

3. Detection of β -actin expression at translational level

In order to investigate the role of actin polymerization during HSV-1 entry in activated T lymphocytes, cyto D treatment at 0, 2.5, 5.0 $\mu\text{g}/\text{mL}$ were performed. Cyto D treated, activated T lymphocytes were infected with HSV-1 at MOI of 10 for 30 minutes. β -actin and GAPDH bands were detected by SDS-PAGE and Western blot. β -actin expression during HSV-1 entry was measured as the relative ratio between β -actin and GAPDH intensities. The result was compared to cyto D treated activated T lymphocytes without HSV-1 and non-activated T lymphocytes with or without HSV-1. The results indicated that β -actin in untreated (0 $\mu\text{g}/\text{mL}$) activated T lymphocytes (1.208 vs 0.873) were increased significantly ($p=0.0477$) at 30 minutes post HSV-1 infection. The similar results were found in non-activated T lymphocytes (1.033 vs 0.758) without statistically significance. After cyto D treatment, the expression of β -actin in both activated and non-activated T lymphocytes were decreased at every time points (Figure 19). Statistic significant reduction of β -actin was found in HSV-1 infected cyto D treated activated T lymphocyte at 2.5 ($p=0.0136$) and 5 ($p=0.0037$) $\mu\text{g}/\text{mL}$ when compared to untreated activated cells. The expression of β -actin from activated and non-activated T lymphocytes without HSV-1 in both concentrations of cyto D treatment (2.5 and 5 $\mu\text{g}/\text{mL}$) were not significantly different (Figure 19). These results implied that cyto D is able to inhibit β -actin polymerization in HSV-1 infected either activated or non-activated Jurkat cells.



| Cyto D concentration | β -actin expression (Mean \pm SEM) | | | |
|----------------------|--|---------------------|-----------------------------|---------------------|
| | Activated T lymphocytes | | Non-activated T lymphocytes | |
| | Without HSV-1 | With HSV-1 (30 mpi) | Without HSV-1 | With HSV-1 (30 mpi) |
| 0 $\mu\text{g/mL}$ | 0.873 \pm 0.049 | 1.208 \pm 0.103 | 0.758 \pm 0.076 | 1.033 \pm 0.152 |
| 2.5 $\mu\text{g/mL}$ | 0.593 \pm 0.131 | 0.610 \pm 0.139 | 0.507 \pm 0.092 | 0.718 \pm 0.090 |
| 5 $\mu\text{g/mL}$ | 0.755 \pm 0.085 | 0.665 \pm 0.059 | 0.543 \pm 0.044 | 0.787 \pm 0.196 |

Figure 19. The expression of β -actin during HSV-1 entry.

(A) β -actin and GAPDH expression in cyto D treated (0, 2.5 and 5 $\mu\text{g/mL}$), activated and non-activated T lymphocytes with or without HSV-1 infection (MOI of 10) were detected by Western blot. (B) The intensities of β -actin and GAPDH bands were quantified by image J software. The relative ratio of β -actin and GAPDH was calculated. The three independent experiments were done. Asterisks indicated significant difference ($p < 0.05$, unpaired t-test). Error bars represented SEM. Act, activated T lymphocytes; Non, non-activated T lymphocytes; mpi, minutes post-infection.

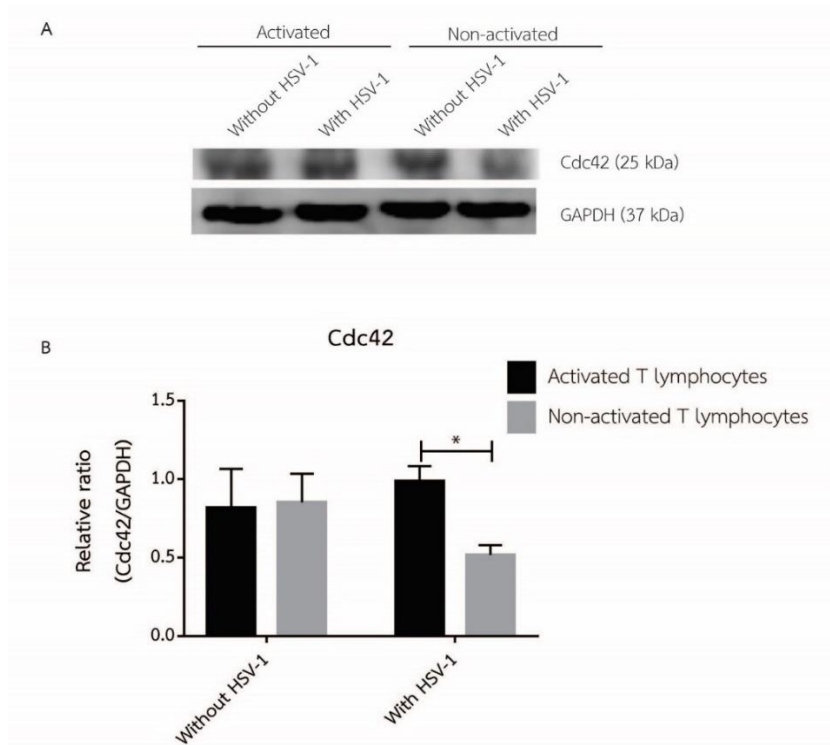
PART IV: Filopodia formation during HSV-1 entry

Actin polymerization was useful to several cellular processes. Three basic types of actin networks were stress fibers, filopodia and lamellipodia (11). These different types of actin depended on Rho GTPase family such as RhoA is known to be involved in stress fiber formation, Rac1 plays role in lamellipodia formation and Cdc42 plays role in filopodia formation. Since the previous results indicated that HSV-1 induced actin expression, the exploration of which type of actin networks occurred in HSV-1 infected activated T-lymphocytes was performed by detection of Rho GTPase family.

1. Rho GTPase family expression

In order to investigate filopodia, lamellipodia and/or stress fiber induced by HSV-1 infection, activated T lymphocytes (1×10^6 cells/mL) were incubated with HSV-1 at MOI of 10 for 10 minutes at 37°C. The proteins from whole cell lysate were separated by SDS-PAGE. Rho GTPase family (Cdc42, RhoA and Rac1) were detected by Western blot. The results showed that, before HSV-1 infection, the mean level expression of Cdc42 in activated and non-activated Jurkat cells were not different (0.817 ± 0.250 vs 0.853 ± 0.813). However, Cdc42 in activated T lymphocytes after HSV-1 infection (10 minutes) compared to mock infected cells (0.987 ± 0.098 vs 0.817 ± 0.250) was increased but the expression of Cdc42 in non-activated T lymphocytes (0.517 ± 0.064 vs 0.853 ± 0.813) was decreased (Figure 20). The Cdc42 expression in HSV-1-infected activated T lymphocytes was significantly different from those in HSV-1-infected non-activated cells (0.987 ± 0.098 vs 0.517 ± 0.064 , $p=0.0127$). The expression of RhoA and Rac1 in non-infected activated cells were lower than non-infected non-activated cells without statistically significance (0.527 ± 0.158 vs 0.710 ± 0.125 and 0.763 ± 0.111 vs 1.003 ± 0.231 , respectively). RhoA and Rac1 expression were increased in HSV-1 infected activated cells when compared to mock control (0.527 ± 0.158 vs 0.943 ± 0.044 and 0.763 ± 0.111 vs 0.913 ± 0.091 , respectively) but decreased in HSV-1 infected non-activated cells when compared to mock

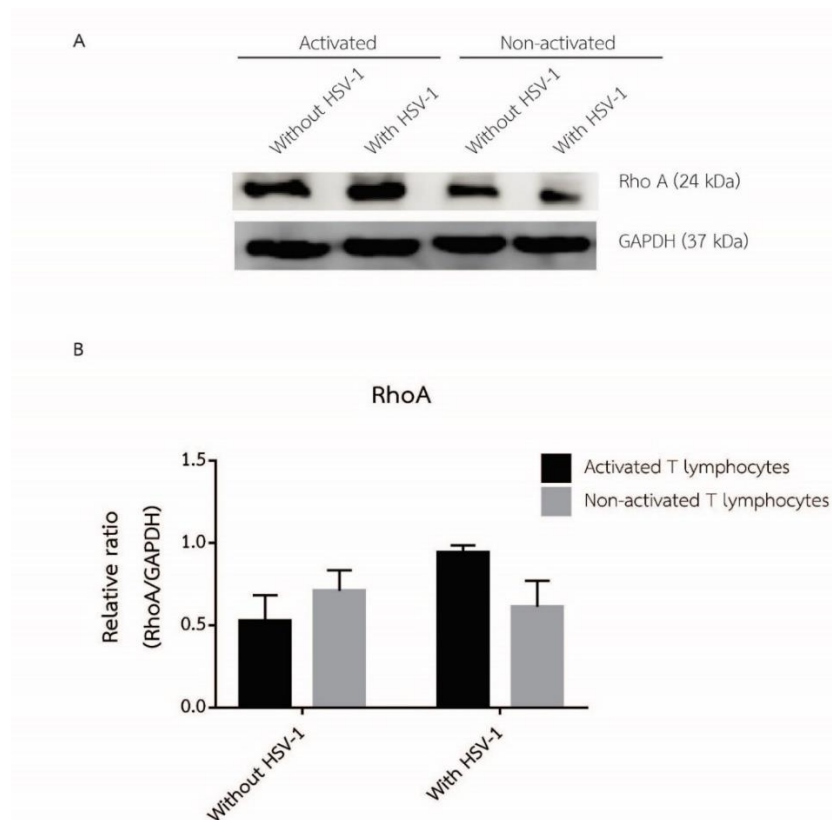
control (0.710 ± 0.125 vs 0.613 ± 0.159 and 1.003 ± 0.231 vs 0.790 ± 0.031 , respectively) (Figure 21 and 22).



| | Cdc42 expression (Mean±SEM) | |
|---------------------|-----------------------------|-----------------------------|
| | Activated T lymphocytes | Non-activated T lymphocytes |
| Without HSV-1 | 0.817±0.250 | 0.853±0.813 |
| With HSV-1 (10 mpi) | 0.987±0.098 | 0.517±0.064 |

Figure 20. The Cdc42 expression during HSV-1 entry.

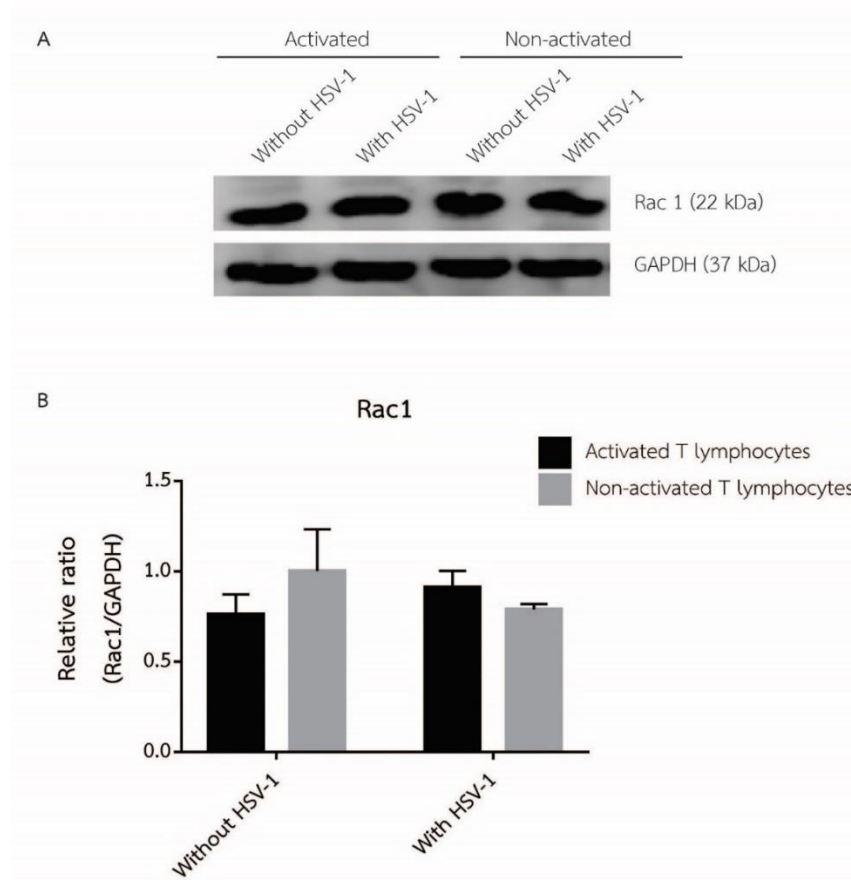
(A) Cdc42 and GAPDH expression in activated and non-activated T lymphocytes with or without HSV-1 infection (MOI of 10) were detected by western blot. (B) The intensities of Cdc42 and GAPDH bands were quantified by image J software. The relative ratio of Cdc42 and GAPDH were calculated. The three independent experiments were done. Asterisks indicated significant difference ($p < 0.05$, unpaired t-test). Error bars represented SEM. mpi; minutes post-infection.



| | RhoA expression (Mean±SEM) | |
|---------------------|----------------------------|-----------------------------|
| | Activated T lymphocytes | Non-activated T lymphocytes |
| Without HSV-1 | 0.527±0.158 | 0.710±0.125 |
| With HSV-1 (10 mpi) | 0.943±0.044 | 0.613±0.159 |

Figure 21. The RhoA expression during HSV-1 entry.

(A) RhoA and GAPDH expression in activated and non-activated T lymphocytes with or without HSV-1 infection (MOI of 10) were detected by western blot. (B) The intensities of RhoA and GAPDH bands were quantified by image J software. The relative ratio of RhoA and GAPDH were calculated. The three independent experiments were done. Asterisks indicated significant difference ($p < 0.05$, unpaired t-test). Error bars represented SEM. mpi; minutes post-infection.



| | Rac1 expression (Mean±SEM) | |
|---------------------|----------------------------|-----------------------------|
| | Activated T lymphocytes | Non-activated T lymphocytes |
| Without HSV-1 | 0.763±0.111 | 1.003±0.231 |
| With HSV-1 (10 mpi) | 0.913±0.091 | 0.790±0.031 |

Figure 22. The Rac1 expression during HSV-1 entry.

(A) Rac1 and GAPDH expression in activated and non-activated T lymphocytes with or without HSV-1 infection (MOI of 10) were detected by western blot. (B) The intensities of Rac1 and GAPDH bands were quantified by image J software. The relative ratio of Rac1 and GAPDH were calculated. The three independent experiments were done. Asterisks indicated significant difference ($P < 0.05$, unpaired t-test). Error bars represented SEM. mpi; minutes post-infection.

2. Detection of HSV-1 and actin on filopodia

Previous data showed that Cdc42 increased significantly in HSV-1 infected activated T lymphocytes indicating possibility of filopodia formation. The filopodia in HSV-1 infected T cells were then determined by staining with rhodamine phalloidin and HSV-1 specific antibody conjugated with FITC and observed under fluorescent microscopy.

First, the concentration of fluorescence dye was optimized. To optimize the suitable concentration of anti-HSV-1 antibody for HSV-1 detection, HSV-1 infected Vero cells were stained with various concentration of goat polyclonal anti-HSV-1 conjugated with FITC (1:5, 1:10, 1:20 and 1:40) and observed under fluorescence microscope. The results indicated that 1:20 of antibody dilution was appropriated for HSV-1 staining (Figure 23). To optimize the suitable concentration for actin staining, HSV-1 infected Vero cell were stained with various concentration of rhodamine phalloidin (1:10, 1:20, 1:40 and 1:80). The results showed that 1:10 dilution was appropriated for actin staining (Figure 24). Thus, 1:20 of goat polyclonal anti-HSV-1 conjugated with FITC and 1:10 goat polyclonal anti-HSV-1 conjugated with FITC were used for further study. To observe the interaction of HSV-1 and filopodia, both fluorescence dyes were co-stained. HSV-1-infected and non-infected Vero cell were stained with the mixture of 1:20 goat polyclonal anti-HSV-1 conjugated with FITC and 1:10 rhodamine phalloidin. Actin-rich protrusions, filopodia formation, was observed. HSV-1 was found at all parts of Vero cell (nucleus, cytoplasm and cytoplasmic membrane) as well as on the filopodia (Figure 25).

To detect the formation of filopodia and the interaction between HSV-1 and filopodia, immunofluorescence assay was performed. Activated T lymphocytes (with or without cyto D treatment) were infected with HSV-1 at MOI of 10 for 30 minutes at 37°C. The virus and actin were co-stained with goat polyclonal anti-HSV-1 conjugated with FITC and rhodamine phalloidin, as described. The results showed that filopodia formation were detected on both cyto D untreated activated T lymphocytes with or

without HSV-1 infection. However, the number of cells forming filopodia in HSV-1-infected activated cells (approximate 30%) were more than activated cells without HSV-1 infection (approximate 11%). The interaction of HSV-1 with filopodia was observed (Figure 26). On the other hand, filopodia formation were not observed in untreated non-activated T lymphocytes (with and without HSV-1 infection) and cyto D treated activated and non-activated T lymphocytes (with and without HSV-1 infection) (Figure 26 and 27).



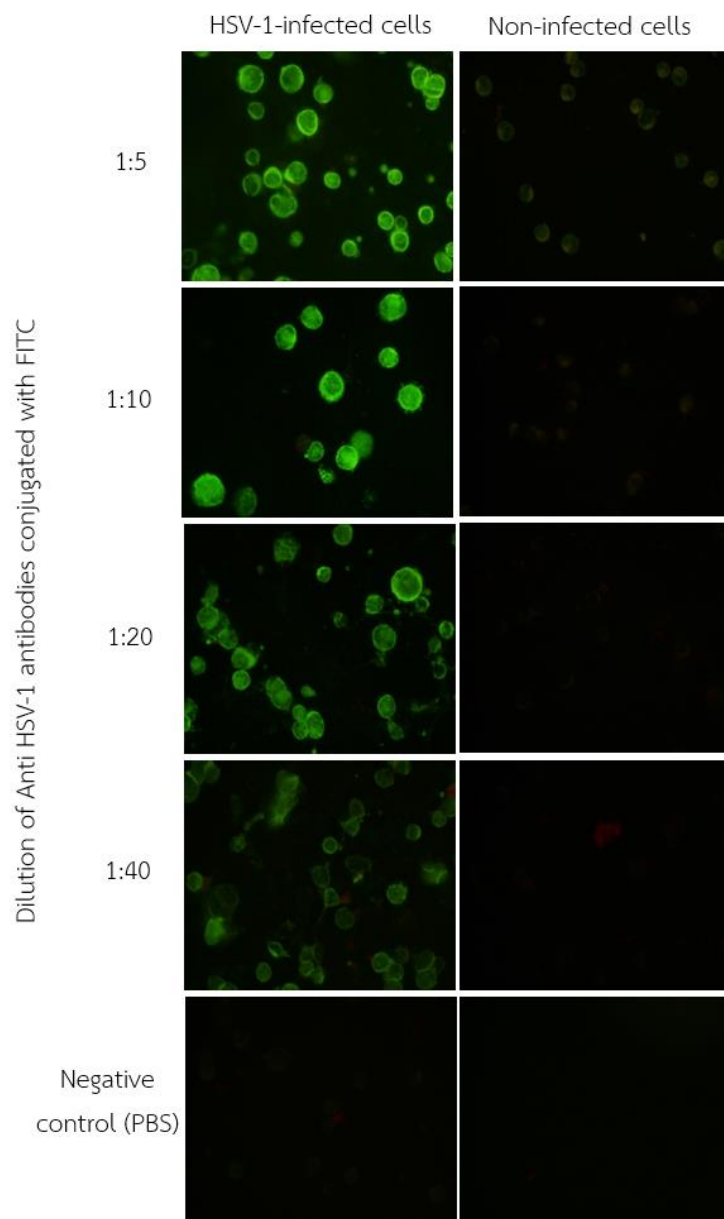


Figure 23. Optimization of goat polyclonal anti-HSV-1 conjugated with FITC.

Vero cells were infected with or without HSV-1 at MOI of 1 for 24 hours and were stained by various concentrations of anti-HSV-1 antibody (1:5, 1:10, 1:20 and 1:40) which were diluted in PBS. The cells were observed under fluorescence microscope (400x). The cells incubated with PBS were used as negative control.

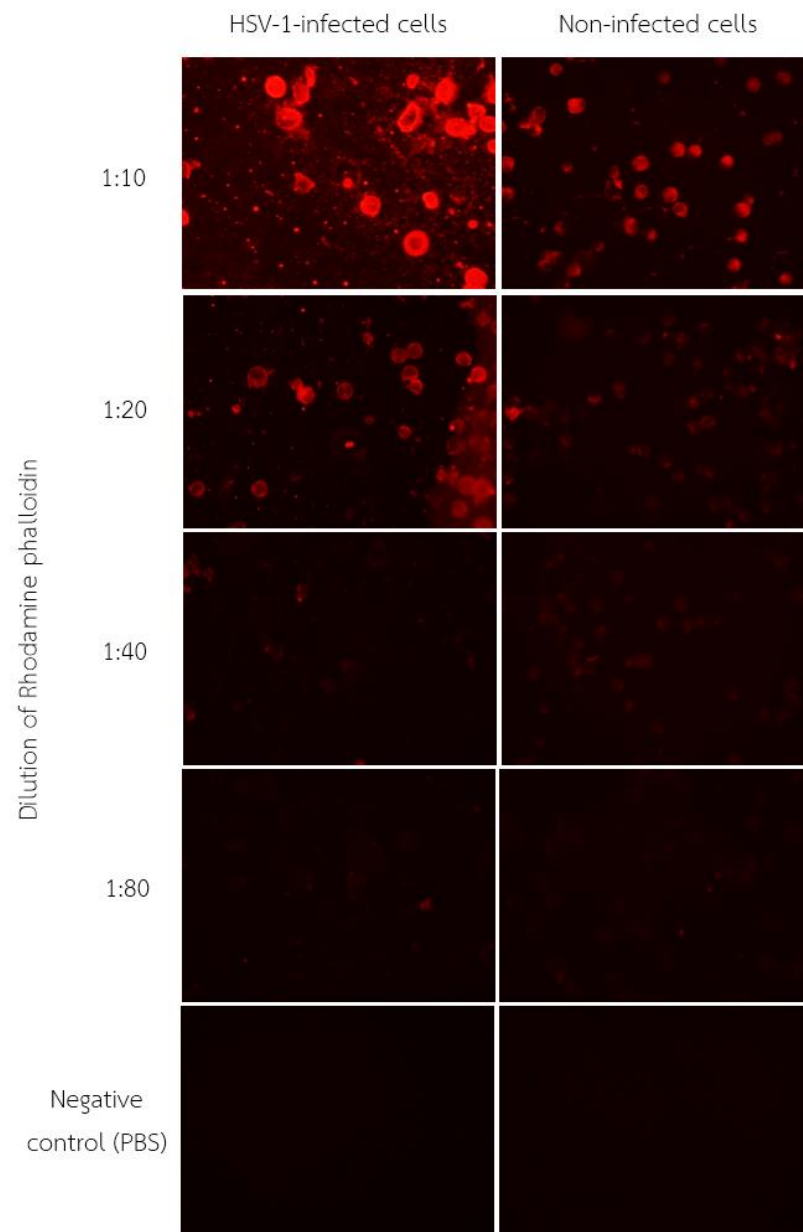


Figure 24. Optimization of rhodamine phalloidin.

Vero cells were infected with or without HSV-1 at MOI of 1 for 24 hours and were stained by various concentrations of rhodamine phalloidin (1:10, 1:20, 1:40 and 1:80) which were diluted in PBS. The cells were observed under fluorescence microscope (400x). The cells incubated with PBS were used as negative control.

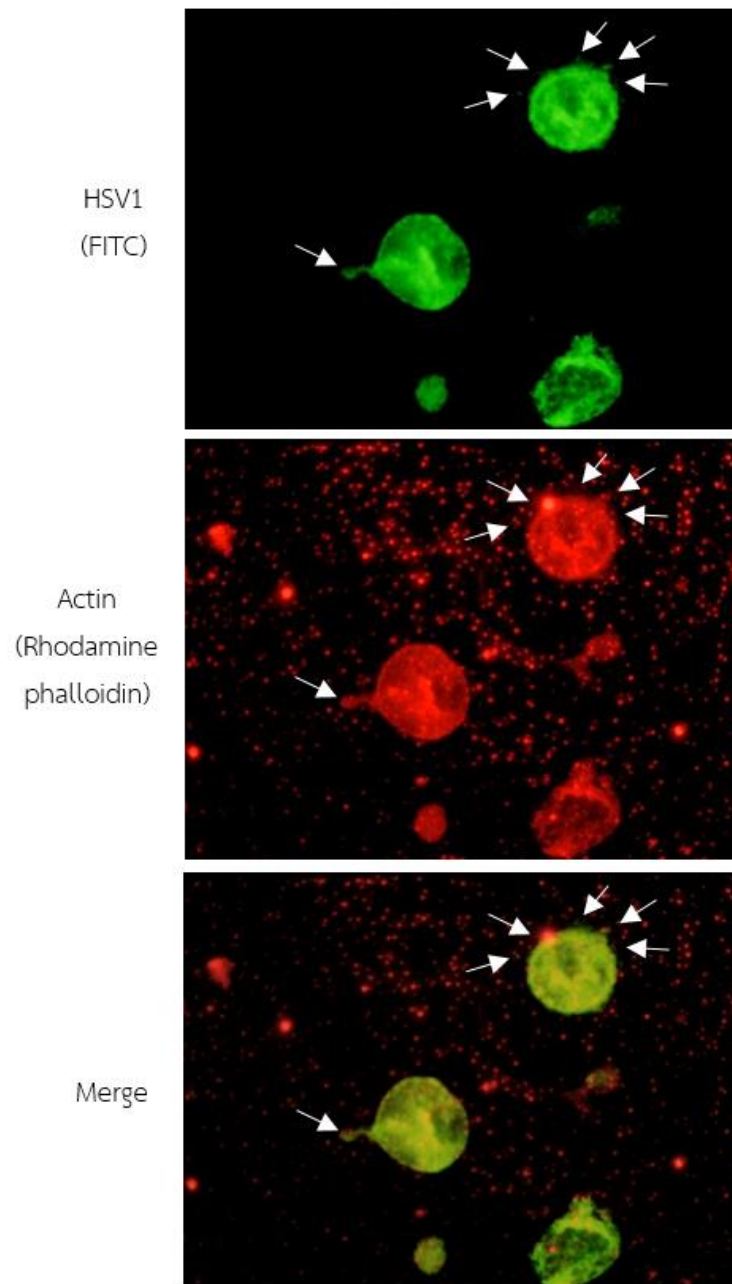


Figure 25. Detection of filopodia formation in HSV-1-infected Vero cell.

Vero cells were infected with HSV-1 at MOI of 1 for 24 hours and were stained with 1:10 rhodamine phalloidin (red) and 1:20 goat polyclonal anti-HSV-1 conjugated with FITC (green) which were diluted in PBS. The cells were observed under fluorescence microscope (1000x). The filopodia were indicated with arrowheads.

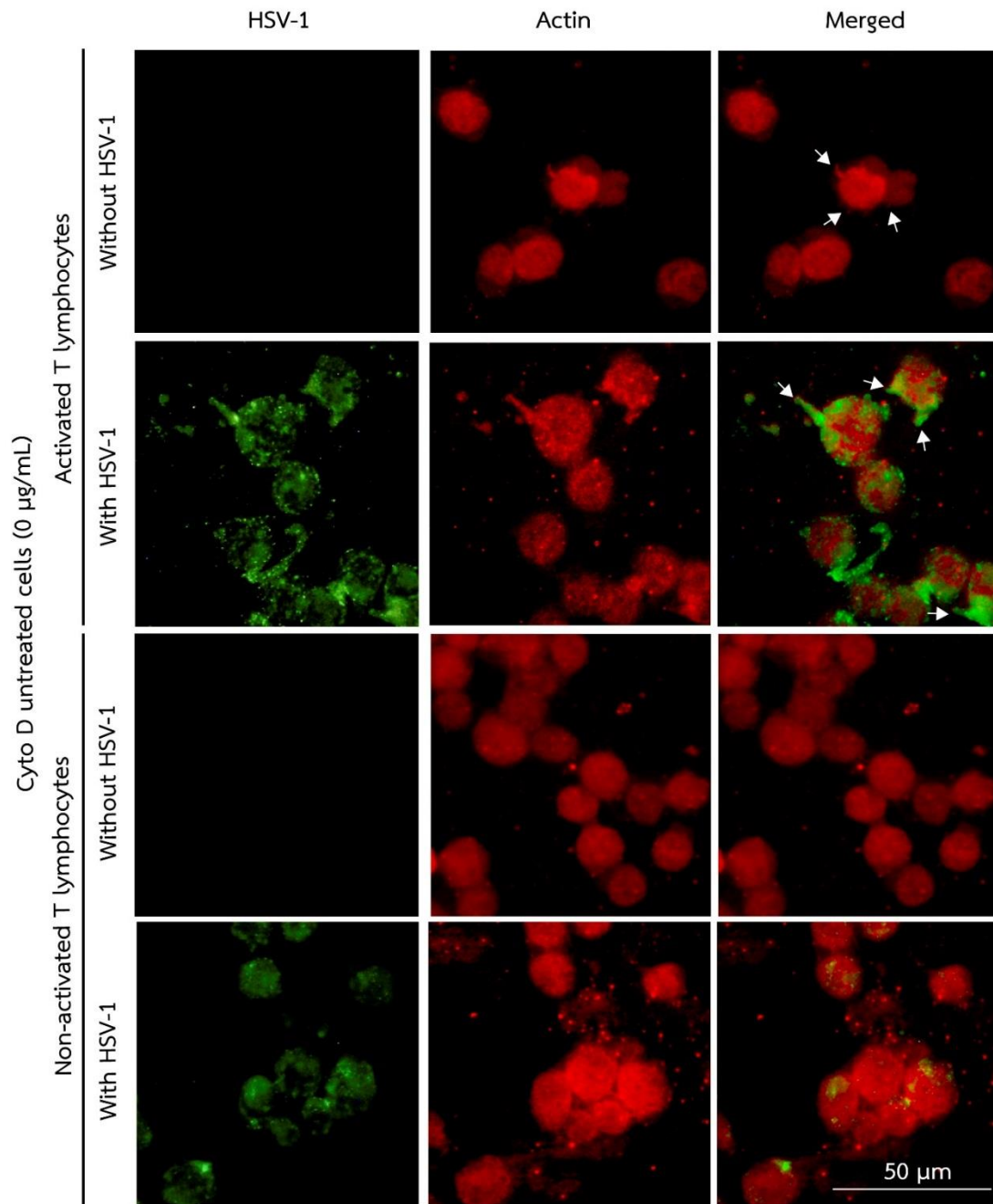


Figure 26. HSV-1 attaches to filopodia on activated T lymphocytes.

Cyto D untreated activated and non-activated T lymphocytes were incubated with HSV-1 at MOI of 10 for 30 minutes. F-actin was visualized by rhodamine phalloidin (red) while HSV-1 was visualized by goat polyclonal anti-HSV-1 conjugated with FITC (green). The interaction of HSV-1 and cells was observed under fluorescence microscope (1000x). Filopodia formation was indicated with arrow head.

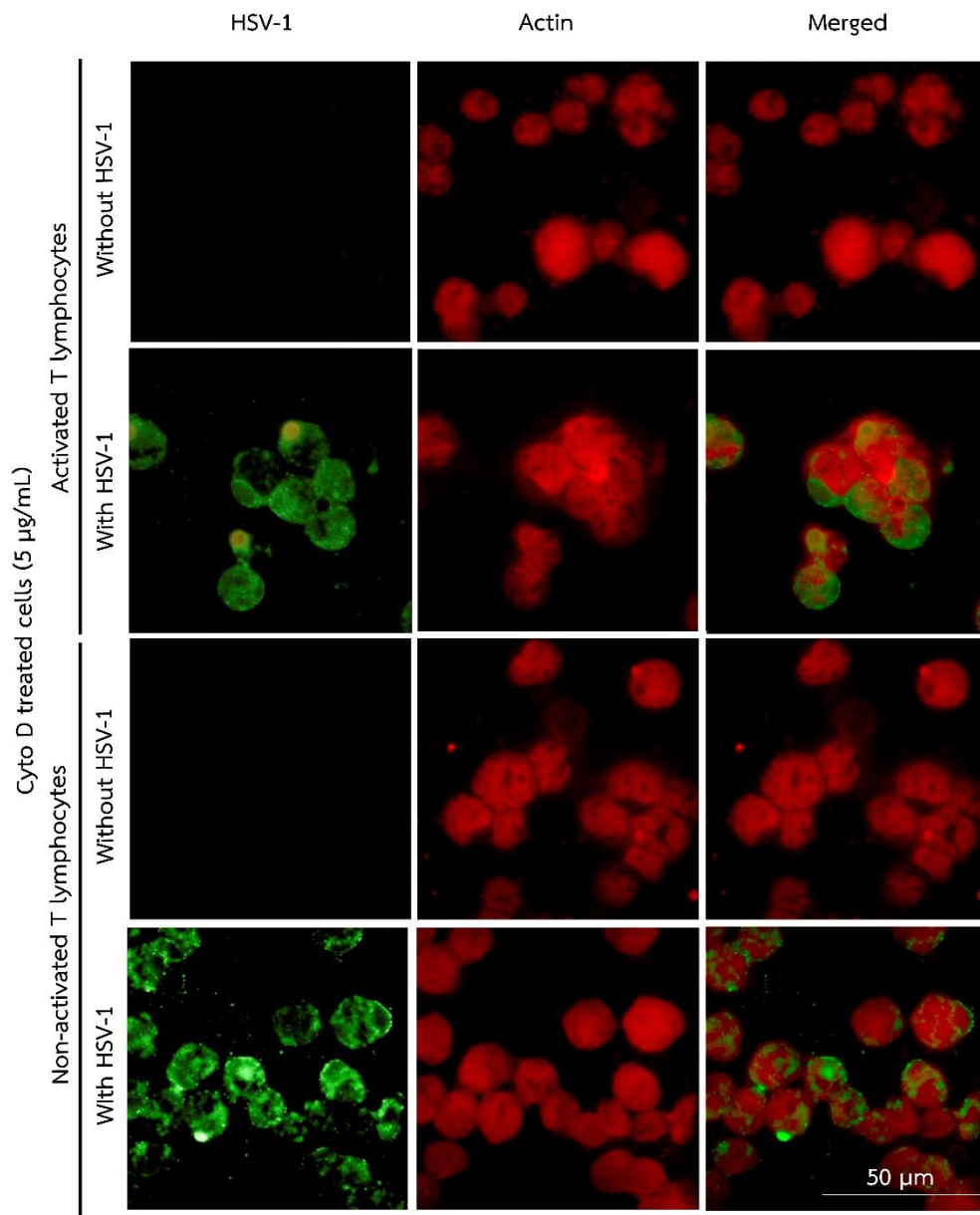


Figure 27. HSV-1 attaches to cyto D treated activated and non-activated T lymphocytes.

Cyto D treated (5 μ g/mL) activated and non-activated T lymphocytes were incubated with HSV-1 at MOI of 10 for 30 minutes. F-actin was visualized by rhodamine phalloidin (red) while HSV-1 was visualized by goat polyclonal anti-HSV-1 conjugated with FITC (green). The interaction of HSV-1 and cells was observed under fluorescence microscope (1000x).

3. Detection of HSV-1 entry and filopodia by electron microscopy

To investigate filopodia formation and HSV-1 entry, electron microscopy was performed. Activated and non-activated T lymphocytes (1.5×10^6 cells/mL) were infected with HSV-1 at MOI of 10 at 37°C for 15 minutes. Cell morphology was observed under transmission electron microscope (TEM). The results showed that filopodia formation was rarely observed in uninfected non-activated T lymphocytes (approximately 12.5%) and HSV-1-infected non-activated T lymphocytes (approximately 20%). But filopodia formation was observed in both HSV-1-infected (approximate 86%) and non-infected (approximate 44%) activated T lymphocytes. Noted that, the length of filopodia extension on activated cells was longer than those on non-activated cells. In addition, the morphology of activated and non-activated cells were different, non-activated cells were round but activated cells were pleomorphic (Figure 28A and B). Moreover, HSV-1 virion associated to filopodia and cell surface on activated T lymphocytes (Figure 28A-a1 and a2) at 15 minutes HSV-1 post-infection was observed. None was found in non-activated T lymphocytes. Only HSV-1 virion bound at cell membrane was demonstrated (Figure 28B-b1). Intracellular HSV-1 virions were observed in activated cells (Figure 28A) whereas there were no intracellular virions in non-activated cells (Figure 28B). It was suggested that HSV-1 could enter into activated T lymphocytes via endocytosis since HSV-1 virion was contained in endosome after 15 minutes post-infection (Figure 28A-a3).

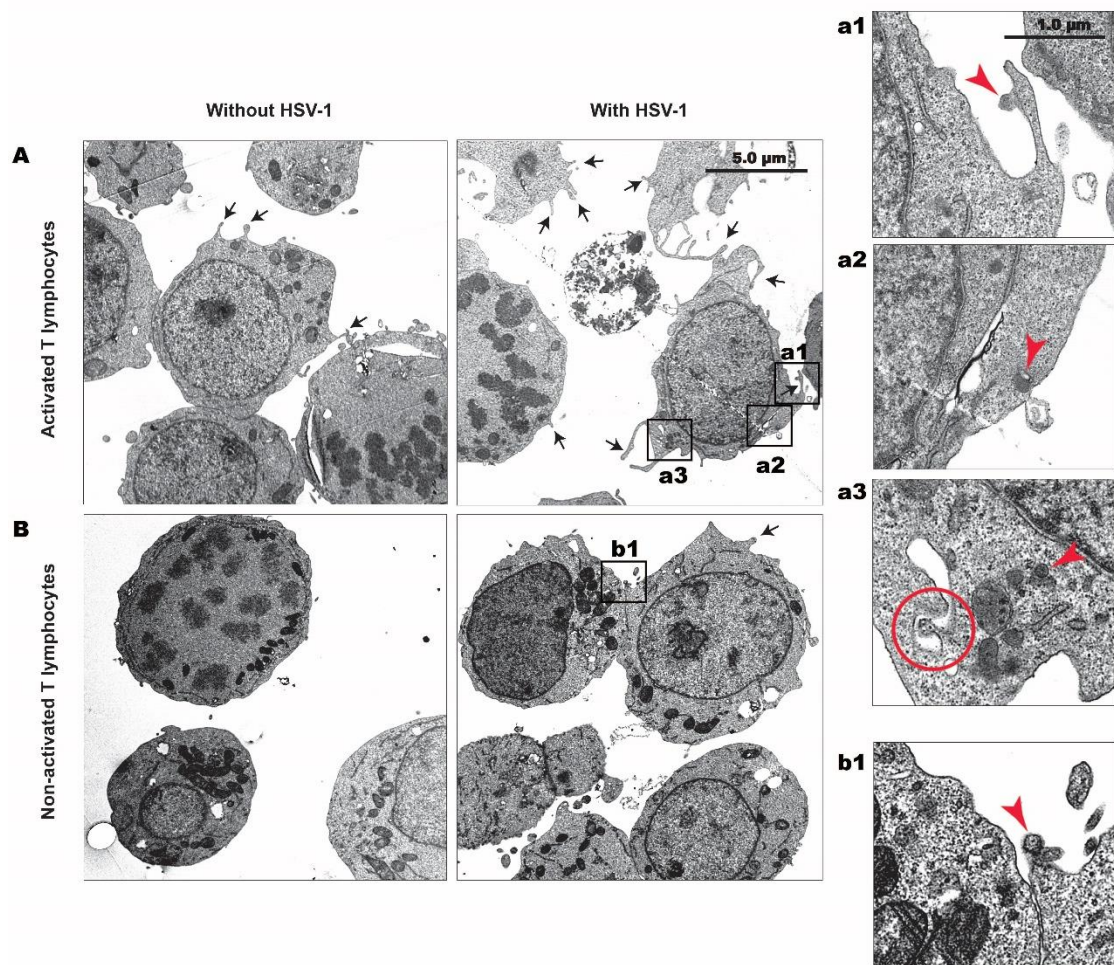


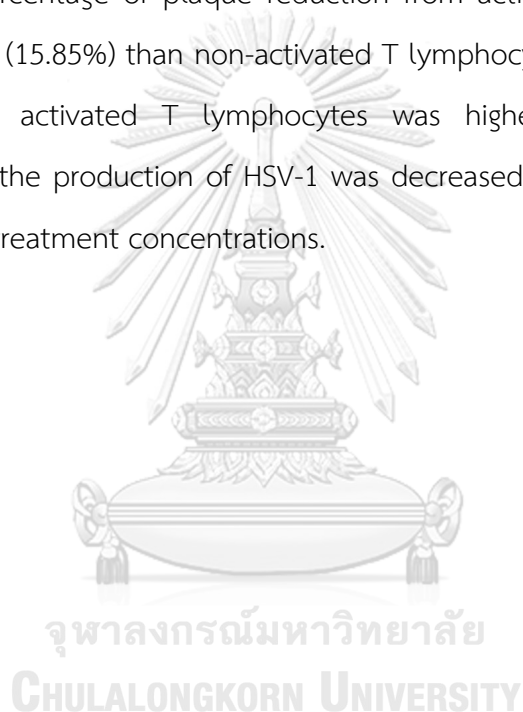
Figure 28. Cell morphology during HSV-1 entry.

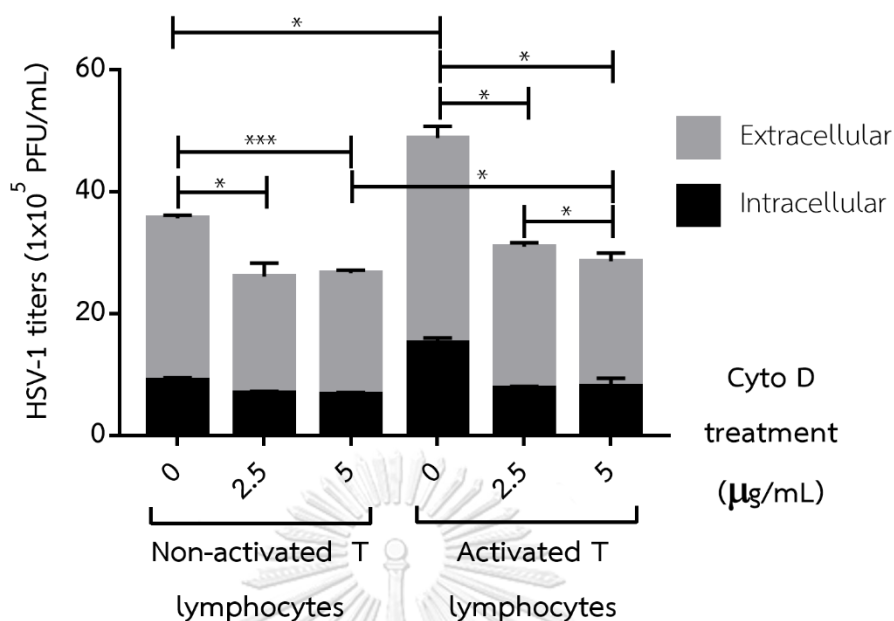
Activated and non-activated T lymphocytes were infected with HSV-1 at MOI of 10 for 15 minutes. Cell morphology was observed under transmission electron microscope (TEM) with magnification of 2,000x (left panel), 12,000x (right panel). (A) Activated T lymphocytes; (a1) HSV-1 bound on filopodia formation, (a2) HSV-1 entered into activated cell by fusion with cell membrane, (a3) HSV-1 entered into the cell via endocytosis (circle). (B) Non-activated T lymphocytes; (b1) HSV-1 attached to surface of non-activated T lymphocytes. Black arrow head indicated filopodia formation, red arrow indicated HSV-1 virion.

PART V: Effect of actin on the yield production of HSV-1 in activated T lymphocytes

Previous experiments indicated that actin expression was increased at 30 minutes after HSV-1 infection and the expression of Cdc42 in HSV-1-infected activated T lymphocytes was higher than in HSV-1-infected non-activated T lymphocytes. According to these results, actin may play role for HSV-1 entry in activated T lymphocytes. In order to determine whether the more HSV-1 entry, the more HSV-1 production should be. If actin played role in HSV-1 entry, HSV-1 titers from cyto D treated cells should be decreased. Activated T lymphocytes were treated with cyto D (0, 2.5 and 5 $\mu\text{g}/\text{mL}$) for 1 hour and were infected with HSV-1 at MOI of 10 for 24 hours. HSV-1 titers were measured by plaque titration assay. The results showed that, extracellular HSV-1 production was significantly higher than intracellular in every cell conditions including in cyto D treated conditions. At 0 $\mu\text{g}/\text{mL}$ of cyto D treatment (untreated cell), total HSV-1 titer from activated T lymphocytes was significantly higher than non-activated T lymphocytes (48.835 ± 2.805 vs 35.700 ± 0.070 , $p=0.0427$). After cyto D treatment, the reduction of HSV-1 production was observed in both activated and non-activated T cells. The mean HSV-1 titer from activated T lymphocytes treated with cyto D at 2.5 $\mu\text{g}/\text{mL}$ was still higher than non-activated T lymphocytes at the same concentration (31.020 ± 0.360 vs 26.140 ± 1.820). The significant difference of HSV-1 production was demonstrated at 5 $\mu\text{g}/\text{mL}$ of cyto D treatment (28.620 ± 0.080 vs 26.655 ± 0.185 , $p=0.0104$), respectively. The yield of total HSV-1 from cyto D untreated (0 $\mu\text{g}/\text{mL}$), activated T lymphocytes was significantly higher than cyto D treated, activated T lymphocytes at 2.5 and 5 $\mu\text{g}/\text{mL}$ (48.835 ± 2.805 vs 31.020 ± 0.360 and 28.620 ± 0.080 , $p=0.0243$ and 0.0187 , respectively). Similar observation was also observed in non-activated T lymphocytes (35.700 ± 0.070 vs 26.140 ± 1.820 and 26.655 ± 0.185 , $p=0.0344$ and 0.0005 , respectively). Moreover, total HSV-1 production from 2.5 $\mu\text{g}/\text{mL}$ cyto D treated, activated T lymphocytes was significantly decreased at 5 $\mu\text{g}/\text{mL}$ treatment (31.020 ± 0.360 vs 28.620 ± 0.080 , $p=0.0228$) while the viral production from 2.5 and 5

$\mu\text{g/mL}$ of cyto D treated, non-activated T lymphocytes were not different (Figure 29). According to these results, the percentage of plaque reduction after cyto D treatment was calculated. HSV-1 titers from 2.5 and 5 $\mu\text{g/mL}$ cyto D treated, activated and non-activated T lymphocytes were compared with untreated, activated or non-activated T lymphocytes. The results indicated that the percentage of plaque reduction from activated T lymphocytes was higher than non-activated T lymphocytes at both of cyto D concentrations, especially in 5 $\mu\text{g/mL}$ of cyto D treatment, the percentage of plaque reduction from activated T lymphocytes was significantly higher (15.85%) than non-activated T lymphocytes (Figure 30). Therefore, HSV-1 titer from activated T lymphocytes was higher than non-activated T lymphocytes and the production of HSV-1 was decreased as dose responsive curve related to cyto D treatment concentrations.

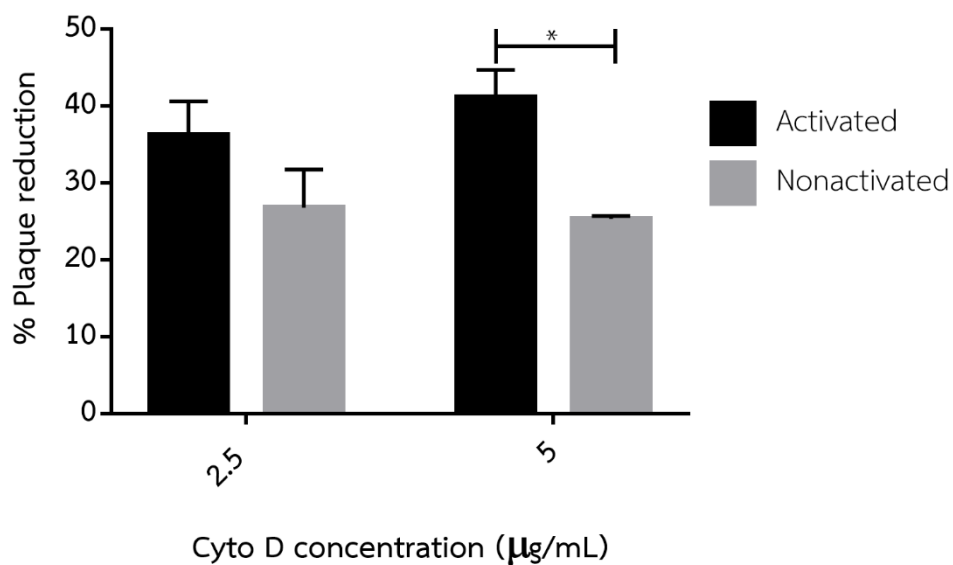




| Cyto D concentration | HSV-1 titers (Mean±SEM x10 ⁵ PFU/mL) | | | | | |
|----------------------|---|-----------------|------------------|------------------|------------------|------------------|
| | Intracellular | | Extracellular | | Total | |
| | Activated | Non-activated | Activated | Non-activated | Activated | Non-activated |
| 0 µg/mL | 15.145 ±0.870 | 9.070 ±0.430 | 33.688 ±1.938 | 26.625 ±0.500 | 48.835 ±2.805 | 35.700 ±0.070 |
| 2.5 µg/mL | 7.795 ±0.295 | 6.906 ±0.346 | 23.220 ±0.655 | 19.231 ±2.169 | 31.020 ±0.360 | 26.140 ±1.820 |
| 5 µg/mL | 8.033 ±1.418 | 6.776 ±0.311 | 20.588 ±1.338 | 19.875 ±0.500 | 28.620 ±0.080 | 26.655 ±0.185 |

Figure 29. The role of actin in HSV-1-infected, activated T lymphocytes after cyto D treatment.

Activated and non-activated T lymphocytes were treated with cyto D (0, 2.5 and 5 µg/mL) and were infected with HSV-1 at MOI of 10 for 24 hours. The viral titer was measured by plaque titration assay. Asterisks indicate significant difference ($p < 0.05$, unpaired t-test). Errors bars represent SEM. The experiment was done in two independent experiments and duplication each.



| Cyto D concentration | Percent plaque reduction (Mean±SEM) | |
|----------------------|-------------------------------------|-----------------------------|
| | Activated T lymphocytes | Non-activated T lymphocytes |
| 2.5 µg/mL | 36.235±4.405 | 26.795±4.965 |
| 5 µg/mL | 41.195±3.535 | 25.345±0.375 |

Figure 30. Percentage of plaque reduction after cyto D treatment.

Asterisks indicate significant difference ($p < 0.05$, unpaired t-test). Errors bars represent SEM. The experiment was done in two independent experiments and duplication each.

CHAPTURE VI

DISCUSSION

HSV-1 replication in T lymphocytes has been reported by several studies (15, 16, 133, 134) and the production of HSV-1 in T lymphocytes was increased after cell activation (17, 133). This phenomenon may mimic *in vivo* situation leading to severe symptoms due to systemic or disseminated infection especially in immunocompromised host. For example, in HIV-infected individuals, HSV viremia was commonly found. One hypothesis is that during HSV reactivation, the virus may spread into blood and multiply in their T lymphocytes which were already activated (136, 137) leading to viremia stage. An *ex vivo* study evaluated HSV-1 titers in HIV-infected PBMCs patients compared to normal healthy donors. The results showed that HSV-1 titers from HIV-PBMCs patients was higher than those from normal related to the number of activated CD3⁺CD38⁺T cells, i.e., 46.51±17.54 vs 27.54±14.12, respectively (138).

The mechanisms that support increased HSV growth in activated T lymphocytes are still unclear. However, enhanced viral entry step was suggested to be one mechanism due to upregulation of HVEA, a HSV receptor, mRNA expression was demonstrated in PHA activated T lymphocytes (17). Exploration on this entry step was attempted. In this study, Jurkat T lymphocytes were activated by anti-CD3/CD28 antibodies. Growth of activated and non-activated Jurkat T cells increased exponentially from 24 hours after activation and stayed stationary phase after 72 hours but the mean growth rate of activated T lymphocytes was slightly lower than that of non-activated T lymphocytes without statistically significant difference (Figure 12). In general, T lymphocytes were proliferated after activation (144) thus higher number of activated cells were expected. The possible explanation of this phenomenon may be due to apoptosis induction. It has been reported that signaling through CD3/TCR complex could induce apoptosis activation in T cell, hybridomas and leukemic cells (145). Therefore, anti-CD3/CD28 activation may induce cell apoptosis.

Since several clones of Jurkat cells are available, the characteristic of Jurkat clone in this study was demonstrated as 97.2% were CD3⁺CD4⁻CD8⁻ (double negative; DN) T lymphocytes (Figure 13). In general, most T lymphocytes normally expressed CD3 molecule on their surface. Two major T cell subsets were CD4⁺ and CD8⁺ T lymphocytes (128) but in some case, CD4 and/or CD8 down-modulation was found, for example, CD4 down regulation in HIV infected patients (146-148). However, DN T cells may also arise *de novo* in blood circulation (149, 150). As previous study using these DN T lymphocytes showed HSV-1 titers were increased after activation (11). Hence, CD3⁺CD4⁻CD8⁻ T lymphocytes were further used.

There were several molecules that express on the surface of activated T lymphocytes, which discriminates from naïve T lymphocytes such as adhesion molecules, receptors, co-stimulatory molecules, chemokine receptors and MHC class II molecules (130). Therefore, the activated Jurkat T cells in this study were phenotypic characterized for the presence of activation markers, i.e., CD69 and CD137 (Figure 14). CD69 was quickly induced on T lymphocytes surface after TCR/CD3 engagement and was also over expressed after 1 hour of anti-CD3/CD28 activation (129, 151, 152). Several study reported that CD137 was up-regulated from 12 hours to up to 5 days after activation (153-155). To make sure that the activation process was succeeded, Jurkat cells were activated by anti-CD3/CD28 at 24, 48 and 72 hours. The expression of CD69 and CD137 was detected in Jurkat T cells comparing with PBMCs after activation. Increase number of Jurkat positive CD69 were observed at 24 hours (8.5%) and 72 hours (3.5%) after stimulation while PBMC showed slightly decrease (0.1%) at 24 hours and increase at 48 (14.48%) and 72 hours (1.42%) (Figure 14). These results contradicted from previous study showing that CD69 expression in PHA-activated PBMCs were maximum increased at 24 hours post-stimulation and stabled till the 72 hours activation period (156). This might be due to different kind of the stimulator. However, median fluorescence intensities (MFI) of CD69 in both Jurkat cells and PBMC were increased at every time point indicating increase of CD69 molecules on surface of the cells. CD137 expression in

stimulated PBMCs were shown similar to CD69 expression while CD137 in activated Jurkat cells showed different. Instead of increase MFI at every time point, CD137 expression was decreased at 72 hours. Previous study showed that CD137 was widely expressed on activated CD8⁺ T lymphocytes (157). This implied that CD137 may not a good activation marker for CD3⁺CD4⁻CD8⁻ T lymphocytes. Other 2 activation markers (CD38 and HLA-DR) were also determined. CD38 was previously reported to be presented on the surface of Jurkat cells (27) while the expression of HLA-DR on human T cells has been regarded primarily as a marker of activated T cells (19, 28). Although the number of CD38⁺ cells and HLA-DR⁺ cells were increased, expression of HLA-DR molecules was barely increased and decrease expression of CD38 molecules was found (Table 4). From all results, the Jurkat used in this study already had CD38 and CD69 presented on their surface while had few HLA-DR. Moreover, CD69 is a good activation marker for anti-CD3/CD28 stimulation in CD3⁺CD4⁻CD8⁻ Jurkat cells at 72 hours since highly increasing MFI of CD69 on Jurkat cells after activation was detected.

The highest yield of HSV-1 production in Jurkat T lymphocytes was at 24 hours post infection in both activated and non-activated cells and then declined afterwards (48 and 72 hpi). However, yield of HSV-1 production in activated T lymphocytes was significantly higher than that found in non-activated cells at 24 hpi (Figure 15), similar to previous study (18). Increased yield of HSV-1 production in activated cells may be due to increased expression of HVEA (17), which, in turn, enhances the viral entry. Detection of ICP4 mRNA, immediate early gene expression of HSV was previously demonstrated in activated T cells 2 hours before that in non-activated T cells, suggesting that there were some factors supporting virus growth presented in the activated cells but not in non-activated cells (18). In addition, the number of HSV-1 virions production from activated and non-activated T lymphocytes were more extracellular than intracellular. This results contradicted with the study in epithelial cells showing that HSV-1 progenies normally attached within the cells and usually disseminated to other cells by cell-to-cell contact (158).

During HSV entry, one of mechanisms supporting HSV-1 uptake in neuronal, fibroblast and epithelial cells was filopodia formation (104, 115, 116, 140). This structure facilitated HSV-1 virions attachment and then surfing toward the cell body. Heparan sulfate (HS), a HSV-1 glycoprotein B receptor, widely expressed on filopodia (27). After HSV-1 attachment on filopodia, underlying cytoskeleton rearrangement was essential for viral surfing along this structure (159). The essential component for filopodia construction was actin which was polymerized toward along the filopodia to increase the length (14, 104). Hence, β -actin mRNA expression in HSV-1 infected activated T lymphocytes was observed. Although β -actin expression was used as housekeeping genes in most kind of cells, expression of this gene was different in various stage of T lymphocytes, especially upon activation (160, 161). In this study, β -actin mRNA expression was observed in anti-CD3/CD28 activated T lymphocytes infected with HSV-1 at MOI of 10 for 30 minutes. Although the expression of this gene between HSV-1 infected and non-infected cells was not significant different, the expression trend was increased as expected after HSV-1 infection in both activated and non-activated T lymphocytes (Figure 16) supported that HSV-1 can induce filopodia formation. As predicted, the β -actin protein expression was also overexpressed after HSV-1 infection in both activated and non-activated T lymphocytes and significant difference was observed between HSV-1 infected and non-infected-activated T lymphocytes (Figure 19). This implied that HSV-1 infection induced β -actin overexpression which may result in cytoskeletal rearrangement in the cells. A study of pseudorabies virus (PRB), a member of alpha-herpesviruses, also induced cytoskeletal rearrangement when the virus bound to its receptor (162). In addition, HSV-1 and PRB induce the formation of actin filaments in nucleus of neurons at 12 hpi has been reported (163). However, in this study, actin expression was shown to upregulate very early after viral attachment, i.e., 30 minutes post-infection. This indicated that overexpression of actin protein and/or actin polymerization may play role in HSV-1 entry. To observe the role of actin polymerization, the cells were treated with cytochalasin D (cyto D), an inhibitor of actin polymerization and depolymerization of actin filaments formed (164) using two

concentrations, 2.5 and 5 $\mu\text{g}/\text{mL}$ (Figure 17-18). Significant reduction of β -actin was observed in HSV-1 infected Cyto D treated activated T cells at 2.5 or 5 $\mu\text{g}/\text{mL}$ compared to HSV-1 infected non-treated cytoD activated T cells (Figure 19). This indicated that actin polymerization was induced by HSV-1 infection at very early of viral attachment. Due to the increase of actin polymerization, HSV-1 may induce filopodia formation in T lymphocytes as same as in epithelial, neuronal and fibroblast cells (27, 28, 115).

Several studies revealed that HSV induced actin cytoskeleton rearrangement to supporting their infectivity in epithelial cells (162, 163). This rearrangement recruited a number of actin bundles to interact together, called actin network. Three basic types of actin networks were stress fibers, filopodia and lamellipodia (11). Rho GTPase activity, including Cdc42, RhoA and Rac1, was essential to generate these actin network structures. Cdc42 induced the formation of filopodia. RhoA regulated stress fibers whereas Rac1 triggered lamellipodia (165). Here, Cdc42 expression was slightly increased in activated T lymphocytes after HSV-1 infection meanwhile the expression in non-activated T lymphocytes was slightly decreased after HSV-1 infection. Interestingly, after HSV-1 infection, Cdc42 expression in activated cells was significant higher than that in non-activated cells (Figure 20). Significant difference in RhoA and Rac1 expression were not observed after HSV-1 infection in both activated and non-activated cells (Figure 21 and 22). These results indicated that filopodia formation were induced by HSV-1 infection through Cdc42 similar to those in epithelial, neural and fibroblast cells. Several studies reported the role of Cdc42 in viral entry. Actin cytoskeleton rearrangement via Cdc42 activation was found in human herpesvirus-8, Epstein-Barr (EBV), influenza, HIV-1, dengue (type 2) and respiratory syncytial virus (RSV) infected cells (107, 166-171). Previous studies revealed that not only filopodia formation but also HSV-1 infection were decreased in Cdc42 downregulated HeLa cells (27). Similar results were demonstrated in HIV infected immature dendritic cell when cdc42 was inhibited (170). Moreover, Cdc42 and Rac1 were activated by signaling through nectin, HSV-1 receptor which widely expresses on epithelial, neural and fibroblast cells, leading to filopodia and

lamellipodia formation (172, 173). In contrast to nectin, signaling through HVEA, a HSV-1 receptor on T lymphocytes, may activate Cdc42 only.

HSV surfing on filopodia, a significant characteristic of HSV entry was demonstrated in HSV infected neuronal, fibroblast and epithelial cells (104, 115, 116, 140). The binding of HSV-1 gB and heparan sulfate (HS), an attachment receptor for HSV-1, on filopodia surface allows virus to surf along the length of filopodia (27, 139). Moreover, upon T cells activation, cytoskeletal actin reorganizes dramatically, resulting in protrusion of filopodia and lamellipodia has been reported (174). Signaling through CD28 can induce filopodia formation (175). Thus, in this study small number of filopodia (11%) was shown possibly from anti-CD3/CD28 activation process. However, HSV-1 increases the formation of filopodia (30%) in activated T cells. None of filopodia was found in non-activated with and without HSV-1 infection (Figure 26). Filopodia constructed from actin polymerization were demonstrated by co-staining of actin and HSV antigens on the same filopodia. Adding cyto D to inhibit actin polymerization, the filopodia formation were not seen (Figure 27), confirming the role of actin in HSV-1 infection in activated T lymphocytes.

In addition, morphology change in the activated T cells during HSV-1 entry was observed under electron microscope. Actin cytoskeleton rearrangement triggered cell morphology changing in activated T cells allowed the formation of the immune synapse and formation of the scaffold for signaling components (176, 177). Not surprisingly, morphology of T lymphocytes was changed after activation and dramatically changed after HSV-1 infection, especially filopodia formation. This experiment confirmed HSV-1 induced filopodia formation in activated T lymphocytes. Moreover, HSV-1 may hijack filopodia on those activated cells supporting their infectivity (Figure 28A). Intracellular HSV-1 virions were observed in activated cells after 30 minutes of inoculation but none of intracellular virions were found in non-activated cells (Figure 28A-B). This indicate that activated cells were more susceptible for HSV-1 entry than non-activated cell. This may be due to the upregulation of HVEA expression together with actin polymerization to form filopodia (17, 18). In

addition, the EM results suggested that HSV-1 may enter into activated T cells via multiple pathways, including endocytosis and fusion. In epithelial and fibroblast cells, HSV-1 preferred one of these mechanisms to enter. HSV preferred fusion with plasma membrane to enter into Vero cells, human neurons, human foreskin fibroblasts and Hep-2 cells (65-67) but entered into retinal pigment epithelial cells, human conjunctival epithelial cells, human epidermal keratinocytes and HeLa cells by endocytosis (62, 68). Decrease in the yield of HSV-1 production after Cyto D treatment in activated T cells was demonstrated (Figure 29-30). Cyto D provided negative affected in filopodia formation by inhibiting actin polymerization which affected HSV-1 entry (30).

In conclusion, this study showed HSV-1 induced filopodia formation through actin polymerization using Cdc42 signaling pathway. The presence of filopodia in activated T lymphocytes enhanced the viral entry into the cells resulting in increase of HSV-1 production in activated T lymphocytes. Increase HSV-1 uptake was previously demonstrated due to upregulate HVEA expression in activated T lymphocytes (17). Moreover, the virion production in T lymphocytes was released mainly extracellular. This phenomenon may be a key mechanism in explaining pathogenesis of HSV dissemination in patients with HSV viremia, especially immunocompromised hosts. Thus, this is the first study revealed that entry step of HSV-1 in activated T lymphocytes was similar to those epithelial, fibroblast and neuron cells.

It would be interesting to further investigate the expression of HS on filopodia of activated T lymphocytes. Likewise, if HS play role in HSV attachment on filopodia of epithelial and neuron cells, this molecule will be a key molecule for HSV infection in T lymphocytes. Reducing viral entry by blocking this attachment step is previously demonstrated in epithelial cells. Heparinase treatment provide negative effect for HSV-1 entry since HS which widely express on filopodia are removed after treatment (178). Tiwari et al. (2011) demonstrated that HSV-1 infection is blocked by anti-HS peptides (179). Moreover, the similar result has been demonstrated by using the low

molecular weight Heparan sulfate-mimetic (180). In addition, this study also revealed that endocytosis or fusion beside filopodia formation might be also play role on HSV-1 entry in activated T lymphocytes. Further investigation of those pathways may be helpful in understanding HSV pathogenesis.





จุฬาลงกรณ์มหาวิทยาลัย
CHULALONGKORN UNIVERSITY

REFERENCES

1. Slifer CM, Jennings SR. Battling the spread: Herpes simplex virus and encephalitis. *Immunology and cell biology*. 2015;93(10):839-40.
2. Crane LR, Lerner AM. Herpetic whitlow: a manifestation of primary infection with herpes simplex virus type 1 or type 2. *The Journal of infectious diseases*. 1978;137(6):855-6.
3. Pardo J, Yogev Y, Ben-Haroush A, Hod M, Amir J. Primary herpes simplex virus type 1 gingivostomatitis during the second and third trimester of pregnancy: foetal and pregnancy outcome. *Scandinavian journal of infectious diseases*. 2004;36(3):179-81.
4. Berkovich S, Ressel M. Neonatal herpes keratitis. *The Journal of pediatrics*. 1966;69(4):652-3.
5. Acheson NH. *Fundamentals of Molecular Virology*. 2nd ed: John Wiley & Sons, INC.; 2011.
6. Brooks GF, Carroll KC, Butel JS, Morse SA, Mietzner TA. *Medical Microbiology*. 27th ed: McGraw-Hill Education; 2013.
7. Agelidis AM, Shukla D. Cell entry mechanisms of HSV: what we have learned in recent years. *Future virology*. 2015;10(10):1145-54.
8. Weihing RR. The cytoskeleton and plasma membrane. *Methods and achievements in experimental pathology*. 1979;8:42-109.
9. Weber K, Osborn M. Cytoskeleton: definition, structure and gene regulation. *Pathology, research and practice*. 1982;175(2-3):128-45.
10. Simiczyjew A, Pietraszek-Gremplewicz K, Mazur AJ, Nowak D. Are non-muscle actin isoforms functionally equivalent? *Histology and histopathology*. 2017:11896.
11. Roberts KL, Baines JD. Actin in herpesvirus infection. *Viruses*. 2011;3(4):336-46.
12. Perrin BJ, Ervasti JM. The actin gene family: function follows isoform. *Cytoskeleton*. 2010;67(10):630-4.
13. Harborth J, Elbashir SM, Bechert K, Tuschl T, Weber K. Identification of essential genes in cultured mammalian cells using small interfering RNAs. *Journal of cell science*. 2001;114(Pt 24):4557-65.

14. Mattila PK, Lappalainen P. Filopodia: molecular architecture and cellular functions. *Nature reviews Molecular cell biology*. 2008;9(6):446-54.
15. Teute H, Braun R, Kirchner H, Becker H, Munk K. Replication of herpes simplex virus in human T lymphocytes. *Intervirology*. 1983;20(1):32-41.
16. Bhattarakosol P, Chirathaworn C, Chomma P. Replication of herpes simplex virus in T lymphocytes. *Journal of the Medical Association of Thailand = Chotmaihet thangphaet*. 2002;85 Suppl 1:S399-406.
17. Chomma P, Chirathaworn C, Bhattarakosol P. Increased susceptibility of herpes simplex virus-1 growth in phytohemagglutinin-activated T lymphocytes caused by upregulation of herpesvirus entry mediator A mRNA expression. *Intervirology*. 2004;47(1):14-8.
18. Bhattarakosol P, Donchai P. One of the Mechanisms to Increase HSV-1 Uptake in HSV-1-Infected, Activated T Lymphocytes Is the Formation of Filopodia. *Intervirology*. 2015;58(4):209-17.
19. Bernard NF, Howley PM, Griffin DE, Lamb RA, Martin MA, Roizman B, et al. *Fields Virology* 4th ed: Lippincott Williams & Wilkins Publishers; 2001.
20. Roizman B, Baines J. The diversity and unity of Herpesviridae. *Comparative immunology, microbiology and infectious diseases*. 1991;14(2):63-79.
21. Duran N. [Genital herpes infections]. *Mikrobiyoloji bulteni*. 2003;37(2-3):205-13.
22. Pinninti SG, Kimberlin DW. Neonatal herpes simplex virus infections. *Seminars in perinatology*. 2018. CHULALONGKORN UNIVERSITY
23. Huber MA. Herpes simplex type-1 virus infection. *Quintessence international*. 2003;34(6):453-67.
24. กัทรโกศล ภ. โรคเริม เพื่อนตายของมนุษย์. 1st ed: ศรีเมืองการพิมพ์; 2561.
25. Roizman B, Carmichael LE, Deinhardt F, de-The G, Nahmias AJ, Plowright W, et al. Herpesviridae. Definition, provisional nomenclature, and taxonomy. The Herpesvirus Study Group, the International Committee on Taxonomy of Viruses. *Intervirology*. 1981;16(4):201-17.
26. Epstein MA. Observations on the fine structure of mature herpes simplex virus and on the composition of its nucleoid. *The Journal of experimental medicine*. 1962;115:1-12.

27. Oh MJ, Akhtar J, Desai P, Shukla D. A role for heparan sulfate in viral surfing. *Biochemical and biophysical research communications*. 2010;391(1):176-81.
28. Clement C, Tiwari V, Scanlan PM, Valyi-Nagy T, Yue BY, Shukla D. A novel role for phagocytosis-like uptake in herpes simplex virus entry. *The Journal of cell biology*. 2006;174(7):1009-21.
29. Geraghty RJ, Krummenacher C, Cohen GH, Eisenberg RJ, Spear PG. Entry of alphaherpesviruses mediated by poliovirus receptor-related protein 1 and poliovirus receptor. *Science*. 1998;280(5369):1618-20.
30. Warner MS, Geraghty RJ, Martinez WM, Montgomery RI, Whitbeck JC, Xu R, et al. A cell surface protein with herpesvirus entry activity (HveB) confers susceptibility to infection by mutants of herpes simplex virus type 1, herpes simplex virus type 2, and pseudorabies virus. *Virology*. 1998;246(1):179-89.
31. Karasneh GA, Shukla D. Herpes simplex virus infects most cell types in vitro: clues to its success. *Virology journal*. 2011;8:481.
32. Lopez M, Cocchi F, Menotti L, Avitabile E, Dubreuil P, Campadelli-Fiume G. Nectin2alpha (PRR2alpha or HveB) and nectin2delta are low-efficiency mediators for entry of herpes simplex virus mutants carrying the Leu25Pro substitution in glycoprotein D. *Journal of virology*. 2000;74(3):1267-74.
33. Krummenacher C, Baribaud F, Ponce de Leon M, Baribaud I, Whitbeck JC, Xu R, et al. Comparative usage of herpesvirus entry mediator A and nectin-1 by laboratory strains and clinical isolates of herpes simplex virus. *Virology*. 2004;322(2):286-99.
34. Kovacs SK, Tiwari V, Prandovszky E, Dosa S, Bacsa S, Valyi-Nagy K, et al. Expression of herpes virus entry mediator (HVEM) in the cornea and trigeminal ganglia of normal and HSV-1 infected mice. *Current eye research*. 2009;34(10):896-904.
35. Montgomery RI, Warner MS, Lum BJ, Spear PG. Herpes simplex virus-1 entry into cells mediated by a novel member of the TNF/NGF receptor family. *Cell*. 1996;87(3):427-36.
36. Kwon BS, Tan KB, Ni J, Oh KO, Lee ZH, Kim KK, et al. A newly identified member of the tumor necrosis factor receptor superfamily with a wide tissue distribution and involvement in lymphocyte activation. *The Journal of biological chemistry*. 1997;272(22):14272-6.

37. Hung SL, Cheng YY, Wang YH, Chang KW, Chen YT. Expression and roles of herpesvirus entry mediators A and C in cells of oral origin. *Oral microbiology and immunology*. 2002;17(4):215-23.
38. Compaan DM, Gonzalez LC, Tom I, Loyet KM, Eaton D, Hymowitz SG. Attenuating lymphocyte activity: the crystal structure of the BTLA-HVEM complex. *The Journal of biological chemistry*. 2005;280(47):39553-61.
39. Croft M. The evolving crosstalk between co-stimulatory and co-inhibitory receptors: HVEM-BTLA. *Trends in immunology*. 2005;26(6):292-4.
40. Mauri DN, Ebner R, Montgomery RI, Kochel KD, Cheung TC, Yu GL, et al. LIGHT, a new member of the TNF superfamily, and lymphotoxin alpha are ligands for herpesvirus entry mediator. *Immunity*. 1998;8(1):21-30.
41. Zhang N, Yan J, Lu G, Guo Z, Fan Z, Wang J, et al. Binding of herpes simplex virus glycoprotein D to nectin-1 exploits host cell adhesion. *Nature communications*. 2011;2:577.
42. Allen SJ, Mott KR, Ghiasi H. Overexpression of herpes simplex virus glycoprotein K (gK) alters expression of HSV receptors in ocularly-infected mice. *Investigative ophthalmology & visual science*. 2014;55(4):2442-51.
43. Allen SJ, Rhode-Kurnow A, Mott KR, Jiang X, Carpenter D, Rodriguez-Barbosa JI, et al. Interactions between herpesvirus entry mediator (TNFRSF14) and latency-associated transcript during herpes simplex virus 1 latency. *Journal of virology*. 2014;88(4):1961-71.
44. O'Donnell CD, Shukla D. A novel function of heparan sulfate in the regulation of cell-cell fusion. *The Journal of biological chemistry*. 2009;284(43):29654-65.
45. Shukla D, Spear PG. Herpesviruses and heparan sulfate: an intimate relationship in aid of viral entry. *The Journal of clinical investigation*. 2001;108(4):503-10.
46. O'Donnell CD, Tiwari V, Oh MJ, Shukla D. A role for heparan sulfate 3-O-sulfotransferase isoform 2 in herpes simplex virus type 1 entry and spread. *Virology*. 2006;346(2):452-9.
47. Xu D, Tiwari V, Xia G, Clement C, Shukla D, Liu J. Characterization of heparan sulphate 3-O-sulphotransferase isoform 6 and its role in assisting the entry of herpes simplex virus type 1. *The Biochemical journal*. 2005;385(Pt 2):451-9.

48. Tiwari V, Clement C, Duncan MB, Chen J, Liu J, Shukla D. A role for 3-O-sulfated heparan sulfate in cell fusion induced by herpes simplex virus type 1. *The Journal of general virology*. 2004;85(Pt 4):805-9.
49. Xia G, Chen J, Tiwari V, Ju W, Li JP, Malmstrom A, et al. Heparan sulfate 3-O-sulfotransferase isoform 5 generates both an antithrombin-binding site and an entry receptor for herpes simplex virus, type 1. *The Journal of biological chemistry*. 2002;277(40):37912-9.
50. Tiwari V, Tarbutton MS, Shukla D. Diversity of heparan sulfate and HSV entry: basic understanding and treatment strategies. *Molecules*. 2015;20(2):2707-27.
51. Tiwari V, Clement C, Xu D, Valyi-Nagy T, Yue BY, Liu J, et al. Role for 3-O-sulfated heparan sulfate as the receptor for herpes simplex virus type 1 entry into primary human corneal fibroblasts. *Journal of virology*. 2006;80(18):8970-80.
52. Yakoub AM, Rawal N, Maus E, Baldwin J, Shukla D, Tiwari V. Comprehensive analysis of herpes simplex virus 1 (HSV-1) entry mediated by zebrafish 3-O-Sulfotransferase isoforms: implications for the development of a zebrafish model of HSV-1 infection. *Journal of virology*. 2014;88(21):12915-22.
53. Tiwari V, O'Donnell C, Copeland RJ, Scarlett T, Liu J, Shukla D. Soluble 3-O-sulfated heparan sulfate can trigger herpes simplex virus type 1 entry into resistant Chinese hamster ovary (CHO-K1) cells. *The Journal of general virology*. 2007;88(Pt 4):1075-9.
54. Campadelli-Fiume CF, Menotti L, Lopez M. The novel receptors that mediate the entry of herpes simplex viruses and animal alphaherpesviruses into cells. *Reviews in medical virology*. 2000.
55. Heldwein EE, Lou H, Bender FC, Cohen GH, Eisenberg RJ, Harrison SC. Crystal structure of glycoprotein B from herpes simplex virus 1. *Science*. 2006;313(5784):217-20.
56. Satoh T, Arase H. HSV-1 infection through inhibitory receptor, PILRalpha. *Uirusu*. 2008;58(1):27-36.
57. Suenaga T, Satoh T, Somboonthum P, Kawaguchi Y, Mori Y, Arase H. Myelin-associated glycoprotein mediates membrane fusion and entry of neurotropic herpesviruses. *Proceedings of the National Academy of Sciences of the United States of America*. 2010;107(2):866-71.

58. Gianni T, Salvioli S, Chesnokova LS, Hutt-Fletcher LM, Campadelli-Fiume G. alphavbeta6- and alphavbeta8-integrins serve as interchangeable receptors for HSV gH/gL to promote endocytosis and activation of membrane fusion. *PLoS pathogens*. 2013;9(12):e1003806.
59. Turner A, Bruun B, Minson T, Browne H. Glycoproteins gB, gD, and gH/gL of herpes simplex virus type 1 are necessary and sufficient to mediate membrane fusion in a Cos cell transfection system. *Journal of virology*. 1998;72(1):873-5.
60. Pertel PE, Fridberg A, Parish ML, Spear PG. Cell fusion induced by herpes simplex virus glycoproteins gB, gD, and gH-gL requires a gD receptor but not necessarily heparan sulfate. *Virology*. 2001;279(1):313-24.
61. Muggeridge MI. Characterization of cell-cell fusion mediated by herpes simplex virus 2 glycoproteins gB, gD, gH and gL in transfected cells. *The Journal of general virology*. 2000;81(Pt 8):2017-27.
62. Nicola AV, Straus SE. Cellular and viral requirements for rapid endocytic entry of herpes simplex virus. *Journal of virology*. 2004;78(14):7508-17.
63. Nicola AV, McEvoy AM, Straus SE. Roles for endocytosis and low pH in herpes simplex virus entry into HeLa and Chinese hamster ovary cells. *Journal of virology*. 2003;77(9):5324-32.
64. Stefan Pohlmann GS. *Viral entry into host cell. Entry of herpesviruses into cell*. New York: Springer; 2013.
65. Lycke E, Hamark B, Johansson M, Krotochwil A, Lycke J, Svennerholm B. Herpes simplex virus infection of the human sensory neuron. An electron microscopy study. *Archives of virology*. 1988;101(1-2):87-104.
66. Nicola AV, Hou J, Major EO, Straus SE. Herpes simplex virus type 1 enters human epidermal keratinocytes, but not neurons, via a pH-dependent endocytic pathway. *Journal of virology*. 2005;79(12):7609-16.
67. Nicolai R, Cortis E, Rava L, Bracaglia C, Pardeo M, Insalaco A, et al. Herpes Virus Infections During Treatment With Etanercept in Juvenile Idiopathic Arthritis. *Journal of the Pediatric Infectious Diseases Society*. 2016;5(1):76-9.
68. Akhtar J, Shukla D. Viral entry mechanisms: cellular and viral mediators of herpes simplex virus entry. *The FEBS journal*. 2009;276(24):7228-36.

69. Milne RS, Nicola AV, Whitbeck JC, Eisenberg RJ, Cohen GH. Glycoprotein D receptor-dependent, low-pH-independent endocytic entry of herpes simplex virus type 1. *Journal of virology*. 2005;79(11):6655-63.
70. Penfold ME, Armati P, Cunningham AL. Axonal transport of herpes simplex virions to epidermal cells: evidence for a specialized mode of virus transport and assembly. *Proceedings of the National Academy of Sciences of the United States of America*. 1994;91(14):6529-33.
71. O'Hare P, Hayward GS. Three trans-acting regulatory proteins of herpes simplex virus modulate immediate-early gene expression in a pathway involving positive and negative feedback regulation. *Journal of virology*. 1985;56(3):723-33.
72. Cai W, Astor TL, Liptak LM, Cho C, Coen DM, Schaffer PA. The herpes simplex virus type 1 regulatory protein ICP0 enhances virus replication during acute infection and reactivation from latency. *Journal of virology*. 1993;67(12):7501-12.
73. Phelan A, Dunlop J, Patel AH, Stow ND, Clements JB. Nuclear sites of herpes simplex virus type 1 DNA replication and transcription colocalize at early times postinfection and are largely distinct from RNA processing factors. *Journal of virology*. 1997;71(2):1124-32.
74. Samaniego LA, Webb AL, DeLuca NA. Functional interactions between herpes simplex virus immediate-early proteins during infection: gene expression as a consequence of ICP27 and different domains of ICP4. *Journal of virology*. 1995;69(9):5705-15.
75. Post LE, Roizman B. A generalized technique for deletion of specific genes in large genomes: alpha gene 22 of herpes simplex virus 1 is not essential for growth. *Cell*. 1981;25(1):227-32.
76. Hill A, Jugovic P, York I, Russ G, Bennink J, Yewdell J, et al. Herpes simplex virus turns off the TAP to evade host immunity. *Nature*. 1995;375(6530):411-5.
77. Gao M, Knipe DM. Potential role for herpes simplex virus ICP8 DNA replication protein in stimulation of late gene expression. *Journal of virology*. 1991;65(5):2666-75.
78. Travis J Taylor MAB EEMaDMK. Herpes simplex virus. *Frontiers in Biosciences*. 2002;7.
79. Weller SK, Coen DM. Herpes simplex viruses: mechanisms of DNA replication.

Cold Spring Harbor perspectives in biology. 2012;4(9):a013011.

80. Steiner I, Kennedy PG, Pachner AR. The neurotropic herpes viruses: herpes simplex and varicella-zoster. *The Lancet Neurology*. 2007;6(11):1015-28.
81. Kramer T, Enquist LW. Directional spread of alphaherpesviruses in the nervous system. *Viruses*. 2013;5(2):678-707.
82. Saleh D, Bermudez R. Herpes, Simplex, Type 1. *StatPearls*. Treasure Island (FL)2018.
83. Scherer J, Yaffe ZA, Vershinin M, Enquist LW. Dual-color Herpesvirus Capsids Discriminate Inoculum from Progeny and Reveal Axonal Transport Dynamics. *Journal of virology*. 2016.
84. Deshmane SL, Fraser NW. During latency, herpes simplex virus type 1 DNA is associated with nucleosomes in a chromatin structure. *Journal of virology*. 1989;63(2):943-7.
85. Bloom DC, Giordani NV, Kwiatkowski DL. Epigenetic regulation of latent HSV-1 gene expression. *Biochimica et biophysica acta*. 2010;1799(3-4):246-56.
86. Thellman NM, Triezenberg SJ. Herpes Simplex Virus Establishment, Maintenance, and Reactivation: In Vitro Modeling of Latency. *Pathogens*. 2017;6(3).
87. Hafezi W, Lorentzen EU, Eing BR, Muller M, King NJ, Klupp B, et al. Entry of herpes simplex virus type 1 (HSV-1) into the distal axons of trigeminal neurons favors the onset of nonproductive, silent infection. *PLoS pathogens*. 2012;8(5):e1002679.
88. Conn KL, Schang LM. Chromatin dynamics during lytic infection with herpes simplex virus 1. *Viruses*. 2013;5(7):1758-86.
89. Mador N, Goldenberg D, Cohen O, Panet A, Steiner I. Herpes simplex virus type 1 latency-associated transcripts suppress viral replication and reduce immediate-early gene mRNA levels in a neuronal cell line. *Journal of virology*. 1998;72(6):5067-75.
90. Cliffe AR, Coen DM, Knipe DM. Kinetics of facultative heterochromatin and polycomb group protein association with the herpes simplex viral genome during establishment of latent infection. *mBio*. 2013;4(1).
91. Maillet S, Naas T, Crepin S, Roque-Afonso AM, Lafay F, Efstathiou S, et al. Herpes simplex virus type 1 latently infected neurons differentially express latency-associated and ICP0 transcripts. *Journal of virology*. 2006;80(18):9310-21.

92. Nicoll MP, Hann W, Shivkumar M, Harman LE, Connor V, Coleman HM, et al. The HSV-1 Latency-Associated Transcript Functions to Repress Latent Phase Lytic Gene Expression and Suppress Virus Reactivation from Latently Infected Neurons. *PLoS pathogens*. 2016;12(4):e1005539.
93. Perng GC, Jones C, Ciacci-Zanella J, Stone M, Henderson G, Yukht A, et al. Virus-induced neuronal apoptosis blocked by the herpes simplex virus latency-associated transcript. *Science*. 2000;287(5457):1500-3.
94. Gupta A, Gartner JJ, Sethupathy P, Hatzigeorgiou AG, Fraser NW. Anti-apoptotic function of a microRNA encoded by the HSV-1 latency-associated transcript. *Nature*. 2006;442(7098):82-5.
95. Thompson RL, Sawtell NM. Evidence that the herpes simplex virus type 1 ICP0 protein does not initiate reactivation from latency in vivo. *Journal of virology*. 2006;80(22):10919-30.
96. Knipe DM, Cliffe A. Chromatin control of herpes simplex virus lytic and latent infection. *Nature reviews Microbiology*. 2008;6(3):211-21.
97. Sonja Kuhn HGM. *The Actin Cytoskeleton and Bacterial Infection*: Springer International; 2017.
98. H L, A B, L ZS, P M, D B, J D. *Molecular Cell Biology*. 4th ed. New York: W. H. Freeman; 2000.
99. Bergeron SE, Zhu M, Thiem SM, Friderici KH, Rubenstein PA. Ion-dependent polymerization differences between mammalian beta- and gamma-nonmuscle actin isoforms. *The Journal of biological chemistry*. 2010;285(21):16087-95.
100. Welch MD, Mullins RD. Cellular control of actin nucleation. *Annual review of cell and developmental biology*. 2002;18:247-88.
101. Etienne-Manneville S, Hall A. Rho GTPases in cell biology. *Nature*. 2002;420(6916):629-35.
102. Hall A. Rho GTPases and the actin cytoskeleton. *Science*. 1998;279(5350):509-14.
103. Chimini G, Chavrier P. Function of Rho family proteins in actin dynamics during phagocytosis and engulfment. *Nature cell biology*. 2000;2(10):E191-6.
104. Chang K, Baginski J, Hassan SF, Volin M, Shukla D, Tiwari V. Filopodia and Viruses: An Analysis of Membrane Processes in Entry Mechanisms. *Frontiers in microbiology*.

2016;7:300.

105. Taylor MP, Koyuncu OO, Enquist LW. Subversion of the actin cytoskeleton during viral infection. *Nature reviews Microbiology*. 2011;9(6):427-39.
106. Quetglas JI, Hernaez B, Galindo I, Munoz-Moreno R, Cuesta-Geijo MA, Alonso C. Small rho GTPases and cholesterol biosynthetic pathway intermediates in African swine fever virus infection. *Journal of virology*. 2012;86(3):1758-67.
107. Xiang Y, Zheng K, Ju H, Wang S, Pei Y, Ding W, et al. Cofilin 1-mediated biphasic F-actin dynamics of neuronal cells affect herpes simplex virus 1 infection and replication. *Journal of virology*. 2012;86(16):8440-51.
108. Smith JL, Lidke DS, Ozburn MA. Virus activated filopodia promote human papillomavirus type 31 uptake from the extracellular matrix. *Virology*. 2008;381(1):16-21.
109. David AT, Baghian A, Foster TP, Chouljenko VN, Kousoulas KG. The herpes simplex virus type 1 (HSV-1) glycoprotein K(gK) is essential for viral corneal spread and neuroinvasiveness. *Current eye research*. 2008;33(5):455-67.
110. Farnsworth A, Johnson DC. Herpes simplex virus gE/gI must accumulate in the trans-Golgi network at early times and then redistribute to cell junctions to promote cell-cell spread. *Journal of virology*. 2006;80(7):3167-79.
111. Mothes W, Sherer NM, Jin J, Zhong P. Virus cell-to-cell transmission. *Journal of virology*. 2010;84(17):8360-8.
112. Watts KR, Morinaka BI, Amagata T, Robinson SJ, Tenney K, Bray WM, et al. Biostructural features of additional jaspakinolide (jaspamide) analogues. *Journal of natural products*. 2011;74(3):341-51.
113. Yarmola EG, Somasundaram T, Boring TA, Spector I, Bubb MR. Actin-latrunculin A structure and function. Differential modulation of actin-binding protein function by latrunculin A. *The Journal of biological chemistry*. 2000;275(36):28120-7.
114. Morton WM, Ayscough KR, McLaughlin PJ. Latrunculin alters the actin-monomer subunit interface to prevent polymerization. *Nature cell biology*. 2000;2(6):376-8.
115. Dixit R, Tiwari V, Shukla D. Herpes simplex virus type 1 induces filopodia in differentiated P19 neural cells to facilitate viral spread. *Neuroscience letters*. 2008;440(2):113-8.

116. Burnham LA, Jaishankar D, Thompson JM, Jones KS, Shukla D, Tiwari V. Liposome-Mediated Herpes Simplex Virus Uptake Is Glycoprotein-D Receptor-Independent but Requires Heparan Sulfate. *Frontiers in microbiology*. 2016;7:973.
117. Whitley RJ, Corey L, Arvin A, Lakeman FD, Sumaya CV, Wright PF, et al. Changing presentation of herpes simplex virus infection in neonates. *The Journal of infectious diseases*. 1988;158(1):109-16.
118. Xu F, Schillinger JA, Sternberg MR, Johnson RE, Lee FK, Nahmias AJ, et al. Seroprevalence and coinfection with herpes simplex virus type 1 and type 2 in the United States, 1988-1994. *The Journal of infectious diseases*. 2002;185(8):1019-24.
119. Zhang J, Liu H, Wei B. Immune response of T cells during herpes simplex virus type 1 (HSV-1) infection. *Journal of Zhejiang University Science B*. 2017;18(4):277-88.
120. Groettrup M, Kraft R, Kostka S, Standera S, Stohwasser R, Kloetzel PM. A third interferon-gamma-induced subunit exchange in the 20S proteasome. *European journal of immunology*. 1996;26(4):863-9.
121. Schroder K, Hertzog PJ, Ravasi T, Hume DA. Interferon-gamma: an overview of signals, mechanisms and functions. *Journal of leukocyte biology*. 2004;75(2):163-89.
122. Azwa A, Barton SE. Aspects of herpes simplex virus: a clinical review. *The journal of family planning and reproductive health care*. 2009;35(4):237-42.
123. Jennings SR, Rice PL, Kloszewski ED, Anderson RW, Thompson DL, Tevethia SS. Effect of herpes simplex virus types 1 and 2 on surface expression of class I major histocompatibility complex antigens on infected cells. *Journal of virology*. 1985;56(3):757-66.
124. McNearney TA, Odell C, Holers VM, Spear PG, Atkinson JP. Herpes simplex virus glycoproteins gC-1 and gC-2 bind to the third component of complement and provide protection against complement-mediated neutralization of viral infectivity. *The Journal of experimental medicine*. 1987;166(5):1525-35.
125. Aubert M, Krantz EM, Jerome KR. Herpes simplex virus genes Us3, Us5, and Us12 differentially regulate cytotoxic T lymphocyte-induced cytotoxicity. *Viral immunology*. 2006;19(3):391-408.
126. Cooper PD. The plaque assay of animal viruses. *Advances in virus research*. 1961;8:319-78.

127. Actor JK. Immunology and Microbiology. 2 ed. USA: Elsevier; 2007.
128. Abbas AK, Lichtman AH, Pillai S. Cellular and Molecular Immunology. 9 ed. USA: Elsevier; 2018.
129. Trickett A, Kwan YL. T cell stimulation and expansion using anti-CD3/CD28 beads. *Journal of immunological methods*. 2003;275(1-2):251-5.
130. Shipkova M, Wieland E. Surface markers of lymphocyte activation and markers of cell proliferation. *Clinica chimica acta; international journal of clinical chemistry*. 2012;413(17-18):1338-49.
131. Holling TM, Schooten E, van Den Elsen PJ. Function and regulation of MHC class II molecules in T-lymphocytes: of mice and men. *Human immunology*. 2004;65(4):282-90.
132. Giorgi JV, Liu Z, Hultin LE, Cumberland WG, Hennessey K, Detels R. Elevated levels of CD38+ CD8+ T cells in HIV infection add to the prognostic value of low CD4+ T cell levels: results of 6 years of follow-up. The Los Angeles Center, Multicenter AIDS Cohort Study. *Journal of acquired immune deficiency syndromes*. 1993;6(8):904-12.
133. Braun RW, Teute HK, Kirchner H, Munk K. Replication of herpes simplex virus in human T lymphocytes: characterization of the viral target cell. *Journal of immunology*. 1984;132(2):914-9.
134. Rinaldo CR, Jr., Richter BS, Black PH, Callery R, Chess L, Hirsch MS. Replication of herpes simplex virus and cytomegalovirus in human leukocytes. *Journal of immunology*. 1978;120(1):130-6.
135. Pongpanich A, Bhattarakosol P, Chirathaworn C. Induction of apoptosis by herpes simplex virus in Jurkat cells is partly through caspase-3, -8 and -9 activation. *Journal of the Medical Association of Thailand = Chotmaihet thangphaet*. 2004;87 Suppl 2:S140-5.
136. Mahalingam M, Peakman M, Davies ET, Pozniak A, McManus TJ, Vergani D. T cell activation and disease severity in HIV infection. *Clinical and experimental immunology*. 1993;93(3):337-43.
137. Biancotto A, Iglehart SJ, Vanpouille C, Condack CE, Lisco A, Ruecker E, et al. HIV-1 induced activation of CD4+ T cells creates new targets for HIV-1 infection in human lymphoid tissue ex vivo. *Blood*. 2008;111(2):699-704.

138. Yamsuwan T, Chirathaworn C, Hansasuta P, Bhattarakosol P. HIV-1 replication in HIV-infected individuals is significantly reduced when peripheral blood mononuclear cells are superinfected with HSV-1. *TheScientificWorldJournal*. 2012;2012:102843.
139. Choudhary S, Burnham L, Thompson JM, Shukla D, Tiwari V. Role of Filopodia in HSV-1 Entry into Zebrafish 3-O-Sulfotransferase-3-Expressing Cells. *The open virology journal*. 2013;7:41-8.
140. Tiwari V, Shukla D. Phosphoinositide 3 kinase signalling may affect multiple steps during herpes simplex virus type-1 entry. *The Journal of general virology*. 2010;91(Pt 12):3002-9.
141. Tiwari V, Oh MJ, Kovacs M, Shukla SY, Valyi-Nagy T, Shukla D. Role for nectin-1 in herpes simplex virus 1 entry and spread in human retinal pigment epithelial cells. *The FEBS journal*. 2008;275(21):5272-85.
142. Akhtar J, Tiwari V, Oh MJ, Kovacs M, Jani A, Kovacs SK, et al. HVEM and nectin-1 are the major mediators of herpes simplex virus 1 (HSV-1) entry into human conjunctival epithelium. *Investigative ophthalmology & visual science*. 2008;49(9):4026-35.
143. Joseph R, Srivastava OP, Pfister RR. Downregulation of beta-actin gene and human antigen R in human keratoconus. *Investigative ophthalmology & visual science*. 2012;53(7):4032-41.
144. Meuer SC, Hodgdon JC, Hussey RE, Protentis JP, Schlossman SF, Reinherz EL. Antigen-like effects of monoclonal antibodies directed at receptors on human T cell clones. *The Journal of experimental medicine*. 1983;158(3):988-93.
145. Mercep M, Bluestone JA, Noguchi PD, Ashwell JD. Inhibition of transformed T cell growth in vitro by monoclonal antibodies directed against distinct activating molecules. *Journal of immunology*. 1988;140(1):324-35.
146. Neri F, Giolo G, Potesta M, Petrini S, Doria M. CD4 downregulation by the human immunodeficiency virus type 1 Nef protein is dispensable for optimal output and functionality of viral particles in primary T cells. *The Journal of general virology*. 2011;92(Pt 1):141-50.
147. Doria M. Role of the CD4 down-modulation activity of Nef in HIV-1 infectivity. *Current HIV research*. 2011;9(7):490-5.

148. Marodon G, Warren D, Filomio MC, Posnett DN. Productive infection of double-negative T cells with HIV in vivo. *Proceedings of the National Academy of Sciences of the United States of America*. 1999;96(21):11958-63.
149. Schonrich G, Kalinke U, Momburg F, Malissen M, Schmitt-Verhulst AM, Malissen B, et al. Down-regulation of T cell receptors on self-reactive T cells as a novel mechanism for extrathymic tolerance induction. *Cell*. 1991;65(2):293-304.
150. Mehal WZ, Crispe IN. TCR ligation on CD8+ T cells creates double-negative cells in vivo. *Journal of immunology*. 1998;161(4):1686-93.
151. Cibrian D, Sanchez-Madrid F. CD69: from activation marker to metabolic gatekeeper. *European journal of immunology*. 2017;47(6):946-53.
152. Simms PE, Ellis TM. Utility of flow cytometric detection of CD69 expression as a rapid method for determining poly- and oligoclonal lymphocyte activation. *Clinical and diagnostic laboratory immunology*. 1996;3(3):301-4.
153. Watts TH. TNF/TNFR family members in costimulation of T cell responses. *Annual review of immunology*. 2005;23:23-68.
154. Cannons JL, Lau P, Ghumman B, DeBenedette MA, Yagita H, Okumura K, et al. 4-1BB ligand induces cell division, sustains survival, and enhances effector function of CD4 and CD8 T cells with similar efficacy. *Journal of immunology*. 2001;167(3):1313-24.
155. Dawicki W, Watts TH. Expression and function of 4-1BB during CD4 versus CD8 T cell responses in vivo. *European journal of immunology*. 2004;34(3):743-51.
156. Mardiney M, 3rd, Brown MR, Fleisher TA. Measurement of T-cell CD69 expression: a rapid and efficient means to assess mitogen- or antigen-induced proliferative capacity in normals. *Cytometry*. 1996;26(4):305-10.
157. Shuford WW, Klussman K, Tritchler DD, Loo DT, Chalupny J, Siadak AW, et al. 4-1BB costimulatory signals preferentially induce CD8+ T cell proliferation and lead to the amplification in vivo of cytotoxic T cell responses. *The Journal of experimental medicine*. 1997;186(1):47-55.
158. Johnson DC, Huber MT. Directed egress of animal viruses promotes cell-to-cell spread. *Journal of virology*. 2002;76(1):1-8.
159. Lehmann MJ, Sherer NM, Marks CB, Pypaert M, Mothes W. Actin- and myosin-driven movement of viruses along filopodia precedes their entry into cells. *The Journal*

of cell biology. 2005;170(2):317-25.

160. Bas A, Forsberg G, Hammarstrom S, Hammarstrom ML. Utility of the housekeeping genes 18S rRNA, beta-actin and glyceraldehyde-3-phosphate-dehydrogenase for normalization in real-time quantitative reverse transcriptase-polymerase chain reaction analysis of gene expression in human T lymphocytes. *Scandinavian journal of immunology*. 2004;59(6):566-73.

161. Roge R, Thorsen J, Topping C, Ozbay A, Moller BK, Carstens J. Commonly used reference genes are actively regulated in in vitro stimulated lymphocytes. *Scandinavian journal of immunology*. 2007;65(2):202-9.

162. Lyman MG, Enquist LW. Herpesvirus interactions with the host cytoskeleton. *Journal of virology*. 2009;83(5):2058-66.

163. Feierbach B, Piccinotti S, Bisher M, Denk W, Enquist LW. Alpha-herpesvirus infection induces the formation of nuclear actin filaments. *PLoS pathogens*. 2006;2(8):e85.

164. Cooper JA. Effects of cytochalasin and phalloidin on actin. *The Journal of cell biology*. 1987;105(4):1473-8.

165. Nobes CD, Hall A. Rho, rac, and cdc42 GTPases regulate the assembly of multimolecular focal complexes associated with actin stress fibers, lamellipodia, and filopodia. *Cell*. 1995;81(1):53-62.

166. Puls A, Eliopoulos AG, Nobes CD, Bridges T, Young LS, Hall A. Activation of the small GTPase Cdc42 by the inflammatory cytokines TNF(alpha) and IL-1, and by the Epstein-Barr virus transforming protein LMP1. *Journal of cell science*. 1999;112 (Pt 17):2983-92.

167. Sharma-Walia N, Naranatt PP, Krishnan HH, Zeng L, Chandran B. Kaposi's sarcoma-associated herpesvirus/human herpesvirus 8 envelope glycoprotein gB induces the integrin-dependent focal adhesion kinase-Src-phosphatidylinositol 3-kinase-rho GTPase signal pathways and cytoskeletal rearrangements. *Journal of virology*. 2004;78(8):4207-23.

168. Zamudio-Meza H, Castillo-Alvarez A, Gonzalez-Bonilla C, Meza I. Cross-talk between Rac1 and Cdc42 GTPases regulates formation of filopodia required for dengue virus type-2 entry into HMEC-1 cells. *The Journal of general virology*. 2009;90(Pt

12):2902-11.

169. Krzyzaniak MA, Zumstein MT, Gerez JA, Picotti P, Helenius A. Host cell entry of respiratory syncytial virus involves macropinocytosis followed by proteolytic activation of the F protein. *PLoS pathogens*. 2013;9(4):e1003309.

170. Nikolic DS, Lehmann M, Felts R, Garcia E, Blanchet FP, Subramaniam S, et al. HIV-1 activates Cdc42 and induces membrane extensions in immature dendritic cells to facilitate cell-to-cell virus propagation. *Blood*. 2011;118(18):4841-52.

171. Wang S, Li H, Chen Y, Wei H, Gao GF, Liu H, et al. Transport of influenza virus neuraminidase (NA) to host cell surface is regulated by ARHGAP21 and Cdc42 proteins. *The Journal of biological chemistry*. 2012;287(13):9804-16.

172. Kawakatsu T, Shimizu K, Honda T, Fukuhara T, Hoshino T, Takai Y. Trans-interactions of nectins induce formation of filopodia and Lamellipodia through the respective activation of Cdc42 and Rac small G proteins. *The Journal of biological chemistry*. 2002;277(52):50749-55.

173. Honda T, Shimizu K, Kawakatsu T, Fukuhara A, Irie K, Nakamura T, et al. Cdc42 and Rac small G proteins activated by trans-interactions of nectins are involved in activation of c-Jun N-terminal kinase, but not in association of nectins and cadherin to form adherens junctions, in fibroblasts. *Genes to cells : devoted to molecular & cellular mechanisms*. 2003;8(5):481-91.

174. Reicher B, Barda-Saad M. Multiple pathways leading from the T-cell antigen receptor to the actin cytoskeleton network. *FEBS letters*. 2010;584(24):4858-64.

175. Salazar-Fontana LI, Barr V, Samelson LE, Bierer BE. CD28 engagement promotes actin polymerization through the activation of the small Rho GTPase Cdc42 in human T cells. *Journal of immunology*. 2003;171(5):2225-32.

176. Serrador JM, Nieto M, Sanchez-Madrid F. Cytoskeletal rearrangement during migration and activation of T lymphocytes. *Trends in cell biology*. 1999;9(6):228-33.

177. Dustin ML, Cooper JA. The immunological synapse and the actin cytoskeleton: molecular hardware for T cell signaling. *Nature immunology*. 2000;1(1):23-9.

178. Immergluck LC, Domowicz MS, Schwartz NB, Herold BC. Viral and cellular requirements for entry of herpes simplex virus type 1 into primary neuronal cells. *The Journal of general virology*. 1998;79 (Pt 3):549-59.

179. Tiwari V, Liu J, Valyi-Nagy T, Shukla D. Anti-heparan sulfate peptides that block herpes simplex virus infection in vivo. *The Journal of biological chemistry*. 2011;286(28):25406-15.
180. Nyberg K, Ekblad M, Bergstrom T, Freeman C, Parish CR, Ferro V, et al. The low molecular weight heparan sulfate-mimetic, PI-88, inhibits cell-to-cell spread of herpes simplex virus. *Antiviral research*. 2004;63(1):15-24.



APPENDIX A
REGENTS, MATERIALS AND INSTRUMENTS

A. Media and Reagents

| | |
|---|-------------------------------------|
| 0.5 Tris-HCl Buffer | (Biorad, USA) |
| 1.5 Tris-HCl Buffer | (Biorad, USA) |
| 2,4,6-Tris(dimethylaminomethyl)phenol (DMP-30) | (Electron microscopy sciences, USA) |
| 2-Mercaptoethanol | (BioRad, China) |
| 2xLaemmli Sample Buffer | (BioRad, China) |
| 4-(2-hydroxyethyl)-1-piperazineethanesulfonic acid (HEPES, Free acid) | (Bio Basic, Canada) |
| 40% Acrylamide/Bis | (BioRad, USA) |
| Acetic acid | (Emsure, Germany) |
| Acetone | (Emsure, Germany) |
| Ammonium Peroxodisulfide (APS) | (Panreac Applichem, Germany) |
| Bovine serum albumin | (Sigma, USA) |
| Complete Lysis-M, EDTA-free | (Roche, Germany) |
| Coomasie Blue R-250 | (Thermo Scientific, USA) |
| Crystal Violet | (Merck, Germany) |
| Cytochalasin D (Cyto D) | (Sigma, USA) |
| DAPI (4',6-diamidino-2-phenylindole) | (Biolegend, USA) |



| | |
|--|--|
| Dimethyl sulfoxide (DMSO) | (Panreac Applichem, Germany) |
| Dodecenylsuccinic anhydride (DDSA) | (Merck, Germany) |
| Dynabeads® Human T-Activator CD3/CD28 | (Invitrogen, USA) |
| Embed 812 resin 14900 (Epon) | (Electron microscopy sciences, USA) |
| Ethanol | (Emsure, Germany) |
| Ethyl alcohol 70% | (Defence Pharmaceutical Factory, Thailand) |
| Ethylenediaminetetraacetic acid (C ₁₀ H ₁₆ N ₂ O ₈ ; EDTA) | (Bio Basic, Canada) |
| Fetal bovine serum (FBS) | (Gibco, USA) |
| Formedehyde 37% m/v | (CARLO ERBA, France) |
| Glycine | (BioRad, USA) |
| Isopropanol (2-Propanol) | (Emsure, Germany) |
| L-Glutamine | (Bio Basic, Canada) |
| Luna® Universal qPCR Master Mix | (New England Biolabs, UK) |
| Medium 199 | (Gibco, USA) |
| Methanol (MeOH) | (Univar, Australia) |
| Mounting fluid | (Diagnostic Hybrids, USA) |
| Nadic Methyl Anhydride (NMA) | (Electron microscopy sciences, USA) |

| | |
|--|----------------------------------|
| NucleoSpin RNA plus | (MACHEREY-NAGEL, Germany) |
| Penicillin G | (Bio Basic, Canada) |
| Potassium chloride (KCl) | (Merck, Germany) |
| Potassium phosphate monobasic (KH ₂ PO ₄) | (Bio Basic, Canada) |
| Rhodamine phalloidin | (Invitrogen, USA) |
| RPMI 1640 Medium | (Gibco, USA) |
| Sensitivity Substrate | USA) |
| Sodium Chloride | (Bio Basic, Canada) |
| Sodium dodecyl sulfate (SDS) | (Bio Basic, Canada) |
| Sodium hydroxide (NaOH) | (Sigma, USA) |
| Sodium phosphate | (Bio Basic, Canada) |
| Streptomycin | (Sigma, USA) |
| SuperScript™ III Reverse Transcriptase | (Invitrogen, USA) |
| SuperSignal® West Femto Maximum | (Thermo ScientificScientific, |
| TBS (Tris-buffered saline) | (Life science, USA) |
| TEMED (N,N,N',N'-Tetramethylethylenediamine) | (Thermo scientific, USA) |
| Tetra Z reagent | (Biolegend, USA) |
| Tragacanth | (Sigma, UK) |
| Tris-HCl | (Vivantis, USA) |
| Trypan blue | (Invitrogen, USA) |

Trypsin (Bio Basic, USA)

Tween 20 (USB, USA)

B. Antibodies

Brilliant violet 421 conjugated anti-human CD8 antibody (Biolegend, USA)

FITC conjugated anti-human CD4 antibody (Biolegend, USA)

Goat pAb polyclonal antibody to mouse IgG conjugated with horseradish peroxidase (HRP) (Abcam, USA)

Goat polyclonal anti-HSV-1 conjugated with FITC (Abcam, USA)

Mouse anti-beta actin antibodies (Santa cruz biotechnology, USA)

Mouse anti-Cdc 42 antibodies (Santa cruz biotechnology, USA)

Mouse anti-GAPDH antibodies (Santa cruz biotechnology, USA)

Mouse anti-Rac1 antibodies (Santa cruz biotechnology, USA)

Mouse anti-RhoA antibodies (Santa cruz biotechnology, USA)

Pacific blue™ mouse anti-Human CD3 Clone: UCHT1 (BD Biosciences Pharmingen, USA)

PE conjugated anti-human CD137 (Biolegend, USA)

PE conjugated anti-human CD69 (Biolegend, USA)

PE/Cy5 conjugated anti-human CD38 (Biolegend, USA)

PE/Cy7 conjugated anti-human CD3 antibody (Biolegend, USA)

PE/Cy7 conjugated anti-human HLA-DR (Biolegend, USA)

C. Materials

| | |
|---------------------------------|--------------------------|
| 1.5 and 0.2 mL tube | (Axygen, USA) |
| 12 well-plate | (Nunc, Denmark) |
| 15 and 50 mL tube | (JetBioFil, China) |
| 24 well-plate | (Nunc, China) |
| 96 well-plate | (Thermo, China) |
| Cell culture flask (T25 and 75) | (Thermo, China) |
| Glass slide | (Thermo Scientific, USA) |
| Hemocytometer | (Spencer, USA) |
| Nitrocellulose membrane | (BioRad, USA) |
| Syringe-driven filters | (JetBioFil, China) |
| Vari-Strip for real-time PCR | (4titude, UK) |

D. Instruments

| | |
|---|-----------------------|
| Autoclave | (Hirayama, Japan) |
| Biohazard safety cabinet | (Flufrance, France) |
| C-Digit blot scanner | (LI-COR, USA) |
| CO ₂ incubator | (Thermo, USA) |
| DynaMag TM -2 magnetic particle concentrator | (Invitrogen, Norway) |
| Flow cytometer (BD FACSAria II) | (BD Biosciences, USA) |
| Fluorescence microscope | (OLYMPUS BX50) |

| | |
|--|------------------------------|
| Fluorescence microscopy | (OLYMPUS BX50, Japan) |
| Heat box | (Bioer technology, china) |
| Hotplate stirrer | (Isolab, Germany) |
| Incubator | (Mettler, Germany) |
| Inverted microscopy | (Leica, Germany) |
| Microcentrifuge | (SelectBioProducts, UK) |
| Microplate reader | (Perkin Eimer, USA) |
| Mixer-vortex | (Scientific industrial, USA) |
| pH meter | (Accmet Basic, Singapore) |
| PowerPac Basic | (BioRad, USA) |
| PowerPac HC | (BioRad, USA) |
| Refrigerated Centrifuge | (Thermo, USA) |
| Roltater | (Thermo, USA) |
| Spindown | (Hercuvan, Malaysia) |
| Step One Plus Real-Time PCR System | (Applied Biosystems. USA) |
| Trans-blot SD semi-dry transfer cell | (BioRad, USA) |
| Transmission electron microscope (TEM) | (JEM-1400 series, USA) |
| Water bath | (Julabo, Germany) |



APPENDIX B

REAGENTS PREPARATION

REAGENTS AND MEDIA FOR CELL CULTURE

1. 5x M199

| | | |
|--|------|---|
| M199 with L-glutamine | 10.4 | g |
| Sterilized Double-distilled water (DDW) | 100 | g |
| Sterilized by filtration (0.2 μ m) and stored at 4°C | | |

2. 10% M199 (growth media for Vero cell)

| | | |
|--|-----|----|
| 5X M199 with Earle's salts, with L-glutamine, without NaHCO ₃ | 20 | mL |
| 1 M HEPES | 1 | mL |
| Pen/Strep antibiotics (10 ⁵ unit/mL) | 0.1 | mL |
| 10% NaHCO ₃ | 1 | mL |
| 5% L-glutamine | 1 | mL |
| Fetal Bovine Serum (FBS) | 10 | mL |
| Sterilized DDW | 67 | mL |
| Stored at 4°C | | |

3. 2% M199 (Maintenance media for Vero cell)

| | | |
|--|-----|----|
| 5X M199 with Earle's salts, with L-glutamine, without NaHCO ₃ | 20 | mL |
| 1 M HEPES | 1 | mL |
| Pen/Strep antibiotics (10 ⁵ unit/mL) | 0.1 | mL |
| 10% NaHCO ₃ | 1 | mL |
| 5% L-glutamine | 1 | mL |
| Fetal Bovine Serum (FBS) | 2 | mL |
| Sterilized DDW | 75 | mL |
| Stored at 4°C | | |

4. 2x RPMI 1640

| | | |
|--|------|----|
| RPMI 1640 with L-glutamine | 10.4 | g |
| Sterilized DDW | 500 | mL |
| Sterilized by filtration (0.2 μ m) and stored at 4°C | | |

5. 10% RPMI (Growth media for Jurkat cell)

| | | |
|---|------|----|
| 2X RPMI with L-glutamine | 50 | mL |
| 1 M HEPES | 1 | mL |
| Pen/Strep antibiotics (10^5 unit/mL) | 1 | mL |
| 10% NaHCO ₃ | 1.5 | mL |
| Fetal Bovine Serum (FBS) | 10 | mL |
| Sterilized DDW | 36.5 | mL |
| Stored at 4°C | | |

6. 2% RPMI (Maintenance media for Jurkat cell)

| | | |
|---|------|----|
| 2X RPMI with L-glutamine | 50 | mL |
| 1 M HEPES | 1 | mL |
| Pen/Strep antibiotics (10^5 unit/mL) | 1 | mL |
| 10% NaHCO ₃ | 1.5 | mL |
| Fetal Bovine Serum (FBS) | 2 | mL |
| Sterilized DDW | 44.5 | mL |
| Stored at 4°C | | |

7. Pen/Strep antibiotic (10^5 units/mL)

| | | |
|--|-----|----|
| Penicillin G | 0.6 | g |
| Streptomycin | 1.5 | g |
| Sterilized DDW | 200 | mL |
| Sterilized by filtration (0.2 μ m) and stored at -20°C | | |

8. HEPES 1 M

| | |
|---|----------|
| HEPES | 11.915 g |
| Sterilized DDW | 50 mL |
| Sterilized by autoclave and stored at 4°C | |

9. 10% NaHCO₃

| | |
|---|-------|
| NaHCO ₃ | 5 g |
| Sterilized DDW | 50 mL |
| Sterilized by autoclave and stored at 4°C | |

10. 10x PBS, pH 7.4

| | |
|---------------------------------|---------|
| NaCl | 80 mL |
| KCl | 2 g |
| NaHPO ₄ | 11.5 g |
| KH ₂ PO ₄ | 2 g |
| DDW | 1000 mL |
| Sterilized by autoclave | |

11. 1x PBS

| | |
|----------------------------|--------|
| 10x PBS | 30 mL |
| Sterilized DDW | 270 mL |
| Stored at room temperature | |

12. 10x Trypsin

| | |
|---|---------|
| Trypsin | 0.5 g |
| EDTA | 0.2 g |
| NaCl | 9.0 g |
| DDW | 1000 mL |
| Sterilized by filtration (0.2 μm) and stored at 4°C | |

13. 1x Trypsin

| | | |
|----------------|---|----|
| 10xTrypsin | 1 | mL |
| Sterilized DDW | 9 | mL |
| Stored at 4°C | | |

14. 2x M199

| | | |
|----------------|---|----|
| 5x M199 | 4 | mL |
| Sterilized DDW | 6 | mL |
| Stored at 4 °C | | |

15. 1.6% Gum tragacanth

| | | |
|---|-----|----|
| Gum tragacanth | 0.8 | g |
| Sterilized DDW | 50 | mL |
| Sterilized by autoclave and stored at 4°C | | |

16. Overlay medium

| | | |
|--|-------|----|
| 2x M199 | 13.35 | mL |
| FBS | 300 | μL |
| Pen/Strep antibiotics (10 ⁵ units/mL) | 300 | μL |
| 1 M HEPES | 150 | μL |
| 10% NaHCO ₃ | 900 | μL |
| 1.6% Gum tragacanth | 15 | mL |

17. 1% Crystal violet

| | | |
|------------------|------|----|
| Crystal violet | 1 | g |
| 5% Isopropanol | 4.75 | mL |
| 10% Formaldehyde | 25 | mL |

18. L-glutamine

| | | |
|----------------|-------|----|
| L-glutamine | 2.922 | g |
| Sterilized DDW | 100 | mL |

Sterilized by filtration (0.2 μ m) and stored at -20°C

19. Washing buffer for Dynabeads (PBS with 0.1% BSA and 2 mM EDTA, pH 7.4)

| | | |
|-----------|------|----|
| 1x PBS | 50 | mL |
| BSA | 0.05 | g |
| 2 mM EDTA | 0.04 | g |

Adjust pH to 7.5 with 1 M HCl, sterilized by filtration (0.2 μ m) and stored at 4°C

REAGENT FOR IMMUNOFLUORESCENCE**1. 1% BSA in PBS**

| | | |
|--------|-----|----|
| BSA | 0.1 | g |
| 1x PBS | 10 | mL |

REAGENTS FOR SDS-PAGE AND WESTERN BLOT**1. 10% Running gel (10% Acrylamide concentration)**

| | | |
|------------------|-----|---------|
| DDW | 7.7 | mL |
| 40% Acrylamide | 4 | mL |
| 1.5M Tris pH 8.8 | 4 | mL |
| 10% SDS | 160 | μ L |
| 10% APS | 160 | μ L |
| TEMED | 16 | μ L |

2. 4% Stacking gel (5% Acrylamide concentration)

| | | |
|------------------|------|---------------|
| DDW | 3.15 | mL |
| 40% Acrylamide | 0.5 | mL |
| 0.5M Tris pH 6.8 | 1.25 | mL |
| 10% SDS | 50 | μL |
| 10% APS | 50 | μL |
| TEMED | 5 | μL |

3. 10% Ammonium persulphate (APS)

| | | |
|-----|------|---------------|
| APS | 0.03 | g |
| DDW | 300 | μL |

4. Coomassie blue R-250 staining solution

| | | |
|----------------------------|-----|----|
| Coomassie blue R-250 stock | 15 | mL |
| Methanol | 250 | mL |
| DW | 200 | mL |
| Acetic acid | 50 | mL |

5. Lysis M

| | | |
|---|----|--------|
| Complete Lysis-M, EDTA-free | 10 | mL |
| Complete tablets, Mini EDTA-free, EASY pack | 1 | tablet |

6. Removal buffer (Mild stripping)

| | | |
|----------|-----|----|
| Glycine | 1.5 | g |
| SDS | 0.1 | g |
| Tween 20 | 1 | mL |

Dissolved in 50 mL distilled water. Adjust pH to 2.2 and bring volume up to 100 mL with distilled water.

7. Tris-buffered saline (TBS)

50 mM Tris-HCl, pH 7.5

150 mM NaCl

To prepare, dissolved 6.05 g Tris-HCl and 8.76 g NaCl in 800 mL of H₂O. Adjust pH to 7.5 with 1 M HCl and make volume to 1 L with H₂O. TBS is stable at 4°C for 3 months.

8. 10x Running buffer for SDS-PAGE (10x Tris/Glycine/SDS Buffer)

| | | |
|-----------|----|---|
| Tris base | 30 | g |
|-----------|----|---|

| | | |
|---------|-----|---|
| Glycine | 144 | g |
|---------|-----|---|

| | | |
|-----|----|---|
| SDS | 10 | g |
|-----|----|---|

| | | |
|----------------------|------|---|
| Distilled water (DW) | 1000 | g |
|----------------------|------|---|

pH should be 8.3-8.4

9. 1x Running buffer (1x Tris/Glycine/SDS Buffer)

| | | |
|--------------------|-----|----|
| 10x Running buffer | 100 | mL |
|--------------------|-----|----|

| | | |
|----------------------|-----|----|
| Distilled water (DW) | 900 | mL |
|----------------------|-----|----|

10. Blotting buffer

| | | |
|-------------------|----|----|
| 1x Running buffer | 80 | mL |
|-------------------|----|----|

| | | |
|----------|----|----|
| Methanol | 20 | mL |
|----------|----|----|

11. TBS + 0.05% Tween (TTBS)

| | | |
|--------|------|----|
| 1x TBS | 1000 | mL |
|--------|------|----|

| | | |
|----------|-----|----|
| Tween 20 | 500 | μL |
|----------|-----|----|

12. 3% BSA in TTBS

| | | |
|------|-----|----|
| TTBS | 20 | mL |
| BSA | 0.6 | g |

13. 1% BSA in TTBS

| | | |
|------|-----|----|
| TTBS | 20 | mL |
| BSA | 0.2 | g |

14. SDS loading buffer (Sample buffer)

| | | |
|--------------------------|-----|---------|
| 2x laemmli sample buffer | 190 | μ L |
| 2 mercapto ethanol | 10 | μ L |

15. 0.1 M NaOH

| | | |
|----------------------|-----|----|
| NaOH | 0.4 | g |
| Distilled water (DW) | 100 | mL |

16. 1 M HCl

| | | |
|----------------------|-------|----|
| HCl (37% w/v) | 4.93 | mL |
| Distilled water (DW) | 45.07 | mL |

17. Destaining solution for Coomassie blue

| | | |
|----------------------|-----|----|
| Methanol | 200 | mL |
| Acetic acid | 100 | mL |
| Distilled water (DW) | 700 | mL |

REAGENT FOR ELECTRON MICROSCOPE

1. Phosphate buffer (PB)

Solution A (0.2 M NaH_2PO_4)

| | | |
|--|-------|----|
| Sodium phosphate monobasic (NaH_2PO_4) | 16.80 | g |
| DW | 500 | mL |

Solution B (0.2 M Na_2HPO_4)

| | | |
|--|-------|----|
| Sodium phosphate dibasic (Na_2HPO_4) | 14.20 | g |
| DW | 500 | mL |

Working solution buffer 0.1 M

| | | |
|------------|------|----|
| Solution A | 19.0 | mL |
| Solution B | 81.0 | mL |
| DW | 100 | mL |

2. Epon 812 (resin)

| | | |
|--|-----|----|
| Nadic Methyl Anhydride (NMA) | 2 | mL |
| Dodecenylsuccinic anhydride (DDSA) | 4 | mL |
| Embed 812 resin 14900 (Epon) | 5 | mL |
| 2,4,6-Tris(dimethylaminomethyl)phenol (DMP-30) | 0.2 | mL |

VITA

NAME Mr. Thanayod Sasivimolrattana

DATE OF BIRTH 28 Mar 1994

PLACE OF BIRTH Bangkok, Thailand

INSTITUTIONS ATTENDED 2012-2016 Bachelor of Science (Industrial Microbiology),
Faculty of Science, King Mongkut's Institute of Technology
Ladkrabang, Bangkok, Thailand.

HOME ADDRESS 15, Amornpan 9 village, Lardprao, Bangkok, 10230,
Thailand

PUBLICATION Thanayod Sasivimolrattana and Parvapan Bhattarakosol.
Filopodia formation plays a key role in HSV-1 entry in
activated T lymphocytes. Proceeding of the 28th Annual
Scientific Meeting, The Virology Association (Thailand).
November 2018